Seismic reliability of Reinforced Concrete buildings erected on hard soil nearby epicenter (case of Guerrero, Mexico)

David Pérez Gómez Pérez-Gómez

UNIVERSITÉ PARIS-EST

École Doctorale : Matériaux, Ouvrages, Durabilité, Environnement et Structures

Pour obtenir le grade de :

DOCTEUR DE L'UNIVERSITE PARIS-EST

Spécialité : *Génie Civil*

Présentée par :

David PÉREZ GÓMEZ

Titre :

Fiabilité séismique des bâtiments en béton armé érigés sur un sol dur avec épicentre proche (cas de Guerrero, Mexique)

Seismic reliability of RC buildings erected on hard soil nearby epicenter (case of Guerrero, Mexico)

Thèse dirigée par : **M. Ahmed MEBARKI**

Soutenue le : 10 Décembre 2009

Jury :

M. LORRAIN Michel Rapporteur

M. BENOUAR Djillali Rapporteur

Dedications

A Dios, por permitirme vivir y realizar este sueño.

A mis Padres, Javier PÉREZ y Guillermina GÓMEZ que con su esfuerzo, dedicación y ejemplo de vida; hicieron de mi un hombre de bien.

A mi esposa Gabriela CASTILLO, a mis hijos Luis Javier y David quienes con palabras de aliento, esperanza, además con su paciencia y amor esperan mi regreso.

A los amigos de la UNAM por la confianza en mi persona, que sin su apoyo incondicional, no lograría esta difícil meta.

Contents

Dedications 3
Contents 5
Summary in English 9
Summary in French 11
Summary in Spanish 13
Acknowledgements 15
List of Symbols 17
Figures 19
Tables 23
Chapter 1 INTRODUCTION 25
1.1 Introduction 25
1.2 Background 26
1.2.1 Seismic events, that caused damage at the Mexican buildings. 26
1.2.2 Geophysics studies and of seismicity 30
a) Accelerographs Network 30
b) Global Positioning System [GPS], Studies. 31
c) Geophysical studies of GAP in the State of Guerrero. 33
1.2.3 Materials and local condition in Guerrero State 36
1.2.4 Studies that have been carried out in the country and in the world on the structural behavior of seismic events with near epicenter. 37
a) Comparative studies of the ground period T_S and the period structure T_E. 38
b) Some reliability studies 38
c) Nowadays, some researches related to reliability 38
d) Examples of revisions to the codes by have quake near epicenter 39
1.3 Justification 40
1.4 General Objective 40
1.4.1 Specific Objectives 40
1.5 Scope of research work 41
1.6 Summary 41
Chapter 2 Theoretical approach of the Reliability and adopted methodology. 43
2.1 Introduction 43
2.2 Reliability and Limit State Function 43
2.2.1 Definitions of the reliability 43
2.2.2 Limit State Functions, (E), general considerations 45
2.3 Mechanical model 50
2.4 Analysis methods 51
2.4.1 Static adaptive pushover analysis with the software SeismoStruct 51
2.4.2 Method of the Incremental dynamic analysis [IDA], with the software SeismoStruct 60

2.5 Study of the buildings 66
2.5.1 Dimension of the buildings 67
2.5.2 Materials used for the construction 69
2.6 Uncertainty in the Resistance of Materials 70
2.6.1 Concrete compressive strength, f 'c 70
2.6.2 Yield stress of Steel, f_y 72
2.6.3 Parameters that define the Stress-Strain curve (fs-ε_S) of steel, proposed by Park and Paulay 72
2.7 Index of Reliability 74
2.8 Summary 78
Chapter 3 Seismic Excitation 79
3.1 Introduction 79
3.2 Origin of the earthquake in Mexico 79
3.2.1 Geological faults 79
3.2.2 Researches on Peak Ground Acceleration [PGA], into survey area. 80
3.3 Survey area and geometry of subduction 82
3.4 Selection of the sample size of the earthquakes 84
3.5 Calculation of the spectra of ground response 94
3.6 Location of epicenters through satellite image with the software Google Earth, distances between the epicenter and the station of the accelerographs, accelerograms and its response spectrum of the ground [Ts] 97
3.7 Summary 101
Chapter 4 Results 103
4.1 Introduction 103
4.2 General Results on the Survey area 104
4.3 Results in the elastic status with the Dynamic Analysis Response to Spectrum [DARS] 105
4.4 Results of Static Adaptive Pushover Analysis [Displacement-base, DAP] 110
4.4.1 Ductility in the buildings 111
4.5 Results with the method of the Incremental dynamic analysis – [IDA] 112
4.6 Indexes of reliability. 114
a) Site effects considering different magnitudes, duration and different distances from the epicenter to the station of the accelerographs, to see Table 16. 115
b) Site effects considering the distance 116
4.7 Summary 127
Chapter 5 Conclusion and recommendations 129
Annex 1 133
Annex 2. 143
Annex 3 149

Annex 4 153
References and Bibliography 155

Summary in English

With real information provided by Mexican Institution, we begin this research. The objective is to measure the indexes of reliability of reinforced concrete buildings subjected to real seismic forces with near epicenter, erected on hard soil. There is a need to assess the uncertainty affecting the buildings in the State of Guerrero, since geophysical researches estimate a GAP of area of 220x90 km^2, which will generate an earthquake of Magnitude Mw=8.4. We expect that the predominant period has a range of 0.034 to 0.36 sec [Pérez D. and Mebarki A., 2007]. We achieved this, with the interpretation of 3600 real earthquake from a database of SMIS, selected by their great magnitude and near epicenter. Where the ordinate of the response spectrum of the ground should be superior than the design spectra, thereby considering the buildings that are at greatest risk of damage or collapse. Three proposals for buildings with different resistance emerge, that are: 1. To calculate according to the properties of the materials in the State of Guerrero. 2. To calculate with the properties of the region central of the country [RCDF], as currently done and. 3. To estimate a degradation of resistance of the buildings for the earthquakes suffered in the past.

The capacity of lateral resistance of the buildings is considered with two analysis types, that are: 1. Static Adaptive Pushover Analysis [DAP], which measures the level of ductility that develops the building, knowing with this, the yield point and the ultimate capacity of each building. 2. Incremental Dynamic Analysis [IDA], in which the resistance of the building is evaluated in the time-history, with real seismic events scaled to know the duration in which the value of the state limit of the building has been exceeded. We observed that the indexes of reliability in the buildings subject to seismic forces with near epicenter are highly dependent on the conditions of ground and the magnitude of the earthquake. The effects of site changes significantly, when the magnitude of the seismic event increases, that make vary the building reliability indexes. These variations show the great importance and attention that should be devoted to properties of the materials in the State of Guerrero, because they influence significantly the fundamental period of the buildings.

Summary in French

Cette recherche s'appuie pour certaines données, fournies par des institutions mexicaines sur des bases de donnée réelle. L'objectif est de mesurer les indices de fiabilité des bâtiments en béton armé soumis à des forces sismiques réelles avec épicentre proche, construits sur un sol rigide. Il existe une nécessité d'évaluer l'effet des incertitudes affectant les bâtiments de l'État de Guerrero, du fait que la recherche géophysique un estime GAP sismique avec une zone de 220x90 km^2, qui produirait un événement sismique de magnitude Mw=8.4. Nous avons déterminé que la période prédominante de site dans un intervalle de 0.034 à 0.36 [Pérez D. and Mebarki A., 2007]. Nous obtenons ceci, avec l'interprétation de 3600 séismes réels d'une base de données de la SMIS, sélectionnés pour leur grande magnitude et épicentre proche. Lorsque l'ordonnée du spectre de réponse du sol est plus grande que celle du spectre du code, on doit approfondir l'analyses des bâtiments qui s'y trouvent du fait du plus grand risque de dommage et effondrement. Trois propositions de bâtiments de différentes résistances apparaissent, à savoir : 1. Calculer avec les propriétés des matériels de l'Etat de Guerrero. 2. Calculer avec les propriétés de la région centre du pays [RCDF], comme l'on fait actuellement, et, 3. Estimer une dégradation de résistance des bâtiments pour les séismes observé dans le passé.

La capacité de résistance latérale du bâtiment est estimée avec deux types d'analyse. Il s'agit de : 1. Static Adaptive Pushover Analysis [DAP], avec laquelle nous mesurons le niveau de ductilité que développe le bâtiment, connaissant le point de plastification et la déformation ultime de chaque bâtiment. 2. Incremental Dynamic Analysis [IDA], pour évaluer en fonction de temps la résistance des bâtiments, soumis à des événements sismiques réels avec changement d'échelle et détermine les moments et la durée de l'état limite du bâtiment a été dépassé. On a observé que les indices de fiabilité dans les bâtiments soumis à des forces sismiques avec épicentre proche, dépendent beaucoup des conditions de sol et de la magnitude du séisme. Les effets de site changent de manière significative quand la magnitude de l'événement sismique augmente, ce qui fait varier les indices de fiabilité des bâtiments. Cette variation montre de l'importance à connaître les propriétés des matériaux de l'État de Guerrero, parce qu'ils influencent grandement sur la période fondamentale de l'édifice.

Summary in Spanish

Con información real proporcionada por instituciones mexicanas iniciamos este trabajo de investigación. El objetivo es medir los índices de confiabilidad de los edificios de concreto reforzado sometidos a fuerzas sísmicas reales con epicentro cercano, construidos sobre un suelo rígido. Existe una necesidad de valorar la certidumbre en los edificios del estado de Guerrero, debido investigaciones de geofísica que estiman un GAP de área de 220x90 km^2 que generaría un evento sísmico de magnitud Mw=8.4. Determinamos que el periodo predominante tiene un intervalo de 0.034 a 0.36 [Pérez D. and Mebarki A., 2007]. Logramos esto, con la interpretación de 3600 sismos reales de una base de datos de la SMIS, seleccionados por su gran magnitud y epicentro cercano. Donde la ordenada del espectro de respuesta del suelo debe ser mayor a la del espectro de diseño, con ello considerar a los edificios que se encuentren con mayor riesgo de daño o colapso. Tres propuestas de edificios de diferentes resistencias surgen, que son: 1. Calcular con las propiedades de los materiales del estado de Guerrero. 2. Calcular con las propiedades de la región centro del país [RCDF], como se hace actualmente y, 3. Estimar una degradación de resistencia de los edificios por los sismos sufridos en el pasado.

La capacidad de resistencia lateral del edificio se estima con dos tipos análisis, estos son: 1. Static Adaptive Pushover Analysis [DAP], con el cuál medimos el nivel de ductilidad que desarrolla el edificio, conociendo con esto, el punto de fluencia y el de capacidad última de cada edificio. 2. Incremental Dynamic Analysis [IDA], se evalúa la resistencia del edificio en la historia del tiempo, con eventos sísmicos reales escalados para conocer el momento en el cuál el valor del estado límite del edificio ha sido excedido. Se observó que los índices de confiabilidad en los edificios sujetos a fuerzas sísmicas con epicentro cercano, dependen mucho de las condiciones de suelo y la magnitud del sismo. Los efectos de sitio cambian de manera considerable cuando la magnitud del evento sísmico aumenta, lo que hace variar los índices de confiabilidad de los edificios. Esta variación le da importancia a conocer las propiedades de los materiales del estado de Guerrero, porque influyen en el periodo fundamental del edificio.

Acknowledgements

This project of doctoral thesis had the collaborations of the following Institutions:

The Sociedad Mexicana de Ingeniería Sísmica [SMIS], for the information of its data base of Strong seismic records and to share their articles published in the International Magazine on the part of their Mexican researchers.

Centro de Instrumentación y Registros Sísmicos, Asociación Civil [CIRES, A. C.], to falicitate the information of historic important happened documents in the world, especially to the responsible of diffusion Ing. Arminda Rangel, to provide the last records of earthquake with magnitude M>5.5 happened in Mexico.

The Centro Nacional de Prevención de Desastres [CENAPRED], in order to provide the information of the designing accelerations for a period of return and also some of the figures of the volcanic zone of the country, to explain the differences of the resistance of the materials that have influence in the f 'c.

The Universidad Nacional Autónoma de México [UNAM], to facilitate the information of the researches Works in the Library of Geophysical and of other researchers.

To United States Geological Survey [USGS], for their educational programs and seismic references of Earthquake Hazard Program.

The Instituto Nacional de Estadística y Geografía [INEGI], to facilitate the information on the population growth.

Ample recognitions are extended to the researcher following:

To Pr. Ahmed MEBARKI, Université Paris-Est Marne la Vallée, for the consultation of this research work, during the period 2005-2009.

To Dr. Mario Ordaz Shroeder, researcher professor of the UNAM; that facilitated to me the software that it elaborated of name: "Degtra" to process all records of real accelerations, that way also for your kindness in providing me the goods of research that he has elaborated on seismicity relative to the survey area. To facilitate references that helped this doctoral project.

I am grateful infinitely to the Dr. Stelios Antoniou and Dr. Rui Pinho. To facilitate a temporary licence to me of the software that they developed with the name of

SeismoSignal and SeismoStruct, that was vey useful to process the records of real accelerations and to make the analyses of: Static adaptive pushover analysis and Incremental Dynamic Analysis [IDA]. With which I take the analysis of structural reliability.

Dr. Luis Esteva and Dr. Orlando J. Díaz for their comments on issues and areas of the engineering that I should study to enrich the thesis work. For giving to me some articles related to this study.

To Master Anselmo Soto, for the information of your Master thesis, in the which after 20 years-old of service by two university laboratories, summarizes evidence of strength of materials used in the preparation of the mixture of the concrete for the State of Guerrero.

To Dr. Vladimir Kostoglodov, researcher professor in the area of Geophysical of the UNAM, to facilitate its works of research through the website of the UNAM, so that they serve as support for other investigations.

To Dr. Jorge Alamilla, researcher of the Instituto Mexicano del Petróleo, to facilitate simulated seismic records to me, that helped to define better the period characteristic of the ground.

To Dr. José Enrique Blanco, for providing some articles concerning the topic of study, mainly research papers published in the Journal of the Earthquake Engineering.

I thank the unswerving support of my family to base oneself on still the most adverse conditions that showed up to me during elaboration of this study.

List of Symbols

Symbol	Definition
DF	City Distrito Federal, México.(The city of the Federal District, Mexico, what in the world is know like the capital city of the country and only under the name of Mexico.)
GPS	Global Positioning System
UNAM	Universidad Nacional Autónoma de México
SAS	Sistema de Alerta Sísmica (The accelerographs Networks that it has 12 accelerograph stations at Guerrero coast, México. Seismic Alert System)
II-UNAM	Instituto de Ingeniería de la Universidad Nacional Autónoma de México
CFE	Comisión Federal de Electricidad.
CIRES, A. C.	Centro de Instrumentación y Registros Sísmicos, Asociación Civil
CICESE	Centro de Investigación Científica y de Educación de Ensenada
CENAPRED	Centro Nacional de Prevención de Desastres
USGS	United States Geological Survey Earthquake Hazard Program
INEGI	Instituto Nacional de Estadística y Geografía.
GAP	It's a Geographic region where earthquake of great magnitude have not historically happened.
SMIS	Sociedad Mexicana de Ingeniería Sísmica
EERI	Earthquake Engineering Research Institute
UAG	Universidad Autónoma de Guerrero.
**	Part of a research text of which it realizes a contribution

For a better understanding in the reading of the tables and figures, next terms of the adopted abbreviations are described.

For the abbreviations of the Buildings Reinforced Concrete, for example, 2-3.5m, we proposed:

2, 3, 4, 5 and 7	The first number means the number of Stories of the building.
-	The sign of difference, is placed as separator
3.5 ó 5	the number after the minus sign, it is the separation to axes of columns.

m	It represents the measure unit that this in meters.
T_E	It is the fundamental period of the structure
Soto A.	He is the researcher that calculation the properties mean of the materials in the State of Guerrero.
RCDF	Properties means calculated and written in the Regulation of Constructions of the Federal District, 2004, for the researchers in the capital of the country.
Degraded	Proposed degradation of the taken resistance of the previous parameter.
Ts	Fundamental period soil
Tm	Mean period
Q	Factor of seismic behavior
PGA	Peak Ground Acceleration
g	Gravity
Sa	Response pseudo-acceleration spectrum of the ground
RC	Reinforced Concrete
c	Coefficient seismic
km	kilometers
Pa	Pascal
MPa	Megapascal
kN	KiloNewton

Figures

Figure 1 Seismic wave and your amplification in the Mexico City. [8]..... 27
Figure 2 Records of Acceleration in site SCT of the city of Mexico, DF. [60] 27
Figure 3 Response spectrum of the ground Ts=2 sec for the record of acceleration in site SCT. [61] 27
Figure 4 Observed response spectrum of response by Tlalli, S. A. de C. V. [22]..... 28
Figure 5 Common damage in the non-reinforced masonry [31] 28
The distance between the epicenter and Mexico City is 591.73 kilometers. It was one of the causes for which damages were not reported in the Distrito Federal [DF], i.e. as city of Mexico. [to see Figure 6c]. 29
Figure 6 Seismic events that have caused damages in the building. [27]..... 29
Figure 7 Global Positioning System installed in Acapulco, [76] and [79]. 32
Figure 8 Observations measured by the system GPS a) Displacement of the North American Plate, displacement measured by GPS statistically until the year 1998. [34] b) Subduction displacement of the Cocos Plate, observations measured with GPS. [34]. 32
Figure 9 Guerrero GAP. [80]..... 33
Figure 10 Critical probable areas of GAP in the State of Guerrero and the distances to their most important cities and to the Mexico City. [27]..... 35
The aforementioned distance is very significant as it could cause serious damages in the capital city of the country and the most important cities of Guerrero State. 36
Figure 11 Volcanic Mexican zone. [15] 36
Figure 12 Relation between seismic magnitude and duration. [81] 39
Figure 13 Delimiting the state zone limit of failure. 44
Figure 14 Probability Density Function of load, resistance, and safety margin.[48] 45
Figure 15 Limit State Functions, a) Complete analyzed Building, b) Inertial Force of the building, c) Lateral capacity of the building, and d) Response Stress-Strain [Stress by base shear Vb vs U_{ult}] in the node of interest. 47
Figure 16 Modal Behavior of the building.[17]..... 47
Figure 17 Procedure for the proposals of preliminary design 50
Figure 18 Use of tangent stiffness in updating the loading vector. [86]..... 53
Figure 19 Shape of loading vector is updated at each analysis step.[86] 54
Figure 20 Behavior of the steel [4] 54
Figure 21 Stress-Strain model for monotonic loading unconfined and confined concrete.[[38],[40] and [75]] 55
Figure 22 Diagram of the Static Adaptive Pushover Analysis [SAPA] 56
Figure 23 Procedure of the Pushover Analysis [51]..... 57
Figure 24 Stress-Strain curve for reloading cases [75]..... 62
Figure 25 Interpretation of the IDA with the equation 2.27 by [72] 64
Figure 26 Diagram of the Incremental Dynamic Analysis [IDA] 65
Figure 27 Diagram for the Dynamic Analysis of Response to Spectrum [DARS] 66
Figure 28 Design spectra considered in the code for Guerrero State, Mexico.[55] 67
Figure 29 The proposed of buildings of study with 2, 3 and 4 stories. For these small structures, we considered two criteria of distance between columns, 3.5 m and 5 m. [20] 69
Figure 30 The propose of buildings of study of 5 and 7 stories, with one criteria of separation of column of 5 m. [20] 69
Figure 31 Stress-Strain diagram of the steel. [52] 72

Figure 32 Three-dimensional representation of a possible Joint density function f_{RS} [48]. 78
Figure 33 Seismic hazard map of Mexico[82] 80
Figure 34 Spectrum of uniforms hazard (Sa, ξ = 5% damping ratio) for two periods of return, of 100 and 500 years for the port of Acapulco, Guerrero, Mexico. [73]. 81
Figure 35 Maximum accelerations for a return period of 100 years [15]..... 81
Figure 36 Geometry of subduction in the zone of Guerrero shows that the Cocos Plate slides underneath the North American Plate. [[39], [27] and [80]] 83
Figure 37 Single-degree-freedom system and ground acceleration. 95
Figure 38 Deformation response of two SDF system with ξ = 0.05 and (a) T_E=0.77 and (b) T_E=0.36.[5]..... 96
Figure 39 All epicenters nearby to the station of the accelerographs with their Magnitude and occurrence days are presented with their date as month/day/year. [27] 98
Figure 40 Distribution of the degradation observed in plant of the buildings. 106
Figure 41 Variation in percentage among the fundamental periods of the mean resistance and a proposed of degradation. 107
Figure 42 Variation in percentage of the yield displacement with the DARS method. .. 108
Figure 43 Variation in percentage due to variables of f'_c and E_c of the RC 108
Figure 44 Variation of the lateral capacity of the maximum basal shear. 110
Figure 45 Observing the displacement of roof with the first increase in acceleration for the station PAPN of magnitude Me = 6.5. 113
Figure 46 Parameters of the soil and the buildings..... 114
Figure 47 Site effects in the station AZIH with different magnitude and distances from station to the epicenter. 115
Figure 48 Site effects with different magnitudes, distances and duration, station PAPN NW0°. 116
Figure 49 Site effects with different magnitudes, distances and duration, station PAPN NW90°. 116
Figure 50 Site effects for Ms=8.1 at different distances, direction NW90°. 117
Figure 51 Site effects for Ms=8.1 at different distances, direction NW0°. 117
Figure 52 Index of reliability of RC buildings with separation between 5 meters columns, once submitted to the force seismic action in the base with M<6.7. 119
Figure 53 Index of reliability of RC buildings with separation between 5 meters columns, once submitted to the force seismic action in the base with M<7.6. 119
Figure 54 Index of reliability of RC buildings with separation between 5 meters columns, once submitted to the force seismic action in the base with M<8.2. 120
Figure 55 Index of reliability of RC buildings with separation between 3.5 meters columns, once submitted to the force seismic action in the base with M<6.7. 121
Figure 56 Index of reliability of RC buildings with separation between 3.5 meters columns, once submitted to the force seismic action in the base with M<7.6. 121
Figure 57 Index of reliability of RC buildings with separation between 3.5 meters columns, once submitted to the force seismic action in the base with M<8.2. 122
Figure 58 Index of reliability of RC building with degradation and separation between columns of 5 meters, for the earthquake with M<6.7..... 122
Figure 59 Index of reliability of RC building with degradation and separation between columns of 5 meters, for the earthquake with M<7.6..... 123
Figure 60 Index of reliability of RC building with degradation and separation between columns of 5 meters, for the earthquake with M<8.2..... 123

Figure 61 Index of reliability of RC building with degradation and separation between columns of 3.5 meters, for the earthquake with M<6.7 124
Figure 62 Index of reliability of RC building with degradation and separation between columns of 3.5 meters, for the earthquake with M<7.6 124
Figure 63 Index of reliability of RC building with degradation and separation between columns of 3.5 meters, for the earthquake with M<8.2 125
Figure 64 Building of 2 Stories symmetric.[20] 134
Figure 65 Hypothesis of the concentrated mass, a) Two stories shear frame, b)forces acting on the two masses.[17] 134
Figure 66 Graphic representation of the frequencies of the oscillator of 1GDL that introduces in the equation 1. 143
Figure 67 Graphic of acceleration time for the algorithm development. 144
Figure 68 Algorithm for make the spectrum of response 147
Figure 69 Station accelerograph CALE with Me=Mw=7.3 a) Record Acceleration, b) Pseudo-acceleration response spectra with $\xi = 0.05$ 149
Figure 70 Station Accelerographs PAPN with Me =6.5 a) Record Acceleration b) Pseudo-acceleration response spectra with $\xi = 0.05$ 149
Figure 71 Station accelerograph BALC with Mc= 6.6 a) Record Acceleration, b) Pseudo-acceleration response spectra with $\xi = 0.05$ 150
Figure 72 Station accelerograph PAPN with Ms=7.5 a) Record Acceleration, b) Pseudo-acceleration response spectra with $\xi = 0.05$ 150
Figure 73 Station accelerograph PETA with Me=6.5 a) Record Acceleration, b) Pseudo-acceleration response spectra with $\xi = 0.05$ 150
Figure 74 Station accelerograph UNIO with Ms=8.1 a) Record Acceleration, b) Pseudo-acceleration response spectra with $\xi = 0.05$ 151
Figure 75 Station accelerograph AZIH with Ms=8.1 a) Record Acceleration, b) Pseudo-acceleration response spectra with $\xi = 0.05$ 151
Figure 76 Station accelerograph AZIH with Ms=7.5 a) Record Acceleration, b) Pseudo-acceleration response spectra with $\xi = 0.05$ 151
Figure 77 Station accelerograph VILE with Ms=8.1 a) Record Acceleration, b) Pseudo-acceleration response spectra with $\xi = 0.05$ 152

Tables

Table 1. Distances of the Gaps to the most important cities of the State of Guerrero, Mexico; and for the capital of the Country, see Figure 10. 35
Table 2. Sequence of the runs generated by the stepping algorithm 65
Table 3. Buildings proposed with the method of analysis of response to spectra with 3 criteria to study. 68
Table 4. Mean value of sampling in work for the structural elements of beam and column with f'c = 25 MPa, Meli y Mendoza(1991). 72
Table 5. Nominal value of the Studies realised by Villanueva y Meli (1984). 73
Table 6. Seismic coefficients of the Guerrero State. Survey area c= 0.44 [55] 80
Table 7. Seismic events that have killed many people [USGS, [81]]..... 85
Table 8. Seismic events that have killed many people and originated many damage. [82] 86
Table 9. Summary of the first sample with twenty real records acceleration seismic events that happened in State of Guerrero, Mexico. With the population mean $\mu \geq 150$ Gals and response of the Ground $c = (Sa, \xi = 0.05)/g$.[78] 87
Table 10. Summary of sample of seismic happened events in Guerrero State, Mexico. [78]..... 94
Table 11. Stories damaged considered for the buildings. 106
Table 12. Fundamental Period due to the properties means and degradation proposed for the buildings. 107
Table 13. Variation in the elastic state due to the properties f'_c and E_c of the RC 108
Table 14. History of the seismic events in the State of Guerrero, Mexico, in the period between September 19, 1985 until October 12, 2009.[78] 109
Table 15. Ductility developed by the proposed buildings 111
Table 16. Effects of site that change the index of reliability in the buildings. 118
Table 17. Recommended target reliability in structural Eurocode. [13] 125
Table 18. Indicative values of index target of reliability β [1] 126

Chapter 1 INTRODUCTION

1.1 Introduction

We began commenting the most important aspects that give importance to this research, for it we showed some examples observed in Mexico and others countries of the world, in which have shown up earthquakes with near epicenter. Experiences that have left damaged and collapsed buildings, with losses of human lives and materials that are directly related with the magnitude of the quake. Nowadays, this type of risk for earthquake goes in increase for the population growth that demands more housing in more and more reduced spaces, what has forced to the development of the housing in a vertical way. These needs, it has provoked modifications in the urban regulation, changes that are not accompanied with the studies of the structural behavior. So, in this chapter one, we will be describe background, the justification, objectives and the scope of research work.

In chapter 2, we propose a methodology according to a limit state function, which considers the parameters from the existing regulation. We show the specification of the parameters mean with which have been carried out the constructions and that reflects the composition of the properties of the materials from the region center of the country, and also, we present the parameters calculated in the State of Guerrero. With the about information, we compare by means of two proposals of dynamic analysis, the level of reliability for the cities located at the coastal region in the State of Guerrero.

In chapter 3, the accelerographs networks are located on hard soil, therefore, we leave of the specification of the regulation and the design spectra for this type of soil. The characteristic of subduction angle generates a response from the pseudo-acceleration spectrum of the ground, different from the other states of the country, so in this chapter we show the location of the real seismic events and their epicenter, that it will help us to determine the minimum distance and the cities in this chapter that more have been exposed to these earthquakes. With these real seismic events, we obtained in an approximate way the characteristic period of the ground T_S, very useful fact to locate to the buildings with fundamental period T_E, near to the periods of the ground T_S, at the end of this chapter introduces a parameter of the mean period of the ground Tm for (Rathje E. M. et al., 1998), in order to observe the current parameters of the regulation of the State of Guerrero.

In Chapter 4, show the results of the analytical methods proposed to the methodology established in chapter 2. At the same time we observe the studies made in the chapter 3 and, with this information. We will explain the reliability index of the buildings built on hard soil. The information thus provided, it is a first reference parameter according to the established research in the scope in this chapter one and the function of state limit from the chapter two.

Finally, in the chapter 5, we present the conclusions and some recommendations that can be continue with this proposed study.

1.2 Background

The backgrounds on researches in the State of Guerrero are scarce about the structural behavior is concerned, for it than to identify "the problem", that is say, the what? We are going to discuss the theme in the following order:

- Why we must developed research works about the structural behavior in function from the real earthquakes in the State of Guerrero, Mexico?
- Geophysics studies and seismicity
- Materials and the reason why of the differences
- Studies that have been carried out in the country and in the world on the structural behavior of seismic events with near epicenter.

1.2.1 Seismic events, that caused damage at the Mexican buildings.

There are seismic events which by caused damage from their great magnitude and epicentre near, gave as response values bigger than the limits specified in the current regulation 2004. Some of these events are:

September 19, 1985, at the City of the Federal District from now on [**DF**], Mexico: An earthquake of great magnitude Ms=8.1 was suffered whose epicenter was located in the coast of Michoacán, near the city of Caleta de Campos. This earthquake had a seismic source at a distance of 349.52 **km** as show in the Figure 6a [27] . This earthquake caused big damages to the buildings of the city of the DF, mainly due to soft soil. Located in the bed of an ancient lake now dry, that served as base to the structures. This ground is unstable and cause the amplification of the seismic wave, which amplification increase with the depth of the sediment [Figure 1].

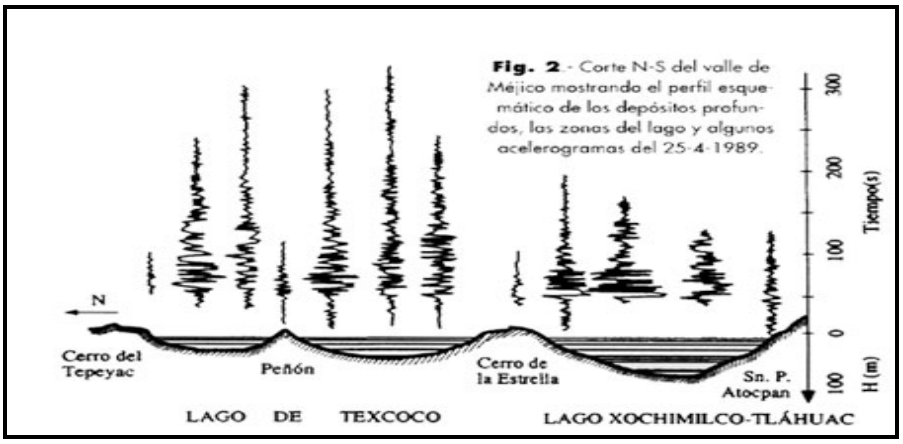

Figure 1 Seismic wave and your amplification in the Mexico City. [8]

The Figure 2 sample the acceleration in Gals of this earthquake in the place of the Secretaria de Comunicaciones y Transportes [SCT] located in downtown of DF. The characteristic response spectrum of the ground for this acceleration is shown in the Figure 3. It gives us the period of the soil [Ts].

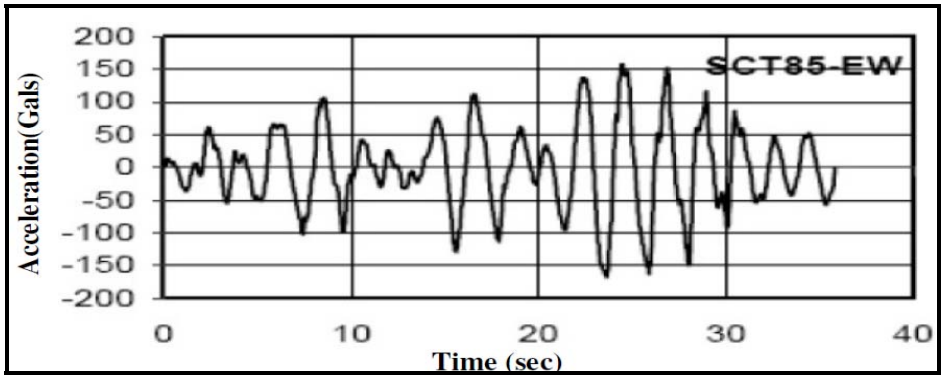

Figure 2 Records of Acceleration in site SCT of the city of Mexico, DF. [60]

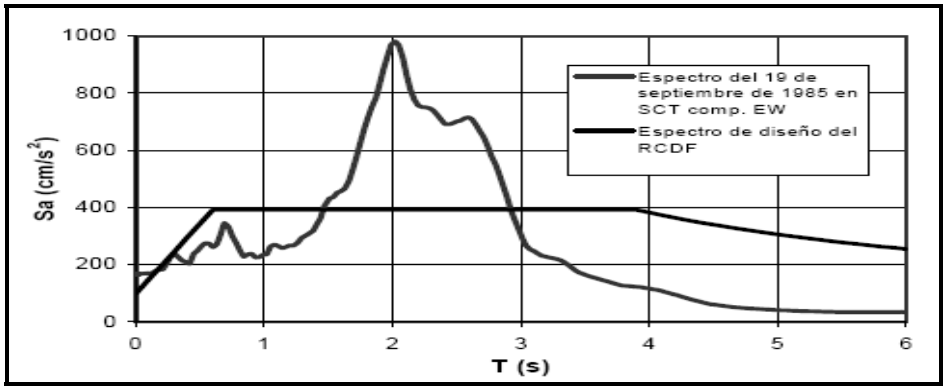

Figure 3 Response spectrum of the ground Ts=2 sec for the record of acceleration in site SCT. [61]

As complement of the Figure 3, the Figure 4 is extracted from [22]. It describes the response spectra of ground in both directions N-S and E-W for the SCT site.

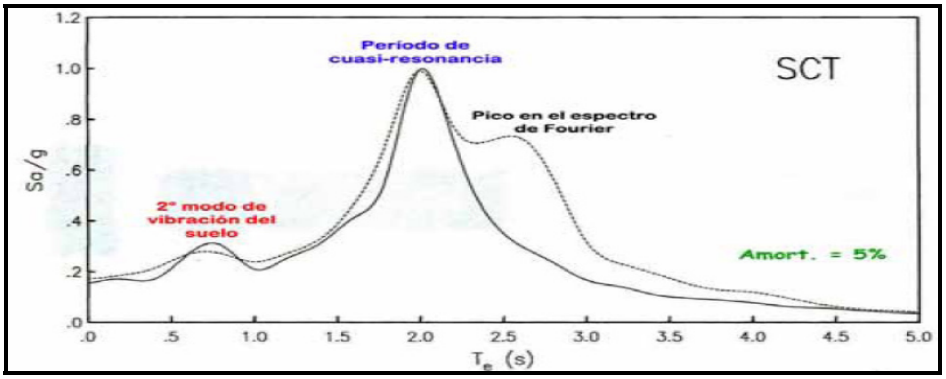

Figure 4 Observed response spectrum of response by Tlalli, S. A. de C. V. [22]

The two Figure 3 and Figure 4 show two peaks. The biggest peak corresponds to the characteristic mode of the ground and it identifies it as the resonance value.

The second peak appears in the Figure 4 as the second ground mode of vibration of the ground. This way explains the reason of buildings collapse from 7 to 15 stories that were next to the period of the ground [Ts]. They might have collapsed by the resonance phenomenon.

The earthquake of Tecomán occurred on January 21, 2003, Mw =7.8 and Ms = 7.6, had a moderate damage reported only in the locality of Colima State (To see Figure 5), and according to the site conditions in some particular zone.

Figure 5 Common damage in the non-reinforced masonry [31]

The epicenter was located at a distance of 108.41 km from the closest city of Tecomán. According to the Sociedad Mexicana de Ingeniería Sísmica [SMIS] and the Earthquake Engineering Research Institute (EERI)[31] (to see Figure 6b).

The distance between the epicenter and Mexico City is 591.73 kilometers. It was one of the causes for which damages were not reported in the Distrito Federal [DF], i.e. as city of Mexico. [to see Figure 6c].

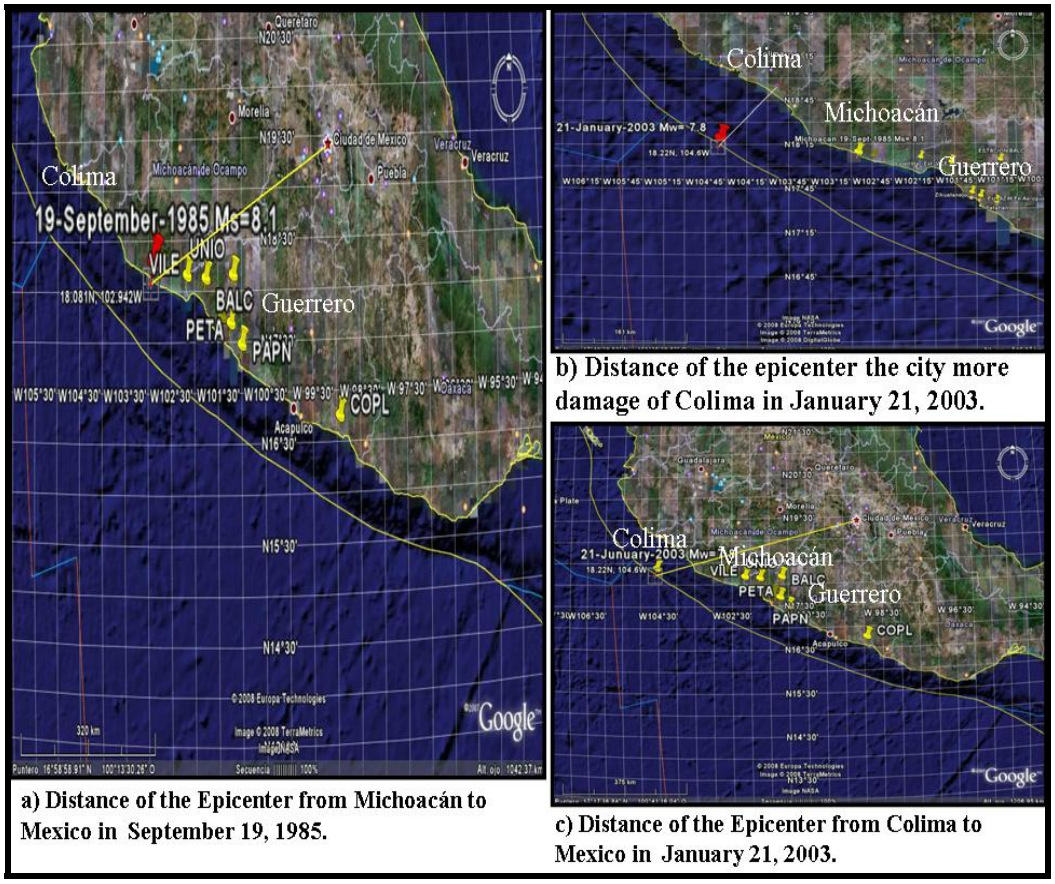

Figure 6 Seismic events that have caused damages in the building. [27]

Other damages have been reported such as stories collapses when not respecting the space of minimum separation among boundaries in the buildings, torsion, effects of shear, and so on. See to reference [Bazán E. y Meli R., 1999]

By aforementioned, all the attention has been concentrated in the GAP of Guerrero, where any seismic event, with epicenter in the coast, could cause considerable damages to constructions, due to the smaller distance to the seismic events.

After the great earthquake many researches have been devoted to improve the response from the buildings, with the aim of separating the structure period [T_E] from the

characteristic ground period [T_S]. They proposed different reinforcements, making more rigid buildings. However, the whole studies have been carried out for the city of DF in which the soil properties differ completely from the area of the coasts in Guerrero State. This State of Guerrero has been selected for an present research work.

1.2.2 Geophysics studies and of seismicity

a) Accelerographs Network

Many geophysical studies have focused on the central area of the country, because it is the city of DF, where are concentrated the biggest institutions with many technological facilities. These institutions have great financial support from the government for projects that minimize the impact of natural phenomena in the Country.

It is important to indicate that of these researches aim to measure the trajectory of the seismic wave in order to take preventive measures such as the evacuation of the buildings. Therefore, installing an Accelerographs Network; especially on the coast zone of the Pacific Ocean, near the faults of subduction in the Cocos Plate and the North American Plate. There is another Fault named: San Andreas, which is a transform fault. [See Figure 33].

These Accelerographs Networks integrated in the Centro de Instrumentación y Registros Sísmicos, A. C. [CIRES, A. C.] fulfill two purposes: first, measure the response of the ground at given magnitude of liberated energy by an earthquake on a certain region for micro-zoning studies. Second, create an alert system, (Sistema de Alerta Sísmica [SAS]) that allows the emission of an alert signal to Mexico City and other important cities. An evacuation of the population from the buildings can be done estimating this time in to approximately 60 seconds. Because the difference that exists between the speeds of propagation of the seismic waves P and S are in the order of 8 to 13 km/s and 4 to 8 km/s respectively, that characteristic depends on the medium in which travel the seismic wave [CIRES, A. C.] [77].

The [SMIS], in collaboration with other organizations in the country, such as Instituto de Ingeniería de la Universidad Nacional Autónoma de México [II-UNAM], Comisión Federal de Electricidad [CFE], [CIRES, A. C.], Centro de Investigación Científica y de Educación de Ensenada [CICESE], Fundación de Ingenieros Constructores y Asociados [Fundación ICA] and Centro Nacional de Prevención de Desastres [CENAPRED]. They

have at present a “Mexican database of strong earthquakes” with 3600 accelerations records. It includes the whole earthquakes that have occurred from 1985 to 2004. To those data of the real records of earthquake that happened in a twenty-year-old period, one may consider the database of SMIS [78]. This database has also considered for section presented later in the present research study. The data collected by this Accelerographs Networking, provided an understanding of the seismic wave amplification of the seismic wave as shown in Figure 1. The following changes were made to the regulations 2004, which are:

A practical and applicable method to estimate important aspects of seismic reliability of engineering systems have been developed. They have influenced the regulations of construction issued by the authorities in 1976, after the earthquake of September 19, 1985. The first modification made was in 1993, which presented other coefficients of seismic design [c], but they maintained the same nomenclature of specifying the soil type classified into 3 categories:

$$Type \quad soils \quad are\left\{\left[I, Hard \quad soil\right], \left[II, Transitional \quad soil\right], \left[III, Soft \quad soil\right]\right\}.$$

On the basis of the instrumentation made by researchers, and the micro zoning studies [to see Figure 1] supported by the observation of the accelerographs network.

The regulations 2004, has changed the value of the seismic coefficients:

All type of soil changed according to the response of ground that modifies every period and the way of ground vibrating for the amplification of the seismic wave. The soil that had the greatest change was the soft soil with the following subdivision: $\{IIIa, IIIb, IIIc, IIId\}$. However, these regulations allow design to enter sometimes in the inelastic range of the structures. In other words, they allow minor possible damages that can be controlled in case of moderate earthquakes, to see Figure 1.

b) Global Positioning System [GPS], Studies.

Other studies that complement the Accelerographs Network have been done with the Global Positioning System [GPS], [see Figure 7], relying on satellite information to assess the various displacements and deformations of the tectonic plates [see Figure 8 a and b].

Figure 7 Global Positioning System installed in Acapulco, [76] and [79].

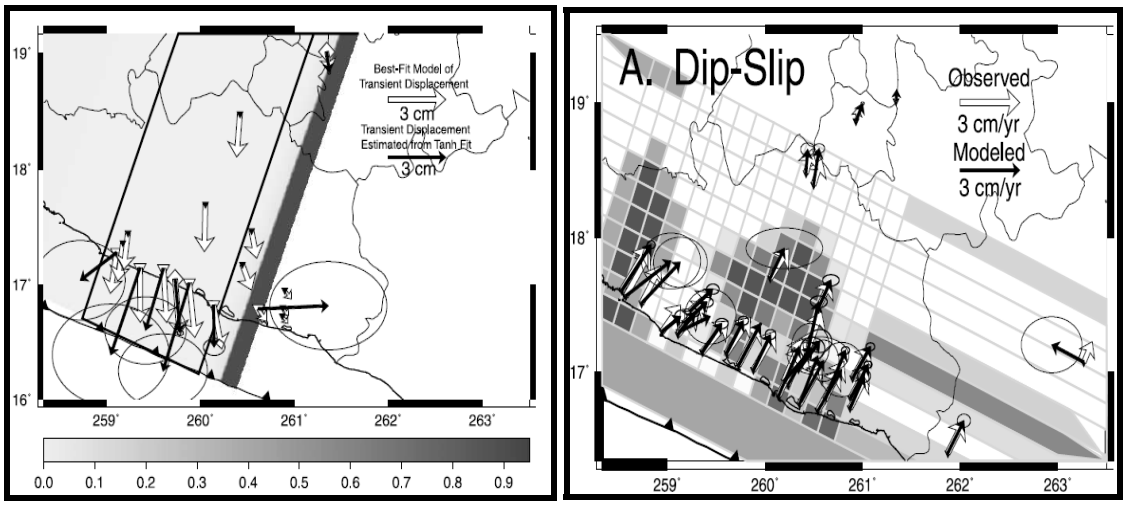

Figure 8 Observations measured by the system GPS a) Displacement of the North American Plate, displacement measured by GPS statistically until the year 1998. [34] b) Subduction displacement of the Cocos Plate, observations measured with GPS. [34].

"These observations of the displacement among the months of October (2002) and June (2003), it is estimated they liberated the equivalent of energy produced by an earthquake of magnitude Mw=7.5". Let us not forget only an estimate, in the Figure 9 are shown some seismic events in the history of the State of Guerrero that they remember our earthquakes of great magnitude that have happened.

It is not clear however, if these measured slips, they imply that only the elastic energy accumulated at the zone is liberating seismogenic, or if efforts are transferring to another connection area in the GAP. The possibility would imply the first thing that at this zone, simply do not have the potential of producing earthquakes of great magnitude. The last, it could imply the occurrence of an earthquake in the future, bigger (bigger magnitude)

than that waited, increasing the level of seismic hazard in turn specifically in Mexico City.

Singh S. K. (2009), suggested that the first possibility is not despicable, if one consider that estimates as to the location of the sequence of events at the region of Guerrero between the years 1890 and 1911, they can have imprecision's of several kilometers due to insufficiency or absence of seismic records of the time.

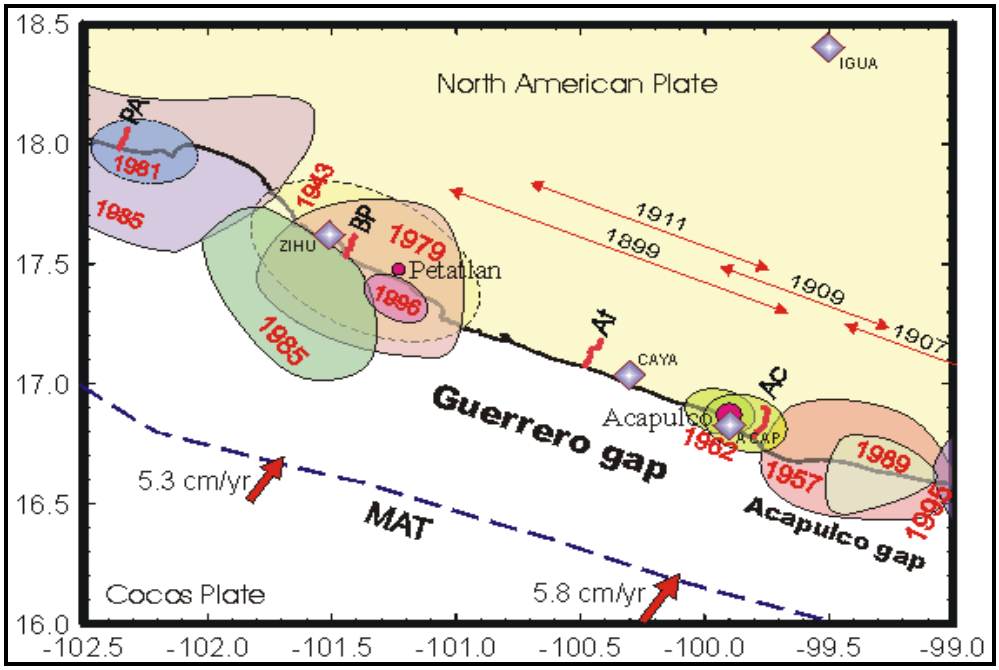

Figure 9 Guerrero GAP. [80]

On the base in the above mentioned, the different epicentral is possible to put forward a scene to the one of an earthquake that you come from the region of the Gap of Guerrero. Earthquakes coming of the seashore of Oaxaca in front of Pinotepa Nacional, where already big earthquakes have shown up in the past, or North-Western good of the coast of the State of Guerrero, close to the population of Petatlán, where there has not been a great earthquake since 1979 " CIRES, 2009,[18]"[18] .

c) Geophysical studies of GAP in the State of Guerrero.

One of the important publications in front of Guerrero States coasts, Mexico, for the information they gather from several research works is [Valdés C. and Novelo D.A., 1997]. They comment the dimensions of the GAP due to that great dimension between the

[18] CIRES, (2009), "Informe del 4 de abril de 2009", Macrosimulacro 2007, Secretaría de Protección Civil, Gobierno del DF., http://www.proteccioncivil.df.gob.mx/macrosimulacro /objetivo_macrosimulacro _3.html , comunicación personal con el investigador del Instituto de Geofísica de la UNAM, Singh S. K.

plates where the energy has not been yet liberated. For the magnitude of the earthquake, they quote the study accomplished by [Suárez G., et al., 1990], in their research, they determined that the seismogenic zone [to see Figure 36]. This area is located between 40 and 60 km., from where subduction starts.

After [Mendoza C., 1993, 1995], using teleseismic body wave and a linear finite-fault inversion scheme, he obtained for the seismogenic zone a distance that varies between 60 and 80 km, for the Zihuatanejo and Petatlan main shocks, respectively. These dimensions coincide with the rupture extent outlined by the aftershocks sequences of Figure 9.

[Valdés C. and Novelo D.A., 1997] made the summary of the points where energy has been liberated. They determine the size of the GAP, then Northwest the earthquakes of 1979 in Petatlán Ms = 7,6 and in 1985 in Zihuatanejo with Ms = 7.5. [to see Figure 9]. Then, towards the Southeast they take the study elaborated by [Nishenko S. P. and Singh S. K., 1987a] and [Nishenko S. P. and Singh S. K,1987^{b}] where they estimated for the 1907 a rupture length of approximate by 160 km extending up to 98.5°W in the Southeast. [Sing S. K and Mortera F., 1991] showed that the rupture of the 1957 earthquake did not extend up to 99°W.

[Valdés C. and Novelo D.A., 1997] suggest the coordinates 99°W and 101°W as the limit of GAP, and the maximum length of prospective rupture is estimated around 220 km, They forgot to write the coordinate of the North position, so we consider the studies by [Suárez G. et al., 1990] and [Mendoza C., 1993, 1995], where they locate the area seismogenic. This and with the help of the Figure 36, we carry out some proposals of the location from the coordinates of the north to build the Figure 10, with the help the Google Earth [27]. These coordinates are then 16° 40' N and 17°32' N.

Finally, to be able to trace this white line and to locate an area of probable rupture we have 99°W with 16° 40'N and 101°W with 17° 32' N. The distance of the oceanic trench toward inside the North American Badge un approximately 60 km is the most critical in the seismogenic area, see Figure 36b. With an area rupture is of 220 x 90 km^2. The relationship between the magnitude and the area [Singh S. K. et al., 1980] gave an expected maximum of magnitude of **Mw = 8.4**.

Therefore, the probable distances of an earthquake epicenter with great magnitude [**Mw=8.4**] to the cities the most important for the survey area, are summarized [To see Table 1 and Figure 10]. [Singh S. K. and Mortera F., 1991] proposed the case of a rupture

longitude among the coordinates from 100°W at 101°W, this would produce an earthquake of **Mw=8.1**. Then with these coordinates we propose again in [27] the coordinates of the North and we have 100°W and 16° 58'N and 101°W with 17° 32'N see Figure 36b. We have the second likely area of rupture in the GAP area that should be considered of high risk [to see yellow line of the Figure 10].

Probable **distance in kilometers** from the city to the epicenter, due to the two possible coordinates of GAP.		
City	GAP for **Mw=8.4**	GAP for **Mw=8.1**
Acapulco	18	15
Ixtapa-Zihuatanejo	59	59
Chilpancingo	67	80
Ometepec	62	170
Tierra Colorada	27	54
And for the capital of the Country, that is Mexico city, [DF]		
Mexico City, [DF]	255	262

Table 1.Distances of the Gaps to the most important cities of the State of Guerrero, Mexico; and for the capital of the Country, see Figure 10.

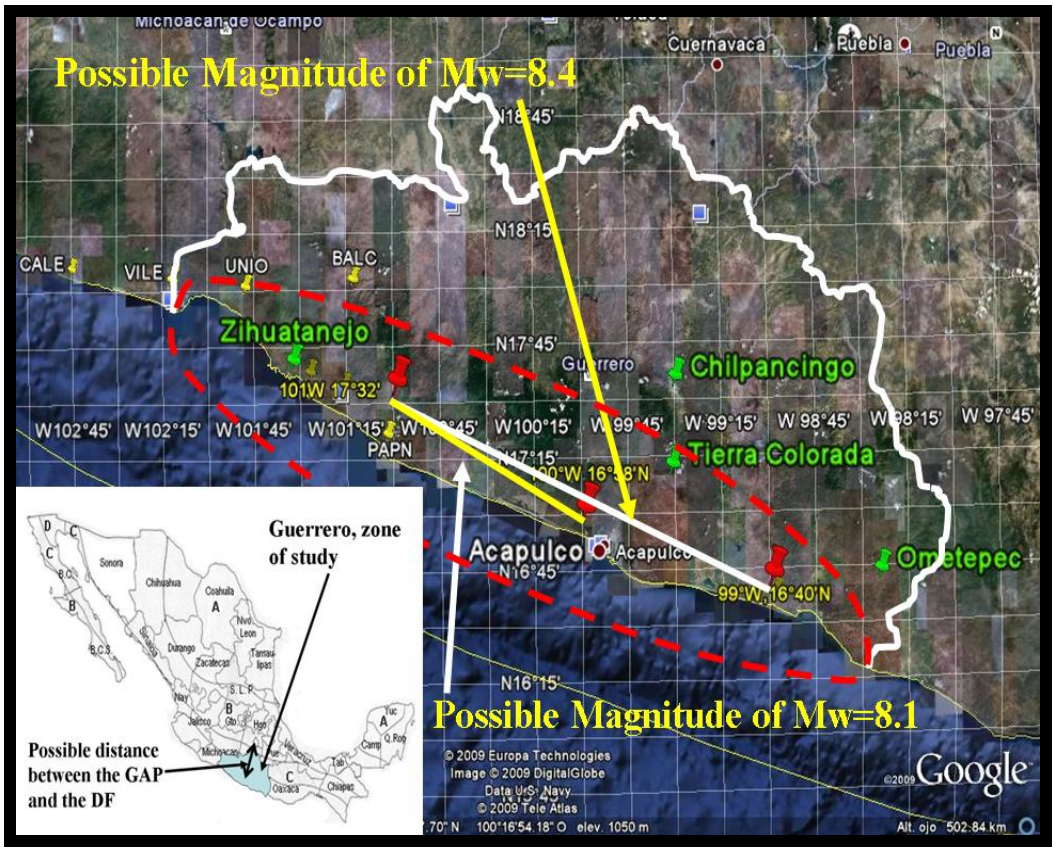

Figure 10 Critical probable areas of GAP in the State of Guerrero and the distances to their most important cities and to the Mexico City. [27]

The aforementioned distance is very significant as it could cause serious damages in the capital city of the country and the most important cities of Guerrero State.

1.2.3 Materials and local condition in Guerrero State

In the metropolitan zone of Mexico City, the regulations in the majority of the municipality, take into account the same constructions parameters than those for Mexico City. Actually the only modification concerns the seismic coefficients [c], but there is has difference in the materials and soils properties.

The cities close to Mexico City and in the same central zone of the country are located inside a volcanic zone. The resistance of the basalt rock is low, because it has higher porosity. The volcanic sand is different in its constitution, and is sometimes contaminated with clays or silt-clay soils [see Figure 11]. The materials in Guerrero coastal region, where there are no volcano, the soil are sandy and the rock is Granit, which gives bigger resistance to these materials and their mixture used reinforced concrete.

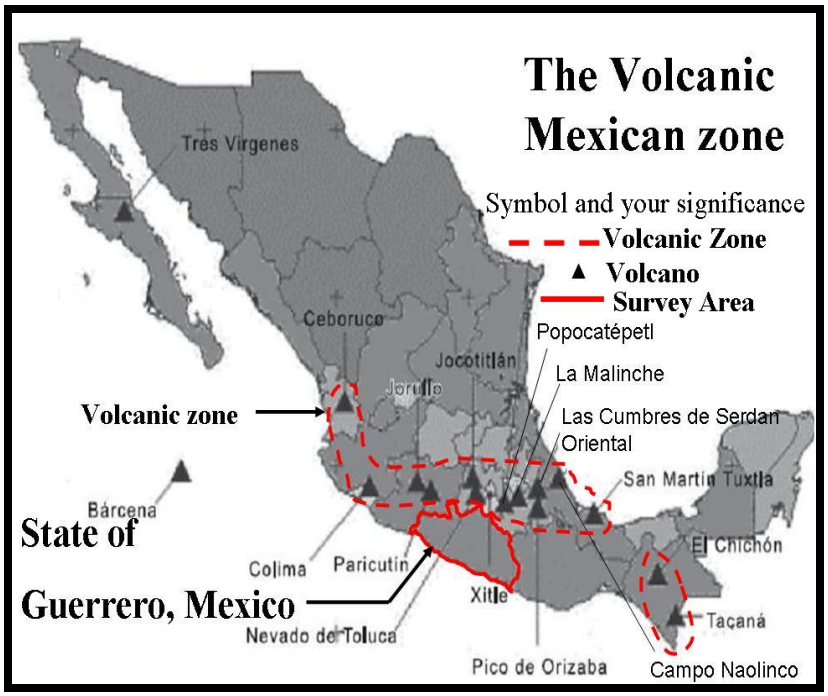

Figure 11 Volcanic Mexican zone. [15]

The Figure 11 show the located of volcano in the country it makes vary the properties of materials in order to produce the mixture of reinforced concrete and as a result the resistance.

In Chapter 2, in the topic 2.5.2, we will develop further the properties of the concrete mixture, used in the construction industry in Guerrero State.

1.2.4 Studies that have been carried out in the country and in the world on the structural behavior of seismic events with near epicenter.

In Mexico, the researches about the effects of the earthquakes on the structure have been developed in the region center of the country. The DF is a place where the expected damages to the buildings and the population are bigger. Some of the studies that deal with reliability of reinforced concrete structures, have been done [Esteva L. et al., 2000], which details the evolution of several researches.

"The estimations of failure probabilities of complex non-linear systems, have been a resource of frequency that have evolved by using the theory of random vibrations or Monte Carlo simulation, to represent stochastic processes of probabilistic prediction for seismic events, where criteria of superposition of modal responses in linear systems of various degrees of liberty are applied (Newmark and Rosenblueth, 1971; Der Kiureghian, 1981; Vanmarcke, 1976).

The government of Mexico City and the federal government of Mexico have taken strict observation of construction regulations. Because before there was little attention in the uncertainty of the properties of the structure's and the definition of failure criteria of non-linear systems of various degrees of liberty for the analysis of failure probabilities on constructions and buildings [Esteva L. et al, 1989] before any seismic action."[23]

Other studies have demonstrated that the distributions of interstorey ductility demands produced by earthquakes, in many-stories buildings, are more irregular than for continuous ductile buildings [Díaz, Mendoza and Esteva, 1994]. Because the probability of the failure depends in an important way on the number of the degrees of liberty and may vary on very broad bands for different combinations of the significant mechanic properties and their distributions of probabilities of resistance before seismic events. It is also very sensible to the irregularities on the plant and elevation of buildings, to spatial distributions of mass, rigidities and resistances, as well as the post-yield and initial rigidity"

[23] Esteva L., Díaz O., Mendoza E., Cruz O., Alamilla J. y Pérez D. (2000), "Confiabilidad de sistemas Estructurales ante sismos", Proyecto CONACYT REF 3663PA.

a) Comparative studies of the ground period T_S and the period structure T_E.

This study is an example that tries to explain the behaviour of the building when T_E approaches to T_s. A study from China based in experimental proofs [Ye Xianguo et al., 2004], considers the earthquakes of 1985 and 1995 in Mexico and the conditions of ground located in the SCT where acceleration peak in the most unfavorable location reach 0.171g and 0.032g respectively. An analytical prediction of seismic response was predicted for a real prototype of a 10 stories building. They determined that to peak ground accelerations between 0.15g and 0.4g. The building already suffers of small deformations and loss of resistance and stiffness. For the peak ground accelerations greater than to 0.4g to 0.6g, the building already suffers considerable deformations changing the structural properties as that of its fundamental period.

b) Some reliability studies

Reliability of reinforced concrete structures has been very extensively studied in the world. In the last years, with the evolution of the technology [computers, software and laboratory team for experimental tests], the reliability studied have contributed in the revisions of the current regulations. [SriVidya A. and Ranganathan R.1995]; [Cheng G., Li and Y. Cai, 1998], [Val D. et al., 1997]. One of the most innovative proposals for the structural reliability that gave birth to a well-known new methodology named Incremental Dynamic Analysis (IDA), is used for the structural revision under seismic loads and was carried out by [Vamvatsikos D. and Cornell C. A., 2002].

c) Nowadays, some researches related to reliability.

The registers have served as a basis to what the new regulations consider "the design spectrum "that contains the current regulations. They were obtained by drawing an envelope of various spectra an oscillator response with one degree of freedom [to see Figure 1]. The spectrum of response represents the values of maximum response of many oscillators characterized by their natural period of vibration and by a given damping, usually 5%. By definition, these spectra do not consider the contribution of the movement of the complete accelerogram, but rather the maximum values [Huerta B. and Reinoso E., 2002].

With the new tendencies of the design by performance, some researchers have considered necessary to observe the duration of the earthquake and the magnitude [Reinoso E. and Ordaz M., 2001]; [Hancock and Bommer, 2006]. The Figure 12 showing the relationship

between the magnitude and the duration of the earthquake is an example extracted from Lisa Wald of the U.S. Geological Survey [81].

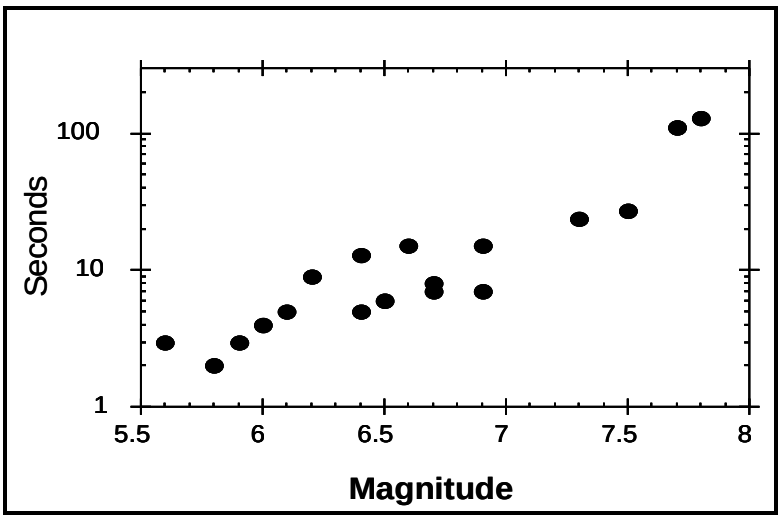

Figure 12 Relation between seismic magnitude and duration. [81]

These two variables have influence upon the behavior of the structural response. These variables, we will further discussed in the chapter 3.

The topography [Boore D., 1973], the contents of frequency and the amplification have also great influence [Boore D. and Joyner, 1997].

d) Examples of revisions to the codes by have quake near epicenter

[Pelin, et al., 2007], conducted a study on the real accelerograms registered during the seismic event of November 12, 1999, with magnitude Mw =7.2 in Duzce, Turkey. This researcher based on 301 horizontal accelerograms and attenuation laws proposes a new design spectrum that takes into account the effects of near earthquakes.

[Laouami N. et al., 2006], have also conducted a similar study for the case of Boumerdes, Algeria, as this region damage by an earthquake of magnitude Mw=6.8 on May 21, 2003. The study is based on strong motion from the 13 stations of the accelerographs Network in Algeria. A peak acceleration of 0.58 g PGA, has been registered at 20 km from the epicenter. Only close to 150 m, a PGA of 0.34g was observed from. With central frequencies about 5 Hz, this acceleration caused the collapse principally of buildings with 3 and 4 Stories.

These last two studies are the most similar to the objectives aimed by our present research of study.

1.3 Justification

The present study focuses on the search for a Reliability index of Reinforced Concrete Structures buildings erected on hard soil at nearby epicenter. Nowadays, there is a big probability of an earthquake occurrence with large magnitude it could cause a great disaster, due to the proximity of the GAP that exists in the coasts of Guerrero. As explained in the previous section. [See Figure 9, Figure 10, Figure 33, Figure 35 and Figure 36]

The Instituto Nacional de Estadística and Geografía e Informática [INEGI, 2005] presented their population census in 2005. It is true that carrying out the comparison of number of inhabitant between the Mexico City with 24.5 million and Acapulco, Guerrero, with 717,766 is a great difference in the population growth.

Nowadays, we have an estimate of over a million and half of people living in Acapulco, Guerrero. Most of the buildings are very old. There are potential seismic risk for cities such as Ixtapa-Zihuatanejo and Acapulco, which represent 70% of the economy of the Guerrero State. The population growth is so great that the buildings are developing in a vertical way, which implies modifications in the urban planning. However, the reviews of the regulations parameters have been neglected for the structural behaviour.

1.4 General Objective

"The revision of the seismic reliability of the Reinforced Concrete buildings, erected on hard soil and nearby epicenter". It considers the effective properties of the local materials in the region. As the new construction proposal developed vertically according to the urban modification and the current regulation, they present appropriate levels of safety and performance regarding a moderate earthquake as well as house adverse conditions in the coasts area of the Guerrero State, Mexico.

1.4.1 Specific Objectives

- Revise first, the parameters of reliability that set regulations for seismic design of structures type B relative to the popular house (according to topology of the regulations of the construction in the DF city and the State of Guerrero that generally follows the same nomenclature) in reinforced concrete.

- Verifying the structural behavior and their level of vulnerability by studying buildings that were projected in their skeletal form, built in a uniform way, symmetrical in plan and elevation, regular and optimal.
- Analyzing real accelerations records Mexican with near epicenter for the construction erected in Guerrero State, with the characteristic period of the ground.
- Sensitivity analysis by considering three cases and measuring the variation of the reliability index. The first of them considers buildings whit the same nomenclature of the regulations than in the region center of the country [Reglamento de Construcciones del Distrito Federal, RCDF 2004]. The second, considers the local means properties of the materials within the survey area [Soto A., 2004]. The third proposal considers preliminary degradation of the buildings and analysis their behaviour during a new seismic event.

1.5 Scope of research work

The research field is very extensive. It is however limited to design only a representative number of regular and skeletal structures in accordance with the regulations. The records accelerations with magnitudes of: Me, Mw, Mc y Ms > 6. [See the catalogue of Magnitudes seismic in the annexe 4] are carefully selected. Knowing the characteristic period of the ground response spectrum [T_S], we consider models of buildings with [T_E] that present a large risk to have a period near to the characteristic period of the ground.

For the proposition of the limit state function, we consider parameters established by regulations. The main reference is the lateral capacity displacement, besides to propose symmetric buildings and with square columns sections in order to eliminate the hypotheses of seismic torsion [Chopra A. K., 2001], [Bozzo, L . M . and Barbat A. H ., 1999], [Nowak A. S. and Collins K. V., 2000].

1.6 Summary

In this first chapter we present the background and the main scientific purposes.

The most important geophysical aspect for the selected survey area concern the existence of a GAP of area 220x90 km^2. Relaying on the relationship of [Singh S. K. et al., 1980], relating the Magnitude and the rupture area gives, one can expect a maximum magnitude of Mw=8.4 in the Guerrero State.

The housing demand is in increase and has modified the urban regulations, allowing building tall buildings in presence of high seismic hazard [see Figure 33 and Figure 36]. Therefore, the main goal of the present research deal with a single limit state function that is focuses on the lateral resistance of the building. We will evaluate the reliability index of the buildings.

Chapter 2 Theoretical approach of the Reliability and adopted methodology.

2.1 Introduction

As a mentioned in the previous chapter, the population growth has led to changes in urban planning in the various cities worldwide. It is observed that the constructions of family housing buildings are developed vertically. These types of housing modifications have not always been accompanied from studies of seismic hazard and risk. For Mexico, the earthquake occurred the September 19, 1985, caused many damages and losses of human lives. The Federal Government created institutions and gives support to universities to develop research projects, aiming to minimize the losses materials and human lives.

To analyse the reliability seismic, we begin with the definitions of reliability, subject excessively complex buildings. Furthermore, we have the need to locate the study area and to define in a simple way the scope from the limit state function according to code 2004.

First, we develop the mechanical model to evaluate the limit state function, which involves random variables, such as the resistance (R), which refers to the properties of materials. In this chapter, we discuss the materials properties and their uncertainties. We focused mainly on the concrete behavior by [Mander et al., 1988] and later modified for the concrete behavior under cyclic load by [Martinez-Rueda and Elnashai, 1997], and also the steel showing idealised elasto-plastic behavior.

For the load variable (S), this chapter considers some parameters that more affect the buildings and the uncertainties from the load earthquakes further discussed in order in the Chapter 3. Finally, we present the mathematical approach in order to evaluate the reliability index.

2.2 Reliability and Limit State Function

2.2.1 Definitions of the reliability

In agreement with Dhillon B.S.(2006), the reliability is defined as the probability that an item performs its assigned mission satisfactorily for the expected lifetime when used according to the specified mission. See also [Lemaire et al. 2005].

The structural reliability is derived from the "Safety margin" for a given limit state function, such as ultimate limit states. For instance, thinking in terms R as the capacity and S as the demand, the performance function or limit state functions can be defined for this mode of failure as [Nowak A. S. and Collins K. V. 2000].

$$E(R,S) = R - S \qquad [2.1]$$

Where: S all loads (or load effects) are represent by the variable and

R total resistance (or capacity)

Then the space of state variables is a two-dimensional space as shown in the Figure 13.

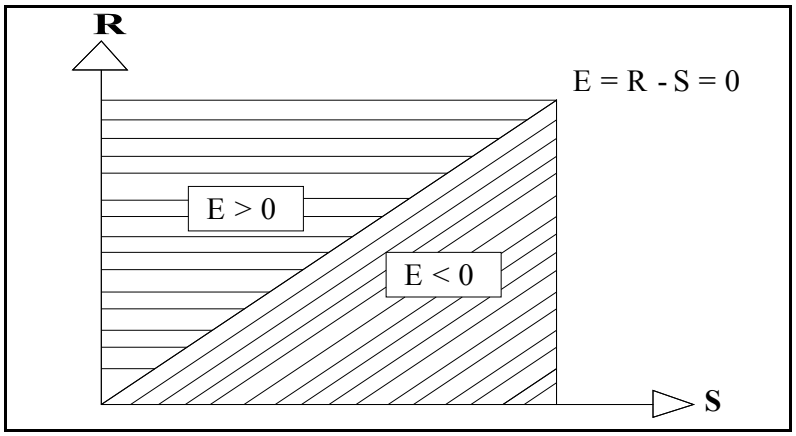

Figure 13 Delimiting the state zone limit of failure.

Within this space, we can separate the "safe domain" from the "failure domain"; the boundary between the two domains describes the limit state function $E(R,S) = 0$.

The probability of failure, Pf, is equal to the probability that an unwilled performance will occur. Mathematically, this can be expressed in terms of the performance function as:

$$Pf = \int_{E \le 0} f_{R,S}(x)dx \qquad [2.2]$$

Where:

f Risk of failure

$f_{R,S}$ Is the joint probability density function of the random variables R and S are assumed Gaussian and independent between them, see Figure 14.

E Limit State functions where: E<0 define the failure domain, see Figure 13.

In Figure 14, we can see than the probability of failure is equal to the probability that the load is greater then the resistance or $P(S > x_i)$.

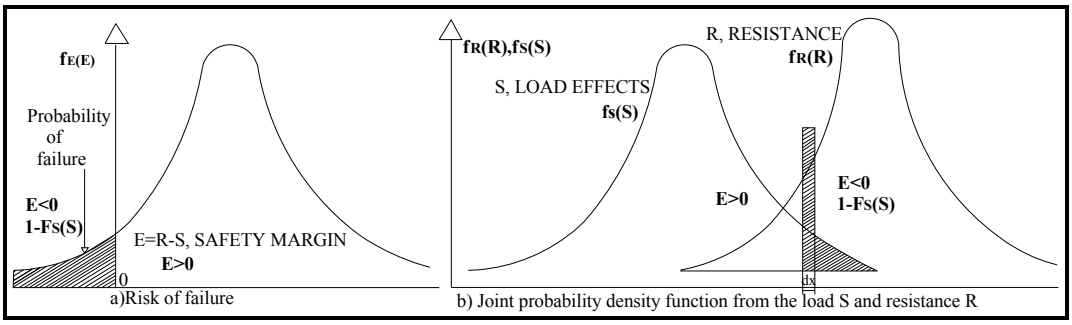

Figure 14 Probability Density Function of load, resistance, and safety margin.[48]

2.2.2 Limit State Functions, (E), general considerations

The limit state functions define a boundary between desired and undesired performance of a structure [Nowak A. S. and Collins K. V. 2000].

Several approaches exist to define a limit status function for reinforced concrete building; we can mention some Ultimate limit states.

E
- Exceeding the moment carrying capacity
- Formation of a plastic hinge
- Crushing of concrete in compression
- Shear failure
- Loss of the overall stability
- Torsion
- Buckling

There are also limit state named as Serviceability limit states. However, for the given arguments developed in the chapter 1 on the possibility of an earthquake of Mw=8.4 [Valdés C., Novelo D.A. 1997] and [Singh S. K. and Mortera F., 1991], we mainly focuse on ultimate limit state as a first step.

The state of the structure can be described using various parameters $X_1, X_2, ..., X_n,$, which are load and resistance parameters such as dead load, live load, earthquake, dimensions, compressive strength, yield strength, and moment of inertia. A limit state function, or performance function, is a function $E(X_1, X_2, ..., X_n)$ of these parameters such that:

With see $E(X_1, X_2, ..., X_n)$ in the Figure 13:

$E(X_1, X_2, ..., X_n) > 0$ for a safe structure

$E(X_1, X_2, ..., X_n) = 0$ Border or Boundary between safe and unsafe state [2.3]

$E(X_1, X_2, ..., X_n) < 0$ for failure

In seismic zones, the most frequent cause of collapse of the buildings is due to inadequate lateral load resistance of the vertical elements that support the structure [Bazán E. and Meli R. 1999].

In the present study, the reliability will concern the degree of lateral resistance for type B buildings in reinforced concrete, which correspond to popular housing designed for a period of 100 years period of return in the coast of Guerrero State, Mexico.

Therefore, for this objective, see equation 2.3, the Limit State Function for this study can expressed mathematically as

$$E[U(t)] = R(t) - S(t) = 0 \quad [2.4]$$

Where: E Limit state function

$U(t)$ is the interstorey drift due to the force for earthquake for any time t.

$R(t)$ total resistance or capacity of the structure at any time t.

$S(t)$ Load effects, but in this study the most important is due to earthquake. These values are derived from real acceleration records from the database obtained by Mexican institutions.

The probability of failure can then be expressed mathematically by:

$$Pf = P(E[U] \leq 0) \quad [2.5]$$

The procedure to calculate the Limit Status Functions is the following:

The calculated dynamic response of the building is compared to the design spectrum give by the code, see Figure 28.

This structural dynamic response provides the rules the interstorey drifts for the whole stories and also the maximum displacement observed along the whole structure (frame), see Figure 15 a, b, c.

In this study, the last resistance lateral capacity of the displacement of the building roof [to see Figure 15]. By assuming that the increases with displacement the fundamental mode T_E [Barbat A. H., 1982] and [Chopra A. K., 2001,] and that the node of interest is located in one of the control frames, an illustration is shown in Figure 15a, b and c.

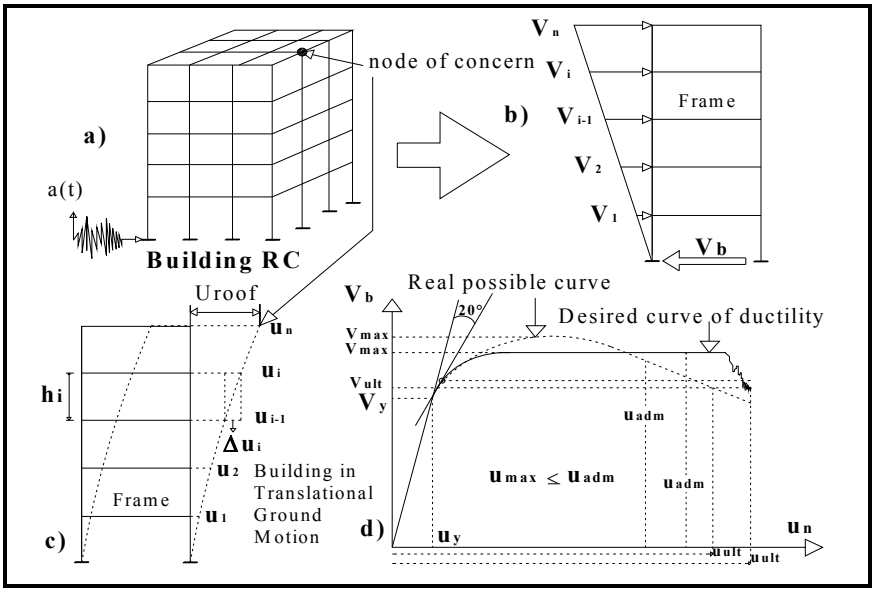

Figure 15 Limit State Functions, a) Complete analyzed Building, b) Inertial Force of the building, c) Lateral capacity of the building, and d) Response Stress-Strain [Stress by base shear Vb vs U_{ult}] in the node of interest.

For the maximum displacement

The maximum displacement for all degrees of freedom of the model can be obtained for all the modes of vibration i, these coefficients are known as "form factors", see Figure 16.

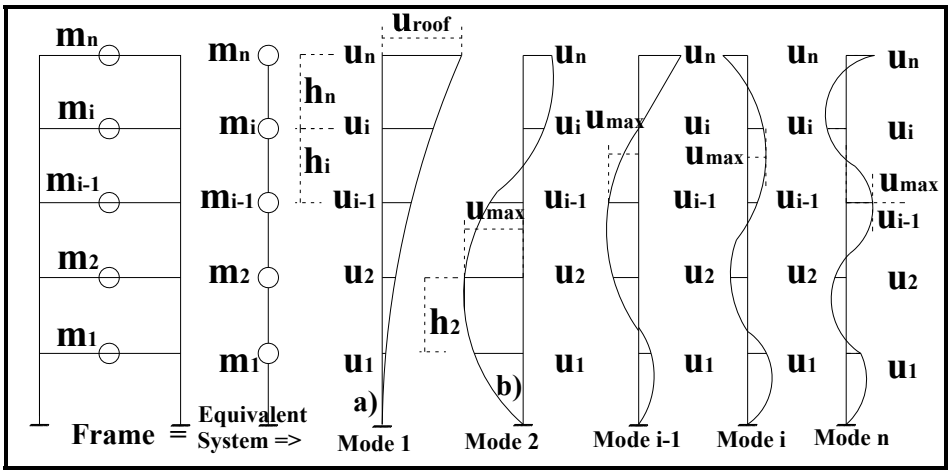

Figure 16 Modal Behavior of the building.[17]

$$U_{\max_{i\in[1\ldots n]}} = \max[u_1, u_2, \ldots, u_{i-1}, u_i, u_n] \qquad [2.6]$$

$U_{\max}$ See Figure 16, represents the maximum displacement for each eigen mode of vibration.

U_{ult} It represents to the ultimate displacement of the building, this happens when some response from the ground due to some seismic event is bigger than the design spectra, therefore, the lateral resistance capacity of the building, see Figure 15d.

Interstorey drifts or Relative displacement between stories.

An important parameters in the structural response is the relative displacement between two successive stories, see Figure 15c, also called the deviation of story. The modal value of this parameter is given by the equation:

$$\Delta U_i = \frac{u_i - u_{i-1}}{h_i} \leq 0.012 = U_{adm} \qquad [2.7]$$

u_i Displacement in the interstorey drifts i

u_{i-1} Displacement in an interstorey drifts immediate inferior of story

h_i It is storey height i.

ΔU_i Relative Displacement or interstorey drifts, see Figure 16a or b

U_{adm} It represents the displacement value than can expected in the range lineal by the building could be a combination or a Complete Quadratic Combination CQC, see Figure 16a, of the maximum displacements $U_{\max}$ in the roof building. This value, for the analysis from the code than consider the Figure 28, is in range elastic, but when we calculated with the time-history from real records acceleration, the buildings enter in the range inelastic.

These interstorey drifts are considered relative to the base of the building that also moves with the movement of soil during the earthquake.

The limit values for the displacement ΔU_{adm} in the roof [Code, 2004]

In the Figure 15d, show the relation lateral load Vb vs lateral displacement in the roof, where the largest value is denoted by ΔU_{adm}. Beyond this limit, the building value cannot

be exceeded is considered in collapse. To each seismic record, corresponds a displacement demand from code 2004, mathematically we can express as:

$$\Delta U_{adm} = \frac{U_{\max(roof)}}{h_{total}} \leq 0.012 \qquad [2.8]$$

ΔU_{adm} Permissible relative displacement in the roof that allow venturing into inelastic range, a parameter that is still considered acceptable by regulation 2004. This value, for the analysis from the code than consider the Figure 28, is in range elastic, but when we calculated with the time-history from real records acceleration, the buildings enter in the range inelastic.

h_{total} It is the height from the buildings

ΔU_{ult} This value was considered by [Vamvatsikos D. and Cornell C.A., 2002], according to FEMA, where for a change in slope of elastic stiffness from 20% defines the point the peak capacity. In addition to this parameter, we considered the elaborate studies by [Esteva et al., 2000] to know the value at which the building has collapsed. i.e. to consider Figure 15d, where we can see that change in slope occurs between the values of effort due to yield-shear Vy and the maximum shear stress Vmax for which guide lines were drawn and when observe that there is no lateral capacity load in this base shear Vb to the 20% from the change of slope, that is where we place the last deformation.

The regulations (2004), allow sometimes the use of factor for seismic behaviour Q, used to reduce the force for earthquake, this value is considered according to the characteristics of the structure, in our study we used $Q = 2$, that it considers most of the constructions of the region, then the acceptable interstorey drifts becomes expressed mathematically as:

$$\Delta U_{adm} = \frac{0.012}{Q} \qquad [2.9]$$

ΔU_{adm} Admissible interstorey drift

Q It is the factor of seismic behaviour. In this study $Q = 2$

Having defined the displacement, the limit state functions are:

$$E_1 = E\left[U_{adm}, U_{ult}\right] \qquad [2.10]$$

$$E_2 = E\left[\Delta U_{adm}, \Delta U_{ut}\right] \qquad [2.11]$$

E_1 Limit State Function that verifies the relative displacements or interstorey drifts.

E_2 Limit State Function verifies the maximum lateral displacement observed along the whole structure (i.e. roof displacement for first mode, for instance)

None of the 2 limit state should be violated. The limit state becomes then as:

$$E = E_1 \bigcup E_2 \qquad [2.12]$$

E Limit State Function that should not be exceeded in no one of the two cases.

2.3 Mechanical model

The accuracy of the results depends on how the buildings models are close to reality. The objective is to consider various existing buildings and evaluated their reliability level. The existing building are, in fact, building designed according to regulation 2004. The design is performed by the Dynamic Analyses of Response to Spectra [DARS] as shown in Figure 17.

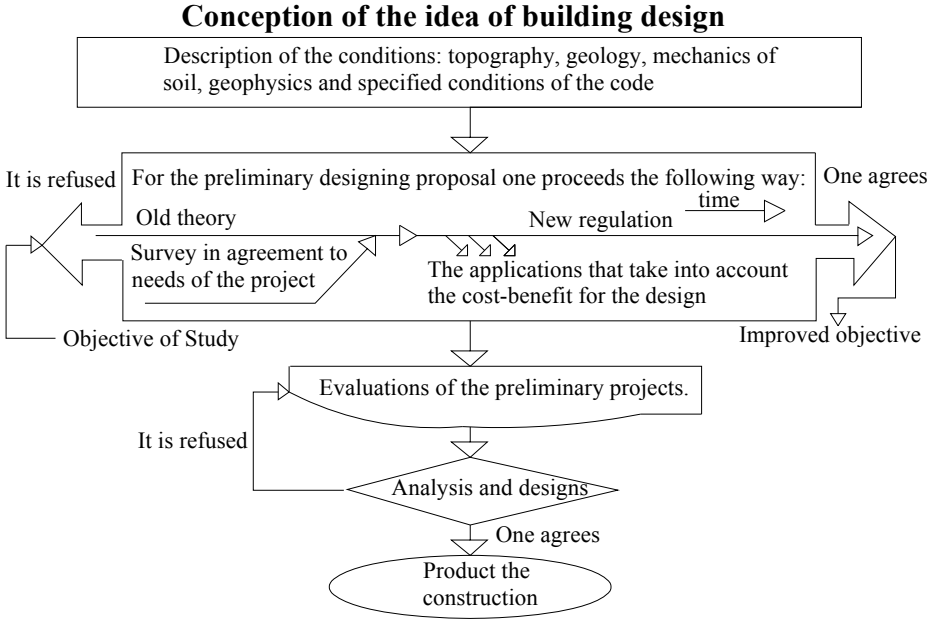

Figure 17 Procedure for the proposals of preliminary design

The analysis and design are still in the elastic range, whereas the values of displacements are close to the value of yield displacement u_y [see Figure 15d].

2.4 Analysis methods

The news Mexican regulation were afforded and published in 2004. The implicit level of safety provided by the structural design is evaluated in the present research study. This later focuses mainly on the safety to lateral load caused by the real earthquakes. The seismic coefficients are changed in the Mexico City, due to studies as Figure 1, furthermore, other parameters that help to the buildings in the development of structural behavior, because they allow higher ductility of the building. The code of the Guerrero State, follows the same nomenclature, but this is not structural behavior and micro-zoning studies. For this reason, we propose the following dynamic analysis to find the reliability index in the Guerrero State with this new code 2004, these analysis are:

- Static Adaptive Pushover Analysis, named [DAP], [Antoniou S. and Pinho R., 2004].
- Incremental Dynamic Analysis, named [IDA], [Vamvatsikos D. and Cornell C. A., 2002].

2.4.1 Static adaptive pushover analysis with the software SeismoStruct[4]

We consider "existing buildings" designed according to the regulation 2004; by the DARS analysis and design method their structural dynamic response and the whole properties of the buildings are required to the Static Adaptive Pushover Dynamic [DAP]. The dynamic analysis is performed with the software developed by [Antoniou S. and Pinho R., 2004].

This study measures the level of ductility and the lateral resistant capacity provided by the building under study.

For instance, a node of concern is proposed as shown in Figure 15d and Figure 22. In Figure 15d, shows the structural behavior obtained by this type of structural analysis. It uses basal shear [Vb] and the total displacement [U_{ult}] concerning the building.

The first version of Pushover analysis began with a proposal based on force, Bracci et al. (1997). After works, Sasaki et al. (1998), arise a great number of proposals and modifications.

[4] Antoniou S. and Pinho R., (2004), "Software SeismoStruct", Version 4.0.3 Temporary License 31/12/2009.

Main steps for the Pushover analysis:

The Pushover analysis is a conventional incremental-iterative solution of the equation of equilibrium 2.13. The iterative process continues until preset limits is reached or until the collapse is detected, see Figure 23, [Papanikolaou V. K. et al. 2005][51].

$$[K]\ \{U\} = \{P\} \qquad [2.13]$$

$[K]$ Is the nonlinear stiffness matrix

$\{U\}$ Is the vector of displacement.

$\{P\}$ Is the load vector applied laterally along the structure height with relatively small increments of load.

In our study the degree of freedom is of greatest interest is translational, i.e. lateral displacement. In stiffness for lateral displacement can be expressed by the equation 2.14:

$$K_{System} = \sum_{columns} \frac{12EI}{L} \qquad [2.14]$$

K_{system} It is the lateral stiffness of each element of the buildings.

E Is the elastic modulus, which depends on the resistance of the element.

I Is the inertia that depends on the geometry of the structural element.

L Is the length of each structural element.

Whenever we assume that, the other elements are axially rigid. As the building is assumed to be symmetrical, this eliminates the torsion in the building.

When the materials enter into their non lineal behavior domain, the global stiffness matrix is [K]; this is replaced by the tangent stiffness matrix $[K_T]$, see Figure 18 and Figure 19. The non lineal behavior of the constitutive concrete and steel is drawn in the Figure 20 and for RC Figure 21.

"To implement the Adaptive Pushover Analysis, we have a side load vector can be forces or displacement. They must necessarily be constant throughout the analysis (fixed pattern)", see Figure 18. At each end of iteration, the vector reaction $\{P_e\}$ of the structure is calculated from the whole contributions of the element [Papanikolaou V. K. et al.

[51] Papanikolaou V. K., Elnashai A. S. And Pareja J. F., (2005), "Limits of applicability of conventional and Adaptive Pushover Analysis for seismic response assessment", Mid-America Earthquake Center civil and environmental engineering Deparment University of Illinois at Urban Champaign

2005]. The forces outside of balance are iteratively re-applied under specified convergence until the expect tolerance is achieved (Bathe, 1982).

$$\Delta U = [K_T]^{-1}(\lambda * P_0 - P_e) \qquad [2.15]$$

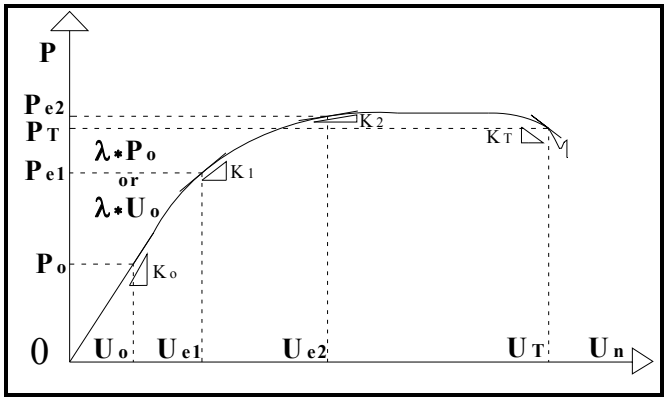

Figure 18 Use of tangent stiffness in updating the loading vector. [86]

ΔU Is the increase of displacement estimated without and iteration

K_T Is the tangent stiffness matrix [see Figure 18, Figure 19 and Figure 22]. It is changing at each step of analysis with the load vector, Figure 18.

λ Is the load factor

P_0 Is the initial load, see Figure 18, Figure 22

P_e Is the equivalent load (reaction) from the previous iteration, see Figure 18, Figure 19 and Figure 22.

To better, understand equation 2.15 we note that there is an initial load P_o, which carries a displacement value U_o. The lateral load pattern is not kept constant during the analysis but it is continuously updated, based on a combination of the instantaneous mode shapes, these mode shapes are determined by performing eigenvalue analysis [using a Lanczos eigenvalue solver] operating on the current tangente stiffness matrix $[K_T]$, K_o until $[K_T]$.[51]

$$P_e = \sum \int_V B^T * \sigma_{NL} * dV \qquad [2.16]$$

[51] Papanikolaou V. K., Elnashai A. S. And Pareja J. F., (2005), "Limits of applicability of conventional and Adaptive Pushover Analysis for seismic response assessment", Mid-America Earthquake Center civil and environmental engineering Deparment University of Illinois at Urban Champaign

B is the matrix deformation-displacement in each element. That value is updated at each step of analysis as explained above. For each increment of loading the matrix K_o is modified by the same strain of the elements [see Figure 18, Figure 19 and Figure 22]

σ_{NL} It is the vector effort of the non-linear element; see Figure 20 for the steel and the Figure 21 for the RC. As far as the load the materials lose their resistance modifying therefore the lateral stiffness matrix, which gives rise to Figure 19.

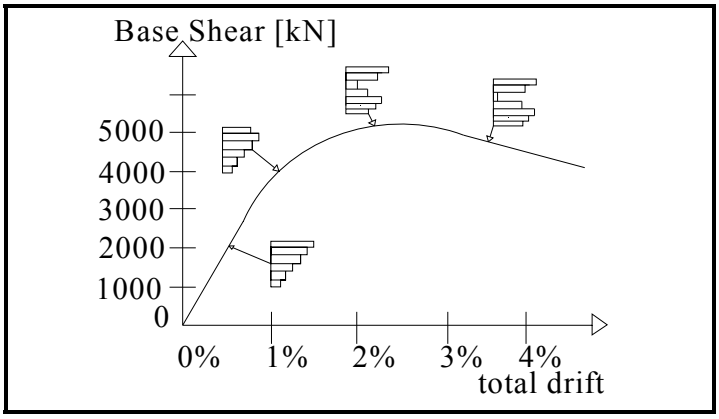

Figure 19 Shape of loading vector is updated at each analysis step.[86]

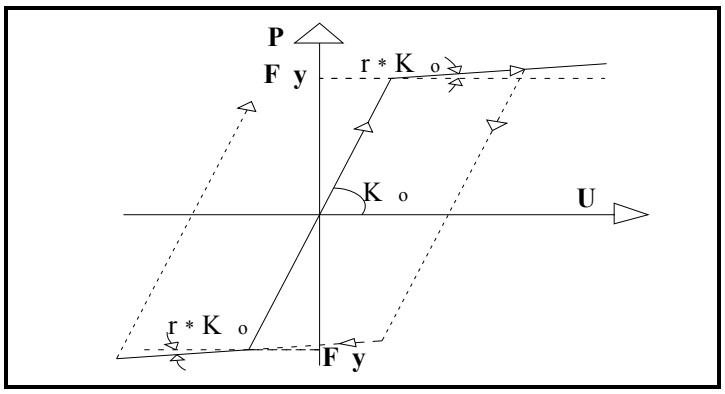

Figure 20 Behavior of the steel [4]

K_o Is the Initial stiffness

F_y Is the Yield force

r Is the Post-yield hardening ratio.

U Is the Strain

Monotonic concrete model: For a uniform confining stress, the monotonic confined compressive stress-strain curve is as show in Figure 21. It is given by [[38], [40] and [75]]:

$$fc = \frac{fcc * x * r}{r - 1 + x^r} \qquad [2.17]$$

fc Is the Compression stress

f 'cc Is the Peak of confined compression strength

f 'c Is the cylindrical compression strength in 28 days

$$\left.\begin{aligned} x &= \frac{u_c}{u_{cc}} \\ r &= \frac{E_c}{E_c - E_{\sec}} \\ E_c &= 26.28\sqrt{f_{co}} \ \text{(MPa)} \ \text{ and} \\ E_{\sec} &= \frac{fcc}{u_{cc}} \end{aligned}\right\} \qquad [2.18]$$

U_{co} Is the Strain corresponding to cylindrical compression strength in 28 days

Ec Are the tangent modules of elasticity

$E\sec$ Is the secant module of elasticity

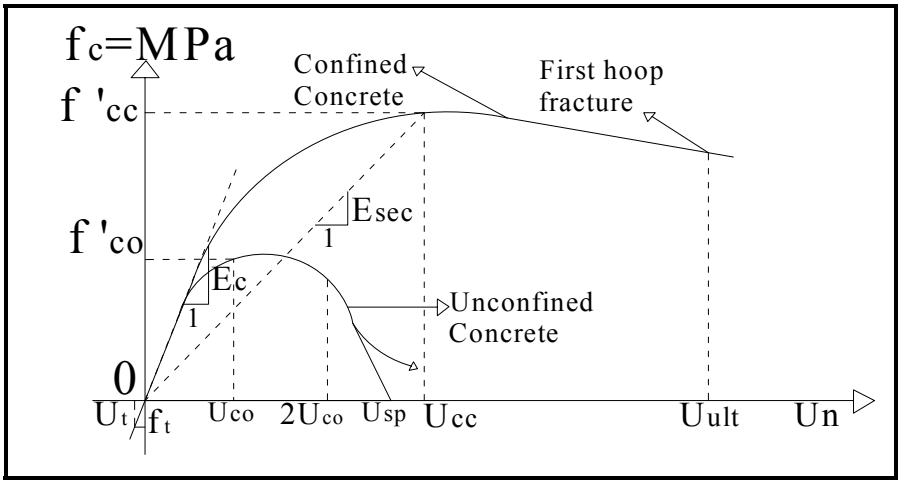

Figure 21 Stress-Strain model for monotonic loading unconfined and confined concrete.[[38],[40] and [75]]

For the unconfined areas, such as the cover of the columns:

$2u_{co}$ In descending branch after, is the concrete compressive strain in the longitudinal direction at peak unconfined stress.

u_{sp} Is defined as a straight line which reaches zero stress at the strain

For monotonic tensile loading, concrete can carry tensile stresses up to a limit, where:

ft is the stiffness equivalent to the modulus of elasticity E_c.

The tensile strength may be affected by initially micro-cracking, and will be lost at the initial stages of cyclic loading. Therefore, in the implementation of the above model the tensile strength was ignored.

The concrete behavior is represented by a nonlinear constant confinement concrete model. It is a good compromise between simplicity and accuracy. It is an uniaxial nonlinear model following the constitutive relationship proposed by (Mander et al 1988), later modified by (Martinez-Rueda and Elnashai 1997**)**. To gravitates numerical stability under large deformations. The constant confinement factor is defined as the ratio between the confined and unconfined compressive stress of the concrete.[4]

The algorithm for this calculation process is shown in the Figure 22:

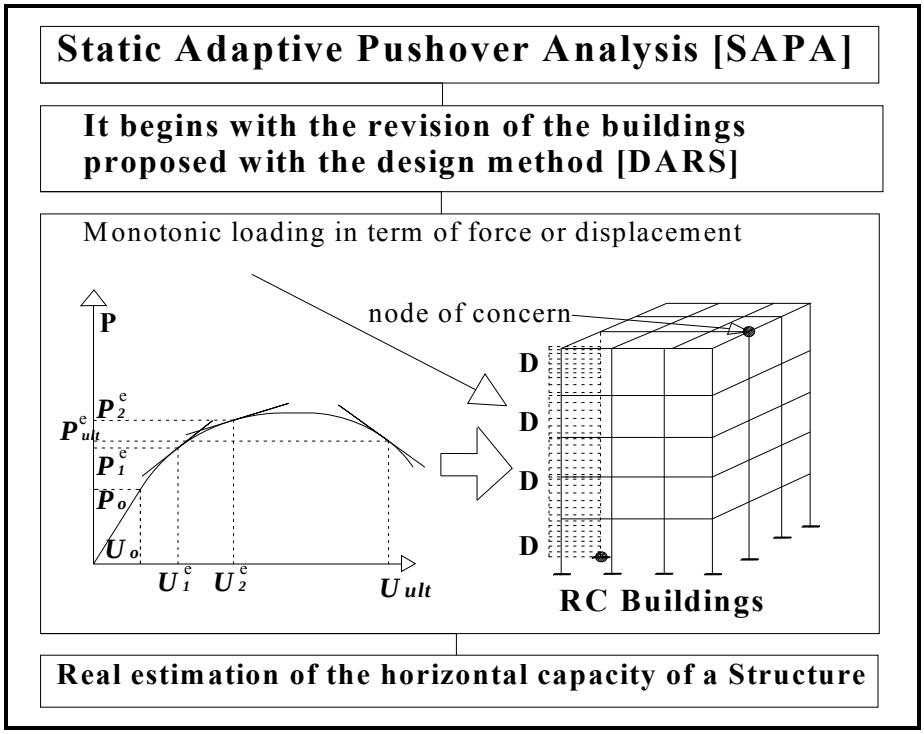

Figure 22 Diagram of the Static Adaptive Pushover Analysis [SAPA]

[4] Antoniou S. and Pinho R., (2004), "Software SeismoStruct", Version 4.0.3 Temporary License 31/12/2009.

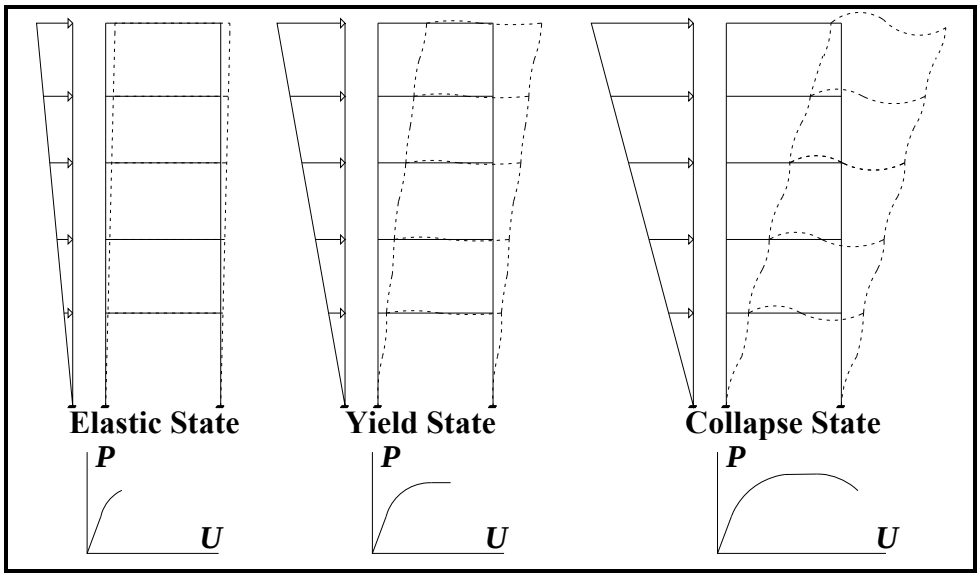

Figure 23 Procedure of the Pushover Analysis [51]

At the present time a new methodology implemented in the software SeismoStruct by Antoniou and Pinho (2004), deals with the Adaptive Static Pushover Analysis [based on the displacements (DPA)].[2]and [3]

"The implementation of this algorithm can be divided into 4 steps which are:

- *Definition of the nominal load vector and inertia mass*
- *Calculation of the load factor*
- *Calculation of normalised scaling vector*
- *Update of loading displacement vector*

The first step is performed only once and the three following are repeated until getting the equilibrium conditions of equation 2.13.

The Basic equation for the analyses DAP is:

$$U = \lambda * U_o \qquad [2.19]$$

U Iis the load vector in terms of displacement

λ *Is the load factor*

[2] Antoniou S. and Pinho R., (2004), "Development and verification of a displacement-based Adaptive Pushover procedure", Journal of Earthquake Engineering, Vol. 8, No. 4

[3] Antoniou S. and Pinho R., (2004), "Advantages and limitations of adaptive and non-adaptive force-based pushover procedures", Journal of Earthquake Engineering, Vol. 8, No. 5

U_o *Is the nominal load vector*

λ *represents the load factor, determined by means of a load control algorithm. This parameter can be introduced by the user.*

U_o *Representing the nominal load vector and we can calculate as follows:*

$\overline{D}$ *is the normalised modal scaling vector, used to determine the shape of the load vector (or load increment vector) at every step. It is computed at the start of every increment. In order for to reflect such scaling the actual stiffness state of the structure, as computed at the end of the previous load increment, an eigenvalue analysis is firstly carried out. For this propose, the Lanczos algorithm [Hughes, 1987] is employed to determine the modal shapes and participations factors of any given pre-defined number of modes.*

The eigenvalues which change the modal load for mode i, applied on the j degree of freedom, as shown in Figure 18, Figure 19 and Figure 22 are defined by equation 2.20: [Papanikolaou V. K. et al. 2005].

The modal load for mode j, applied on the k_{th} degree of freedom is defined by:

$$F_j^k = \Gamma_j * \Phi_j^k * m_k \qquad [2.20]$$

F_j^k is the element of the j-mode eigenvector, referring to the k_{th} degree of freedom

Γ_j is the modal participation factor for the j_{th} mode

m_k is the lumped mass for the k_{th} degree of freedom

$$\Gamma_j = \frac{\Phi_j * M * \delta}{\Phi_j^T * M * \Phi_j} \qquad [2.21]$$

Φ_j is the eigenvector for mode j,

M is the mass matrix and

δ is a unit vector that depends on the mass number of the system to analyze.

For the interstorey drift-based scaling technique, the eigenvectors are thus employed to determine the interstorey drift for each mode Δ_{ij}, like the next equation 2.22, Antoniou S. and Pinho R., (2004):

$$D_i = \sum_{k=1}^{i} \Delta_k \ \text{ con } \ \Delta_i = \sqrt{\sum_{j=1}^{n} \Delta_{ij}^2} = \sqrt{\sum_{j=1}^{n} \left(\Gamma_j [\phi_{i,j} - \phi_{i-1,j}]\right)^2} \qquad [2.22]$$

D_i is the displacement pattern at the i_{th} storey. It is obtained through the summation of the modal-combined interstorey drift of the storey below that level Δ_i, where we can see the mode shape, of one drift Δ_1 to Δ_i but the last interstorey drift is the Δ_n.

For example, in the Figure 16 u_i is the interstorey drift and in this section we change that variable for D_i.

Δ_{ij} Is the summation of the modal-combined of Δ_1 to Δ_i

n Is the total number of modes

$\phi_{i,j}$ Is the normalised mass mode shape value for the i_{th} storey and the j_{th} mode

$\phi_{i-1,j}$ Is the normalised mass mode shape value for the $i_{th}-1$, that is to say, the precedent storey, for the same j_{th} mode.

These will be replaced in the modal matrix Φ to calculate the equation 2.21 for the modal participation factor at the story.

Since only the relative values of storey displacement D_i are of interest in the determination of the normalised modal scaling vector $\bar{D}$, which defines the shape, not the magnitude, of the load or load increment vector (to see point 4). The displacements obtained by equation 2.22 are normalised so that the maximum displacement remains proportional to the load factor, as required within a load control framework:[2]

$$\bar{D}_i = \frac{D_i}{\max D_i} \qquad [2.23]$$

Update of loading displacement vector

The load vector should be updated at each step of analysis, at time t, for example. From Equation 2.23, the starting value was interest $\overline{D_i}$ and a storey where want to measure the displacement of interstorey drifts, for the next step of analysis at time t, the vector that is normalized load vector and its value is $\bar{D}_t$.[2]

[2] Antoniou S. and Pinho R., (2004), "Development and verification of a displacement-based Adaptive Pushover procedure", Journal of Earthquake Engineering, Vol. 8, No. 4

The load factor λ_t has been determined. Knowing the value of the initial nominal load vector Uo, the displacement vector U_t loaded on an analysis in a given analysis step t can be by the following equation:

$$U_t = \lambda_t * \bar{D}_t * Uo \qquad [2.24]$$

The main advantage of DAP hold in the fact that lateral deformations are directly determinate through modal analysis that takes into consideration the stiffness state of the structure at each step, whilst storey shear force distributions result from the requirement of structural equilibrium at each analysis step.

The profiles of DAP displacement, through carrying a permanently positive sign, do, in any case, feature changes of their respective gradient (that is, the trend with which displacement values change from one storey to the next), introduced by the contribution of higher modes.

When such gradient variations imply a reduction of the displacement of a given storey with respect to its two adjacent storey levels, then the corresponding horizontal force applied storey must also be reduced, in some cases to the extent of sign inversion.

In other words, given that in DAP, shear distributions are automatically derived by the program's solver to attain structural equilibrium at the imposed storey drift, rather than being a result of the loads directly applied to the structure. For this reason the equation 2.26, made the substitution of equation 2.21 for the parametric studies carried out by S. Antoniou and R. Pinho (2004).

2.4.2 Method of the Incremental dynamic analysis [IDA], with the software SeismoStruct[4]

[Antoniou S. and Pinho R., 2002] elaborated this algorithm in the software of SeismoStruct, with the theoretical aspects established by [Hamburger et al., 2000; Vamvatsikos and Cornell, 2002], where the structure is subject to a series of nonlinear time-history of increasing intensity. The PGA is incrementally scaled from a low elastic response value up to the attainment of a pre-defined post-yield target limit state. The peak values of base shear are then plotted against their top displacement counterpart, for each

[4] Antoniou S. and Pinho R., (2004), "Software SeismoStruct", Version 4.0.3 Temporary License 31/12/2009.

dynamic runs, giving rise to the so-called dynamic pushover or IDA envelope curves. The algorithm is shown in the Figure 26.

Next it is described in a brief way this method[72]:

The first step in this type of methodology is given in chapter 1, where there is a need to study the characteristics of Guerrero State, region in which there is a high level of seismic hazard and the existence of a GAP. Hence, one of these seismic events can exceed the considerations referred to in the regulations and cause damage and even collapse in structures. Chapter 3 will discuss more extensively the records of real acceleration to be used and the response spectra that characterize the soil. That shows the importance of implementing this analysis method which will gradually increase the maximum acceleration given in the record of acceleration [Figure 26].

The operational procedure consists in:

In our study, we have nine seismic events selected with different magnitude and they are introduced one by one for their analysis inside the software.

The first step is proposing a scale factor λ that goes multiplying the record of accelerations a_1.

$$\lambda * a_1(t) = a_\lambda(t) \qquad [2.25]$$

a_1 is the unscaled accelerogram.

λ is the scale factor.

$a_\lambda(t)$ is the scaled accelerogram.

Such an operation can also be conveniently thought of as scaling the elastic acceleration spectrum by λ or equivalently, in the Fourier domain, as scaling by λ the amplitudes across all frequencies while keeping phase information intact. Each dynamic analysis can be characterized by at least two scalars, an Intensity Measure [IM], which represents the scaling factor of the record [for example, the $\xi = 5\%$ damped spectral acceleration at the structures first-mode period $S_a(T_1,5\%)$].

Hence, we need a Damage Measure [DM], which monitors the structural response of the model (for example, maximum peak interstorey drift $U_{\max}$ or peak roof drift ratio $U_{\max}$ in

[72] Vamvatsikos D. and Cornell C. A. (2002), "Incremental Dynamic Analysis", Earthquake Engineering and Structural Dynamic, Vol. 31, No. 3, pp. 491-514.

the roof). The Damage Measure [DM] or Structural State Variable is a non-negative scalar that characterizes the additional response of the structural model under a prescribed seismic loading.

In this study, the proposed damage index is defined according to the Limit State Function. The behavior of the constitutive parameters of materials in the dynamic analysis are the same as those used in the DAP. The tests that define the material properties and their uncertainties are displayed in the item 2.5.2., see Figure 20. However, the behavior of the reinforced concrete changed, in this section, because there are load earthquakes. Then the model to be followed is the concrete model for cyclic loading. To describe a cyclic model, the unloading and reloading branches should be defined as given below.

On complete unloading.

u_{pl} The stress drops to zero, at a plastic. For strains smaller than u_{pl}, the stress is considered to be zero.

(u_{un}, f_{un}) Is the value of the plastic strain depends on the previous maximum reversal point. The unloading path is of similar form to the monotonic loading of equation 2.17, as show in the Figure 21, but is modified to pass through the point

$(u_{pl},0)$, as shown in Figure 24.

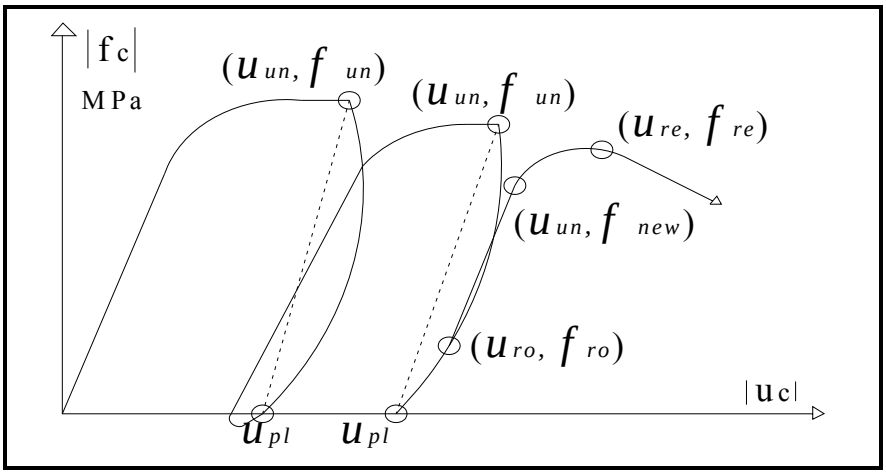

Figure 24 Stress-Strain curve for reloading cases [75]

Mander, Priestly and Park, 1988, on the basis of experimental result, have calibrated the value of initial unloading modulus of elasticity E_u.

The reloading can occur from different previous unloading history cases and hence the different possibilities ought to be considered, for this study, the theme of concern is the reloading to a strain higher than u_{un} .

u_{un} for a strain exceeding and

u_{re} up to u_{un} ,

Mander et al (1988a) suggested a parabolic transition curve between the target point (u_{un}, f_{new}) and a common return point (u_{re}, f_{re}) as shown in the next equation below:

$$u_{re} = u_{un} + \frac{f_{un} - f_{new}}{E_r\left(2 + \frac{f_{cc}}{f_{co}}\right)} \qquad [2.26]$$

u_{re} Value is obtained from equation 2.26, is evaluated by using stiffness higher than the reloading linear branch E_r .

Since the value of $(2 + f_{cc}/f_{co})$ in the denominator is at least three. This does not conform to observation from a number of cyclic experiments conducted on control cylinders.

For the purposes of this works, the value of u_{re} was obtained by dividing E_r by the parenthesis value (instead of multiplying it), and a modified parabolic transition curve has been derived on the same principles.

To derive this second order equation, the three boundary conditions used were the two end points (u_{un}, f_{new}) and (u_{re}, f_{re}) and the gradient at the first point being E_r . The modified transition curve is given by the next equation:

$$f_c = f_{re} + E_{re}x + Ax^2 \qquad [2.27]$$

Where

$$x = (u_c - u_{re})$$

$$A = \frac{(f_{new} - f_{re}) - E_{re}(u_{un} - u_{re})}{(u_{un} - u_{re})^2}$$

For strains higher than u_{re} reloading continues on the monotonic curve as shown as:

Each graph illustrates the demands imposed upon the structure by each ground motion record at different intensities. As we show up in the Figure 25, a single earthquake scaling to different intensities and each of them produces a different response in the building, as mentioned in the points above the quake scaling.

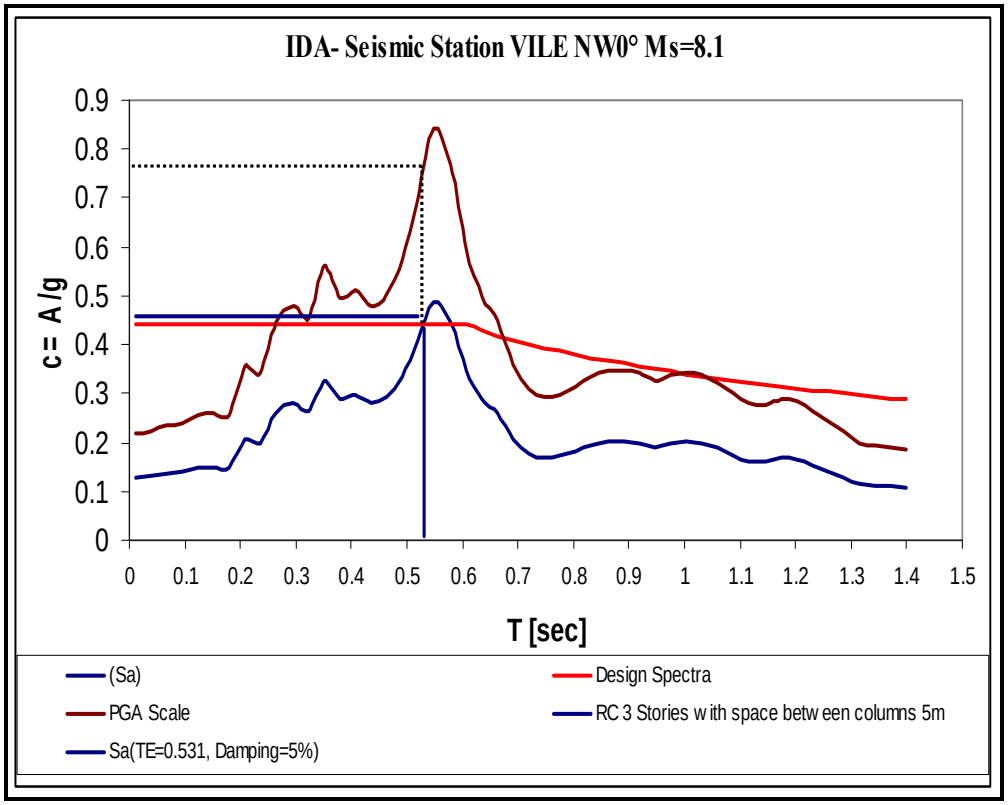

Figure 25 Interpretation of the IDA with the equation 2.27 by [72]

Therefore, for the Intensity Measure in the building of medium height (hence first-mode-dominated) the $\xi = 5\%5$ damped first-mode spectral acceleration $S_a(T_1,5\%)$ will be chosen. It has been proven to be efficient, by minimizing the scatter in the results and requiring only few ground motion records to provide good demand and capacity estimates. It provides also complete characterization of the response without the need for magnitude or source-to-site distance information [Shome and Cornell, 2002].

They consider that a sample of 10 until 20 seismic events represent a good size of the sample with a good accuracy this number will also be adopted in our present study.

Once the scale term $S_a(T_1,5\%)$ has been selected, the algorithm was configured to use an initial step of 0.1g while a maximum of 20 runs was allowed for each record. Thus, we have selected by default a resolution of 0.1g on the global collapse capacity, that is to say,

we expected the model to develop numerical non-convergence and show practically infinite interstorey drifts at some high intensity level. We also wish this level to be known within 0.1g of its IM- value. For example, we can expect one sequence of IM, as in Table 2.

Number	1	2	3	4
Sa (T1, ζ=5%)	0.1	0.2	0.3	0.4
E	0.30%	0.65%	1.15%	1.95%

Table 2. Sequence of the runs generated by the stepping algorithm

With this method, it is easy to calculate IM values for the Limit State Functions [E]. We only need to calculate all the IM that produced E. According to the E concept, we need to find the highest IM value point where the IDA reaches the interstorey drifts in the top storey until the value of E converges, see Figure 25.

With that mentioned previously about IM and DM that takes into account the of limit state function, the run for collapse is fixed on a number of runs for each record, so that IM steps incrementing to determine that the record causes the collapse of the building [see Figure 25].

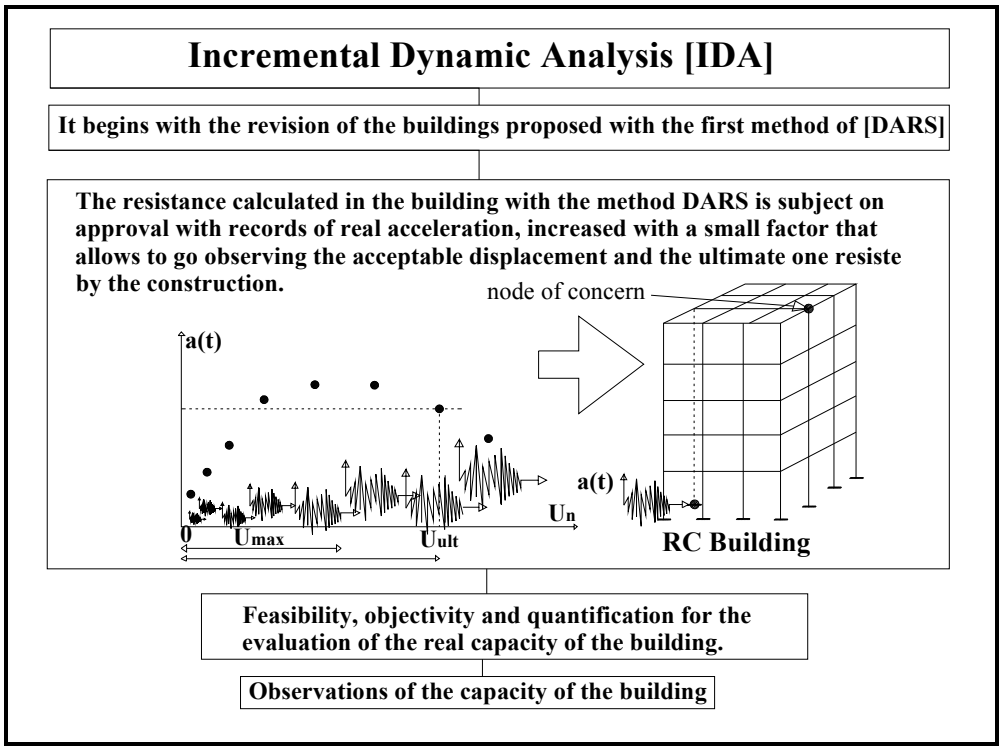

Figure 26 Diagram of the Incremental Dynamic Analysis [IDA]

2.5 Study of the buildings

The purpose of the building designed with the Dynamic Analysis of Response to Spectrum (DARS), according to the algorithm presented in the Figure 27, the procedure aims an optimization of the building design. This analysis is provided by the regulations 2004. It is mainly based on it relies on experimental studies, so that the formulas established in regulations are conservative and, safe against certain parameters (Clough R. W. and Penzien J., 1995):

See the flow chart shown in Figure 27. There are several commercial software available for the design. We used the commercial software ECOgcW [Corona G., 2004]. To perform the dynamic analysis of response to a design spectrum, described in Annex 1. It is supported by the software manuals and books (Barbat A. H., 1982) and (Bozzo L. M. and Barbat A. H., 1999). Although the information on this testing procedure can be found in various programs manuals well known to the community with expertise in the structural area, such as: SAP2000, ETABS, and so on.

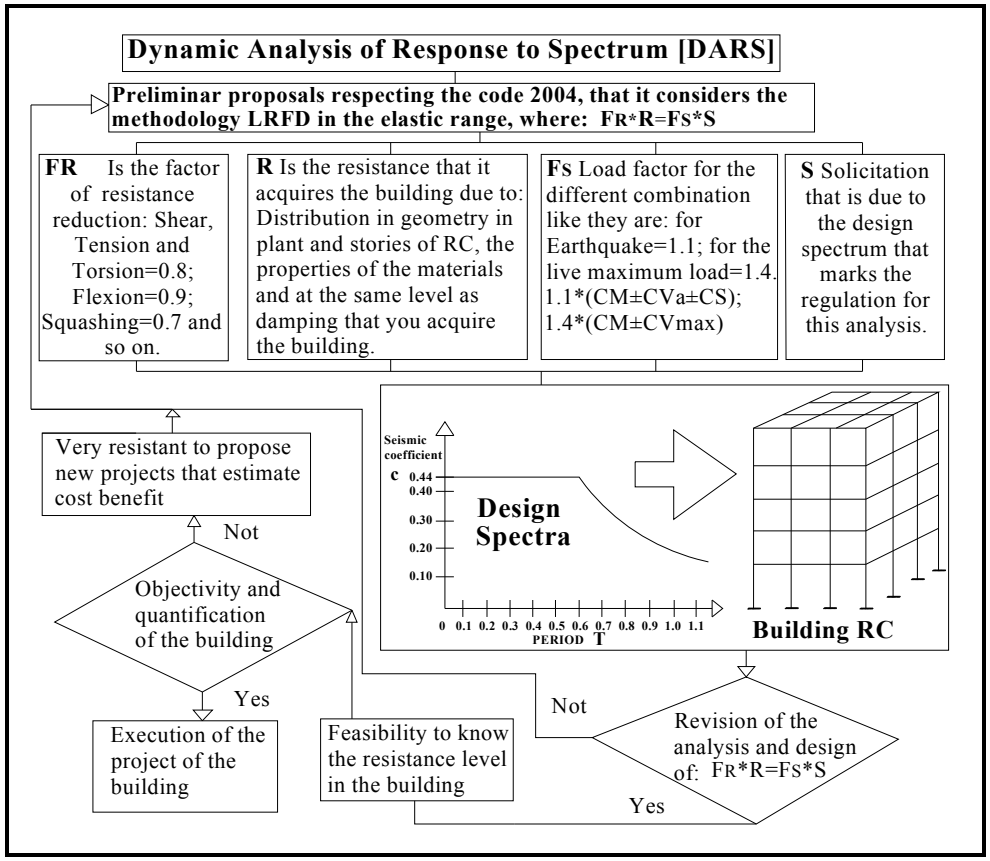

Figure 27 Diagram for the Dynamic Analysis of Response to Spectrum [DARS]

Hereafter, we discuss the general aspects of analysis and design with this software.

The design spectra [Figure 28] involve the responses of soil from seismic events until certain magnitude. In such way, the construction of buildings corresponds to reasonable price and accepts certain level of damage that can be repaired, [Clough R. W. and Penzien J., 1995], [Wilson E. L., 2002], [Huerta B. and Reinoso E., 2002], [Regulations, 2004].

The optimal analysis and design of the buildings are conducted according to the permissible limit state and the seismic force indicated by the regulation 2004, in the case of Guerrero State.

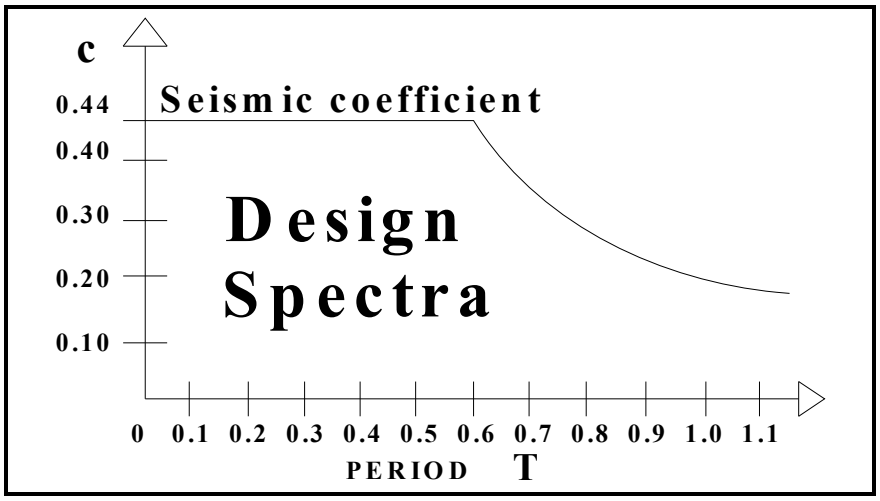

Figure 28 Design spectra considered in the code for Guerrero State, Mexico.[55]

2.5.1 Dimension of the buildings

We selected, for this study, 27 buildings. For which, we are carried out the laboratory tests on materials used in construction for Guerrero State. With the same proportions to produce concrete mixtures, the values were more resistant than those currently provided for the construction of buildings in the central region of the country. The base of the building moves as the effect of seismic force and displacement which resulting values are proportional to the strength, mass and damping of the building. The first proposal considers 9 buildings with resistances satisfy the regulation 2004 in the central region of the country.

In a second instance, another set of 9 buildings seen as structures designed and analyzed with the resistance obtained from the tests of concrete cylinders for the region of the State of Guerrero (Soto A., 2004) this will help to propose observations and recommendations

for the regulation specific of Guerrero. Adopting the suggestion made by [CENAPRED, Gutierrez C., 2004], which says that for cities in which accelerations are presented in the order of 150 Gals or bigger, it is recommended to revise the effective regulations and make proposals for the modification to those norms.

Besides these "existing structures" obtained by running DARS according to regulation 2004, we have also performed a sensitively analysis. Actually, we assumed that a seismic event has occurred has partially damage these "existing structures".

The damage is equivalent to a given loss of the elastic module. The effect on the safety index is investigated for several structures with various levels of damage.

To better, understand the structure of tables and figures; please see the list of symbols at the beginning of this work. Finally, in the Table 3 presents the summary of all the features of the buildings, i.e. dimension of the optimal size of the sections, the fundamental periods, in order to observe the resistance variation between the buildings.

Concept	Summary of the Building Design of Reinforced Concrete [DARS]							
Building RC	2 Stories		3 Stories		4 Stories		5 Stories	7 Stories
space between columns	3.5m	5m	3.5m	5m	3.5m	5m	5m	5m
Columns-Storey 1	30	30	40	40	35	35	50	45
Beams-Storey 1	20X40	20X40	20X40	20X40	20X40	20X40	25X40	30X55
Columns-Storey 2	30	30	35	35	35	35	45	45
Beams-Storey 2	20X40	20X40	20X40	20X40	20X40	20X40	25X40	30X55
Columns-Storey 3			30	30	30	30	45	45
Beams-Storey 3			20X40	20X40	20X40	20X40	25X40	30X55
Columns-Storey 4					30	30	40	40
Beams-Storey 4					20X40	20X40	25X40	25X45
Columns-Storey 5							30	40
Beams-Storey 5							25X40	25X45
Columns-Storey 6								35
Beams-Storey 6								20X40
Columns-Storey 7								35
Beams-Storey 7								20X40
Period T_E RCDF	0.307	0.441	0.360	0.531	0.524	0.773	0.850	0.876
Period T_E Soto	0.306	0.438	0.358	0.528	0.521	0.769	0.845	0.871
T_E with degradation	0.315	0.454	0.370	0.545	0.538	0.794	0.865	0.901

Table 3. Buildings proposed with the method of analysis of response to spectra with 3 criteria to study.

Rigid slabs, which give continuity in both directions of analysis and design, constitute these buildings; its form can be viewed on the skeletal Figure 29 and Figure 30.

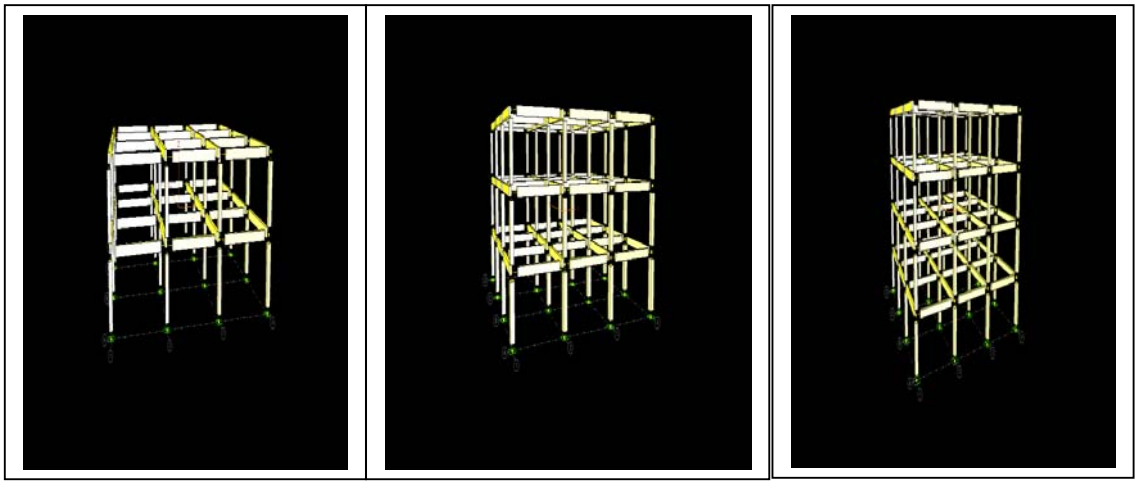

Figure 29 The proposed of buildings of study with 2, 3 and 4 stories. For these small structures, we considered two criteria of distance between columns, 3.5 m and 5 m. [20]

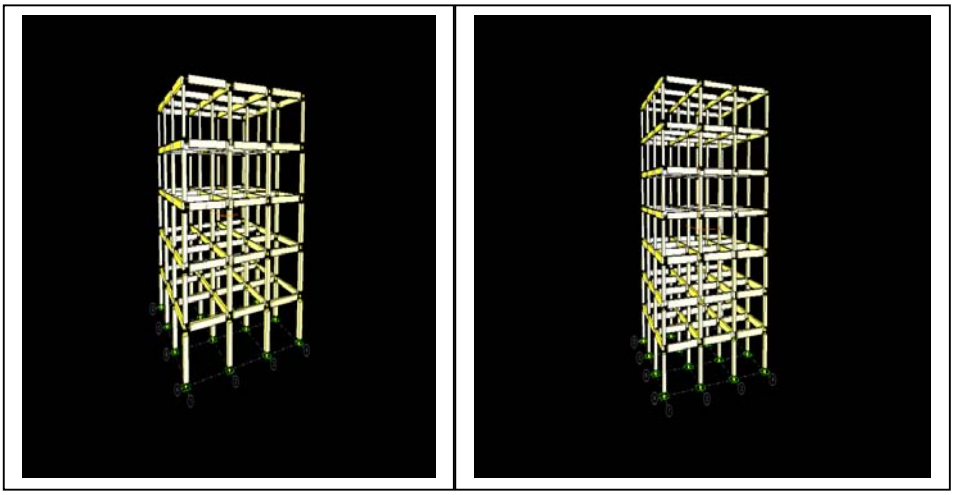

Figure 30 The propose of buildings of study of 5 and 7 stories, with one criteria of separation of column of 5 m. [20]

2.5.2 Materials used for the construction

The Laboratory tests discussed earlier that gave rise to the regulations 2004, have been calibrated to provide a structural behavior of the building made suitable for the central region of the country, as they relate to the resistance of the material in that region.

Therefore, below are the values of these experimental tests of the resistance for the local materials in Guerrero State .

2.6 Uncertainty in the Resistance of Materials

The main subject of this research is study the reliability index influence by the variations in the resistance properties. These differences were summarized after 20 years of research by Professor Anselmo Soto Garcia, who worked in the civil engineering laboratories of educational institutions that are: the UAG and the Instituto Tecnológico de Chilpancingo. He reported then in his thesis entitled "Determinación del módulo de la elasticidad del concreto simple, con resistencia f'c = 250 kg/cm^2, para el municipio de Chilpancingo de los Bravos, Guerrero". [Determination of the elasticity module of simple concrete, with strength f'c = 25MPa for the municipality of Bravos Chilpancingo, Guerrero] (for to obtain the title of Master of Science). In the various places where he analyzed different materials tests for the construction in the region, the information of the elaborated test proved that the nine areas where material is extracted presented various conditions of resistance. From this thesis we selected the representative parameters of the mean resistance values, used in the reinforced concrete elements. Thus, we compare than with those established in the regulations of construction referenced above, as is the basis for all the Mexican country.

2.6.1 Concrete compressive strength, f 'c

The variation in the properties of the concrete in great extent occurs by the difference in the proportions of the materials that compose it. Sometimes these proportions can be adequate, but environmental factors play an important role. Its mixture is also important, since the relation between water and cement, can bring about diminution or increase in the resistance of concrete. Others factors like transport, granulometry of aggregates, strained and cured, the latter depending on the used method, may influence considerably the resistance of the concrete.

Meli and Mendoza (1991) recommend a normal-type distribution function of probabilities, for the resistance to compression of the concrete, has the following statistical parameters:

for $f'_c = 25$ MPa : Mean = 26.8 MPa, Standard deviation = 4.5 MPa.

For our study, the laboratory tests are made for the capital state, which is Chilpancingo, Guerrero. It includes nine banks of materials used in the region, including the Acapulco city, Guerrero (Soto, 2004). To obtain the mean properties and their standard deviation, (Soto, 2004) like (Meli and Mendoza, 1991) used also the normal distribution function, with the same mixture considerations specified by the regulation of constructions for Mexico City, and its complementary practical standards for concrete, as the regulation of Guerrero State is identical in this aspect. For this reason, for a characteristic value of f 'c = 25 MPa; (that it is the most commonly value used in construction in the state), one obtains:

for $f'_c = 25$ MPa: Mean = 27.4 MPa, Standard deviation = 2.6 MPa.

In order to make this study, we will take into account the necessary statistical parameters for the analyses that have been applied in others researches, such as that of Meli (1976). He recommends a resistance to compression of concrete (that considers the difference that exists between the resistance of concrete in work and the one of the cylinders) proposing expressions according to the experimental study made by Petersons (1964).

We use in our study the international units and, in Table 4 and Table 5, we present the values to which make the calculation of the reliability index, for this reason we indicated in the following equations the coefficients with which we operated.

$$\text{Mean} = FC1 = 0.75FC1 + 0.03 \qquad [2.28]$$

$$\text{Standard deviation} = SFC = FC1\sqrt{CVFC1^2 + (0.1)^2} \qquad [2.29]$$

FC1 is the value mean,

SFC the Standard deviation and

CVFC1 the Coefficient of Variation.

FC1 and CVFC1 [see Table 4], [Meli and Mendoza, 1991] for f 'c ≥ 20MPa are defined by means of following expressions:

$$FC1 = f'c + 0.84SFC \qquad [2.30]$$

f ’c Specified compressive strength of concrete

$$CVFC1 = \frac{SFC}{FC1} \qquad [2.31]$$

And for f 'c =25 MPa, the sampled values in work in the cylinders of concrete are displayed in Table 4.

Concepts	Beam	Columns
FC1 =value mean	23.955 Mpa	23.1 Mpa
SFC = Standard deviation	3.84 Mpa	4.50 Mpa
CVFC1 = Coefficient of variation	0.16	0.168

Table 4. Mean value of sampling in work for the structural elements of beam and column with f'c = 25 MPa, Meli y Mendoza(1991).

2.6.2 Yield stress of Steel, f_y

In this work, the statistical parameters employed for the resistance of reinforcement steel were taken from studies made in Mexico City by Villanueva and Meli (1984). For the structural steel bars, they suggest a fluency effort nominal value equal to 420 MPa with a median value of 468 MPa and a standard deviation of 45 MPa. They also recommend that a normal-type distribution of probabilities function is employed, because the family of data adjusts to this type of distribution.

2.6.3 Parameters that define the Stress-Strain curve (fs-ε_S) of steel, proposed by Park and Paulay.

The stress curve, f_s, strain, ε_s, of steel proposed by Park and Paulay (1984) is shown in Figure 31. This curve will serve as reference to determine the resistance of beams and columns.

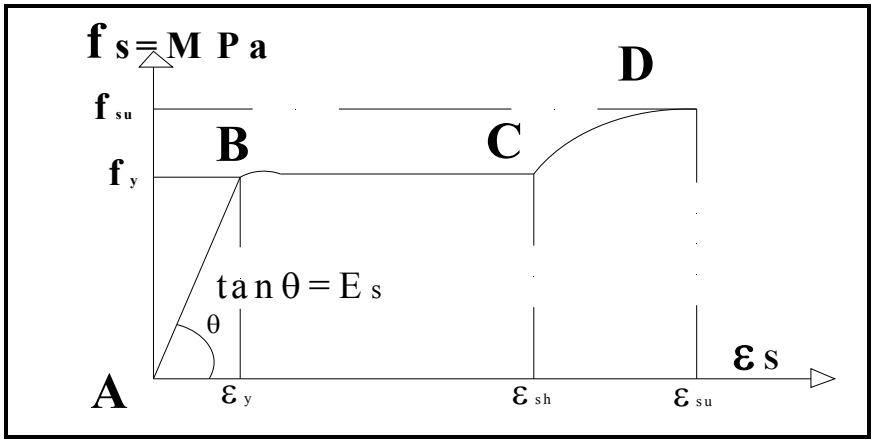

Figure 31 Stress-Strain diagram of the steel. [52]

In Figure 31 three parts are distinguished. Segment AB defines elastic interval, $\varepsilon_s<\varepsilon_y$. The used expression is:

$$f_s = \varepsilon_s E_s \qquad [2.32]$$

E_s elasticity modulus of steel equal to 2.1×10^5 MPa

ε_s unitary steel deformation

ε_y unitary yield deformation

The part BC correspond to the interval $\varepsilon_y \leq \varepsilon_s \leq \varepsilon_{sh}$, and represents the yield zone of structural steel.

$$f_s = f_y \qquad [2.33]$$

ε_{sh} unitary deformation where hardening zone begins

f_y yield stress

The part CD corresponds to the interval $\varepsilon_{sh} \leq \varepsilon_s \leq \varepsilon_{su}$ defined by

$$f_s = f_y\left[\frac{m(\varepsilon_s - \varepsilon_{sh}) + 2}{60(\varepsilon_s - \varepsilon_{sh}) + 2} + \frac{(\varepsilon_s - \varepsilon_{sh})(60 - m)}{2(30r + 1)^2}\right] \qquad [2.34]$$

$$r = \varepsilon_s - \varepsilon_{sh} \qquad [2.35]$$

$$m = \frac{(f_{su}/f_y)(30r + 1)^2 - 60r - 1}{15r^2} \qquad [2.36]$$

Villanueva and Meli (1984) find that the variables $f_{su,}$ ε_{sh}, and ε_{su} present medium values and standard deviations given in the Table 5, obtained from studies done with steel rods made in Mexico.

Concept	Nominal value	Value mean	Standard deviation
f_{su}	720 MPa	760 MPa	75 MPa
ε_{sh}	0.1	0.01175	0.0024
ε_{su}	0.13	0.1175	0.0148
fy	420 MPa	468 MPa	45 MPa
ε_y	0.002	0.00234	0.000225

Table 5. Nominal value of the Studies realised by Villanueva y Meli (1984).

2.7 Index of Reliability

Previously we defined the Limit State Functions. In this section, we develop the procedure for finding the reliability index for the buildings under study.

The random variables are supposed to be:

R Total resistance or capacity of the structure

S Load effects

According to the proposal from the limit state function, the random variables supposed to be independent are expressed as:

$$R = V_R \qquad [2.37]$$

V_R Is the resistant Shear Force

R Is the lateral load resistance that we considered in a single direction, because the building is symmetric, so we can neglect the effect of torsion. Hence, we suppose the storey rigid, and then only the movement is translational.

This random vector R is itself depending in form independent random variables:

Four variables independent that are:

$f'c$ Specified compressive concrete strength

Ec Modulus of elasticity of concrete

f_y Yield stress of steel

Es Modulus of elasticity of steel

In fact, the other geometrical parameters are supposed to be deterministic with constant value along the structural elements:

b Is the width from the structural element.

h Is the depth of the height of the element.

L Is the length of the element.

The random load variables are defined as:

$$S = CM + \left(CV_{\max} \quad or \quad CV_{inst} \right) + C_a \qquad [2.38]$$

CM The dead load depends on the material specific weight and volume of each structural element.

$CV_{\max}$ Is the maximum live load used in the combination $1.4(CM \pm CV_{\max})$ as indicated in Annex 1.

CV_{inst} Is the instantaneous live load used in the combination $1.1(CM \pm CV_{inst} \pm Ca)$ as indicated in Annex 1.

C_a It the beginning of the study, it is the load due to design spectra of the regulation 2004 of Guerrero State, México. After we perform the analysis and design, we will introduce a time-history of one real accelerogram that will be scaled to be able to know the level of structural safety of the buildings

These vectors R and S involve n random variables $X_i = (1,2,...,n)$. In a first step, assume that X_i are statistically independent, with given probability distributions. As a rough approximation, we suppose that the resulting limit state function E will follow a Gaussian distribution [Nowak A.S. and Collins K.R., 2000]

We can find that for the mean and the variance of these vectors, the mathematical expression is:

The means are:

$$\mu_R = \mu_{V_R} \qquad [2.39]$$

$$\mu_S = \mu_{CM} + \left(\mu_{CV_{\max}} \quad or \quad \mu_{CV_{inst}} \right) + \mu_{C_a} \qquad [2.40]$$

Where symbol μ signifies the value mean of the random variables defined previously.

The variances are:

$$\sigma^2{}_R = \sigma^2{}_{V_R} \qquad [2.41]$$

$$\sigma^2{}_S = \sigma^2{}_{CM} + \left(\sigma^2{}_{CV_{\max}} \quad or \quad \sigma^2{}_{CV_{inst}} \right) + \sigma^2{}_{C_a} \qquad [2.42]$$

Where symbol σ^2 signifies the variances of the random variables defined previously.

To be able to define the reliability index it is convenient to convert all random variables to their "standard form" which is a non-dimensional form of the variables. For the basic variables R and S, the standard form can be expressed as:

$$Z_R = \frac{R - \mu_R}{\sigma_R} \qquad [2.43a]$$

$$Z_S = \frac{S - \mu_S}{\sigma_S} \qquad [2.43b]$$

Where Z_R and Z_S are the variables in their "standard form". These variables are called reduced or standardized variables. Hence, rearranging the equations [2.44a and 2.44b], the resistance R and the load S can be expressed in terms of the reduced variables as follows:

$$R = \mu_R + Z_R \sigma_R \qquad [2.44a]$$

$$S = \mu_S + Z_S \sigma_S \qquad [2.44b]$$

These equations [2.44a and 2.44b] in terms of the reduced variables for the limit state function $E(R,S) = R - S$ can be expressed as:

$$E(Z_R, Z_S) = \mu_R + Z_R \sigma_R - \mu_S - Z_S \sigma_S = (\mu_R - \mu_S) + Z_R \sigma_R - Z_S \sigma_S \qquad [2.45]$$

For these equation 2.45, is for any specific value of $E(Z_R, Z_S)$ that represent a straight line in the space of reduced variables Z_R and Z_S.

When we initiated the calculation of the index of reliability, the process goes described firstly by the stage where $E(Z_R, Z_S) > 0$ in which we are still in the range of the elastic behavior, which is the process described until the moment.

When the Limit State Function begins to intrude in the inelastic range, the Limit State Function changes to be a nonlinear function, then the procedure to find the value in which the building arrives to the collapse is as follows:

We can obtain an approximate answer by linearization the nonlinear function using a Taylor series expansion.

Once the function has been transformed in terms of the Limit State Function, the mathematical expression in terms of Taylor series is as:

$$E(X_1, X_2, ..., X_n) \approx E(x_1^*, x_2^*, ..., x_n^*) + \sum_{i=1}^{n} (X_i - x_i^*) \frac{\partial E}{\partial X_i}\bigg|_{evaluated \ \ at (x_1^*, x_2^*, ..., x_n^*)} \quad [2.46]$$

Where

$E(X_1, X_2, ..., X_3)$ Is the expected mean value of the random variables to define the Limit State Function.

X_i Is the terms of random variables uncorrelated integrated.

$(x_1^*, x_2^*, ..., x_n^*)$ Is the point about which the expansion is performed.

$\sum_{i=1}^{n} (X_i - x_n^*) \frac{\partial E}{\partial X_i}$ Is the partial derivative of the mean value with respect to the random variable that produces a value to the point about which the expansion is performed.

One choice for this linearization point is the point corresponding to the mean value of the random variables. Then the last equation 2.46 gives the follow results:

$$E(X_1, X_2, ..., X_n) \approx E(\mu x_1, \mu x_2, ..., \mu x_n) + \sum_{i=1}^{n} (X_i - \mu x_i) \frac{\partial E}{\partial X_i}\bigg|_{evaluated \ \ at \ \ mean \ \ values} \quad [2.47]$$

Since equation 2.47 is a linear function of the X_i variables, it can be rewritten to look exactly like the next equation than is considered as linear limit state function:

$$E(X_1, X_2, ..., X_n) = a_0 + a_1 X_1 + a_2 X_2 + ... + a_n X_n = a_0 + \sum_{i=1}^{n} a_i X_i \quad [2.48]$$

Where:

a_i terms $(i = 0,1,2,...,n)$ are values constants

X_i is the terms of random variables uncorrelated.

Then we can obtain the reliability index β as:

$$\beta = \frac{E(\mu x_1, \mu x_2, ..., \mu x_n)}{\sqrt{\sum_{i=1}^{n} (a_i \sigma x_i)^2}} \quad [2.49]$$

Where

$E(\mu x_1, \mu x_2, ..., \mu x_3)$ It is the mean value of limit state function evaluated at the means values for the whole random variables.

$a_i = \left.\frac{\partial E}{\partial X_i}\right|_{evaluated\ \ at\ \ mean\ \ values}$ Is the partial derivative of the limit state function with respect to the random variable that produces a constant value.

X_i It is the deviation standard of the random variable

And the probability of failure as:

$$Pf = \int_{E \le 0} fX(x)dx = P(E \le 0) = \Phi(-\beta) \qquad [2.50]$$

Where $\Phi(-\beta) =$ cumulative distribution function of the standardized Gaussian distribution

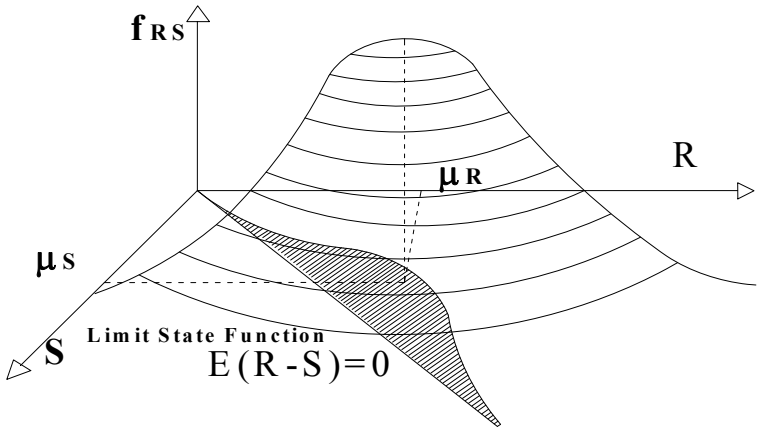

Figure 32 Three-dimensional representation of a possible Joint density function f_{RS} [48].

2.8 Summary

This chapter founds the background information to evaluate the reliability of Reinforced Concrete (RC) buildings against damage by excessive lateral in plane seismic loading: A set of RC buildings is designed according to regulation 2004. They are erected in the Guerrero State with local materials and near source events, the distribution of the materials to the local site. Two dynamics analysis are present in order to evaluate the structural response. 1. Static Adaptive Pushover Analysis [DAP] and 2. Incremental Dynamic Analysis [IDA].

The safety index is calculated is calculating under hypothesis of random independent variables: materials dimensions and load.

Chapter 3 Seismic Excitation

3.1 Introduction

In this chapter we describe the earthquake origin is the Guerrero State. The characteristics of subduction are described as well as the location of the epicenters that are selected for this study. According to the parameters established by [CENAPRED, Gutierrez C., 2004], which define the level of seismic hazard in the area and establish a value of PGA, with the real records acceleration, we calculate the characteristic from the ground such as: period of vibration.

For the selection of real records acceleration, corresponding to spectrum of the ground pseudo-acceleration response greater than the seismic design spectra regulation 2004, as shown in Figure 3.

It is very important to locate the geometry of subduction and the seismogenic zone, that affect the area selected for our study. In chapter 1, we located, the probable distance from a near epicenters to the most important cities in the Guerrero State, which may be affected by an earthquake of great magnitude.

3.2 Origin of the earthquake in Mexico

3.2.1 Geological faults

In the country, there are two regions of high seismic hazard indicated by the letter D, see Figure 33, due to two types of fault in the tectonics plates. The first is the transform fault, caused by the San Andres fault that begins in San Andres in the USA and ends in the North part of the country between the States of Baja California North and Sonora.

The other fault is due to the subduction of the Cocos plate under the North American plate in the Pacific coast. These concern us, because we located the coast of the Guerrero State like our survey area.

The information used in this study is the real acceleration records obtained from 1985 to date [SMIS], and the studies prepared by researchers in Geophysics from the UNAM. They have identified a subduction angle of approximately 10° degrees. So, the hypocenters of the earthquakes have a depth withen 14 to 18 kilometers, with the exception of a seismic event, which had a depth of 55 kilometers.

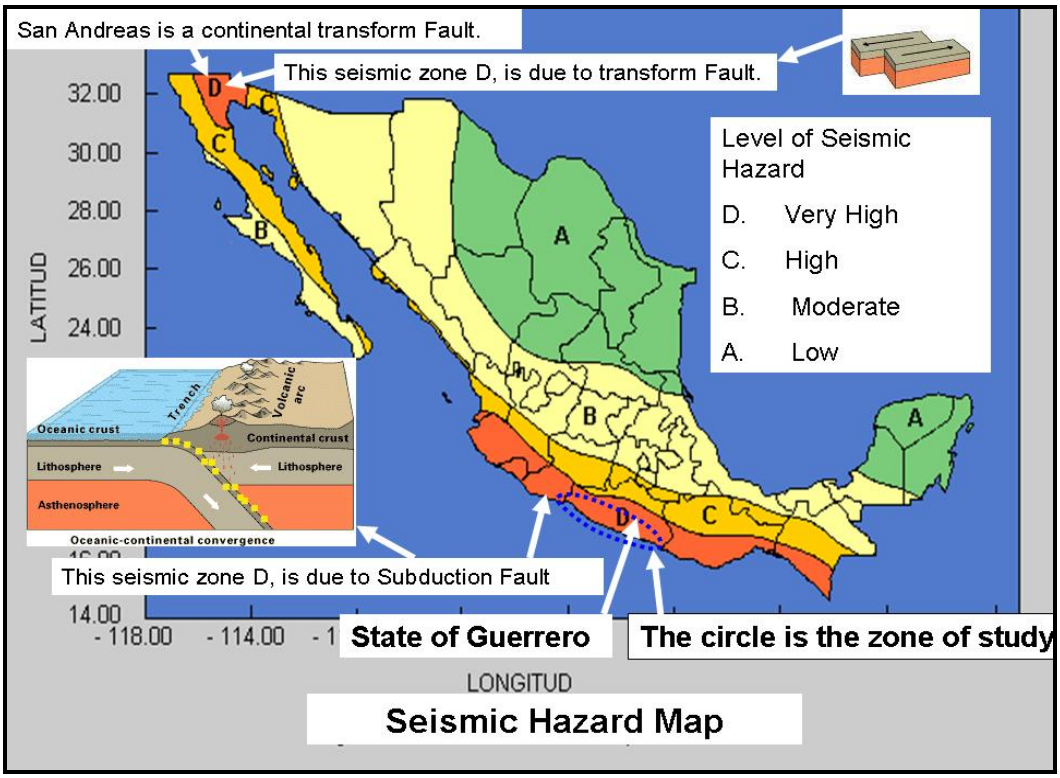

Figure 33 Seismic hazard map of Mexico[82]

According to the regional seismic hazard, the seismic coefficients are presented in the following Table 6, from the article 206 of the building regulations for the state of Guerrero, for the constructions type B of popular housing. With these values of the seismic coefficient, the design spectra are built as illustrated in Figure 28, which are used to carry out the Dynamic Analysis of Response to Spectra.

Seismic zone	Type of soil	Seismic coefficients c = A/g
D	I [Hard] Survey area	0.44
	II [Shallow intermediate]	0.86
	III [Soft]	1.08

Table 6.Seismic coefficients of the Guerrero State. Survey area c= 0.44 [55]

3.2.2 Researches on Peak Ground Acceleration [PGA], into survey area.

The work done by many researchers in the study area are used as a basis for this thesis project. For instance from the research of [Veras L. and Ordaz M., 2004], we consider the uniform hazard spectrum [Figure 34] where the accelerations are shown for two typical return periods for the city of Acapulco, Guerrero. These values are Tr =500 and Tr = 100 years.

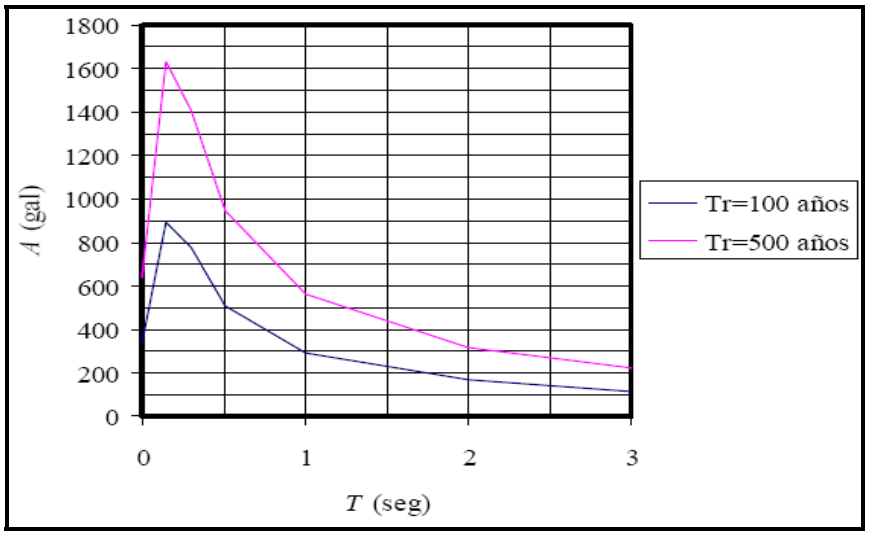

Figure 34 Spectrum of uniforms hazard (Sa, $\xi = 5\%$ damping ratio) for two periods of return, of 100 and 500 years for the port of Acapulco, Guerrero, Mexico. [73].

In the aforementioned, from a total of 3600 registries of accelerations that has the SMIS [78], only 20 registries of real accelerations will be taken into account, among those that did not fulfil the design acceleration for a period of return of 100 years. This reference, is the basic information of several researches which resulted in the report [CENAPRED, Gutiérrez C., 2004, see Figure 35].

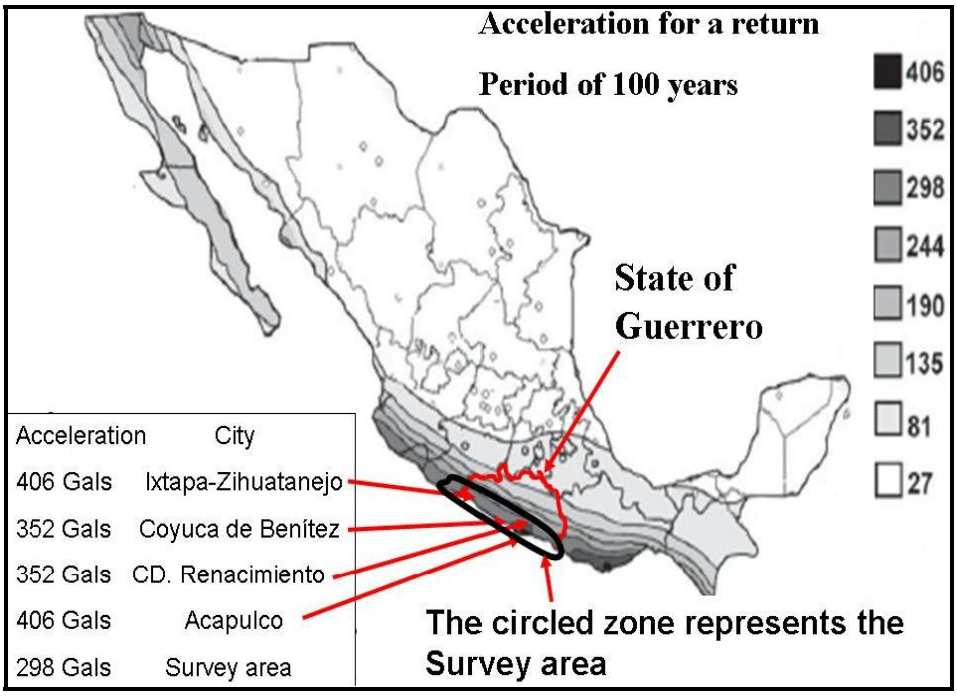

Figure 35 Maximum accelerations for a return period of 100 years [15].

For the zone selected for this study, the values of acceleration to consider are: of 298 Gals for almost all of the state, for a return period of 100 years. But for cities like Acapulco and Ixtapa-Zihuatanejo the value is 406 Gals. The cities that have been annexed to this port like: ciudad Renacimiento, la Venta. A city slightly away is Coyuca de Benítez which presents an acceleration value 352 Gals. One important note that indicates [Gutiérrez C., 2004] is that for accelerations greater to 150 cm/s^2. The constructions may show up given level of damage Figure 5, hence, he suggests the revisions to those regulations.

3.3 Survey area and geometry of subduction

A total of 3600 real records are available in the "Mexican database of strong earthquakes" of the [SMIS]. The accelerographs Networks was born in the country, after earthquake of September 19, 1985; for this reason the SMIS only consider earthquakes whose Magnitude Me, Mw, Mc or Ms $\leq$ 8.1, to see annex 4 for catalogue of seismic magnitude.

For these range of magnitude, we considered all records from the stations concerned. We have processed them with the software **"Degtra"** [Ordaz M. and Montoya C., 2005] and **"Seismosignal"** [Antoniou S. and Pinho R., 2002]. The spectrum of absolute acceleration provides the response of the ground, that is to say, the period characteristics of vibration.

Many of the obtained values did not represent a significant importance measure the reliability of the buildings. Actually, this concerns the seismic events that have values higher than the parameters specified in the regulations 2004, see in Figure 3.

On the other hand, as illustrated in the Figure 6a, the earthquake in Colima State, despite having a magnitude Mw=7.8, does not cause significant damage in some small cities.

Therefore, on the basis of geophysical research [Suarez G. et al., 1990], it appears that the distance from the trench to the seismogenic zone is within an interval of 40 to 60 km. [Mendoza C., 1993, 1995] estimated the distance between 60 and 80 km. The research by [Manea V. C. et al., 2004] they defined the subduction angle to approximately 10° degrees, between the Cocos Plate and the North American plate. Therefore, they located more precisely in this way seismogenic zone, enclosed in the circle, where release of energy by the rupture between the plates, and cause the greatest damages.

The Figure 36, shows the: "Geometry and survey area".

Where:

a) shows the angle of approximately 10° degrees due to subduction. The distance is measured at the bottom of the abscissa axis in km, from the trench to the North American plate, which indicates there a circular area, in which the earthquakes occur in seismogenic zone [39].

b) Located clearly on the distance between the trench and survey area. The distance I got with the software Google Earth [27], ranges from 48 to 62 km. This confirms that the most accurate seismogenic area is provided by [Mendoza C., 1993.1995], and

c) The latter figure shows the two plates where there is subduction of the Rivera Plate and the Cocos Plate to the North American. Right here it shows the many earthquakes that occur in that area, causing a big seismic hazard zone [80].

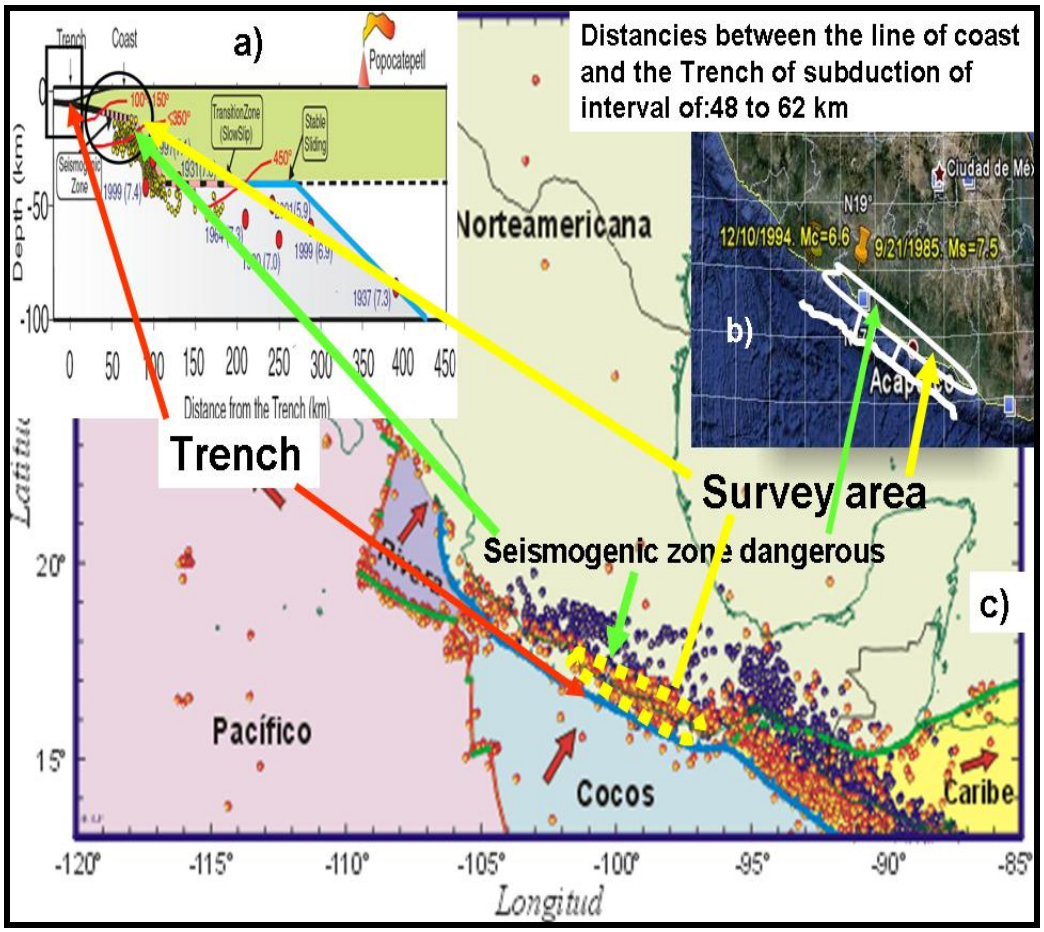

Figure 36 Geometry of subduction in the zone of Guerrero shows that the Cocos Plate slides underneath the North American Plate. [[39], [27] and [80]]

The main points to consider are:

- The distance among all accelerographs stations to the epicenter of the seismic events.
- For the area delimited by the circle, any seismic events with magnitude M>6, can cause a greater intensity in that area near the epicenter, causing damage to building, see Figure 36.
- A final point is that if the earthquake occurs near the surface, i.e. a hypocenter close at a distance smaller 5 km, the released energy is very low.
- Considerer the parameters set [CENAPRED, Gutierrez C., 2004], which provides a value of PGA to consider with a mean value of $\mu = 150$ Gals.

3.4 Selection of the sample size of the earthquakes

The report from seismic events that have caused damage in many cities of the world [see Table 7 and Table 8], and a parameter set by [CENAPRED, Gutierrez C., 2004], show to accelerations greater than 150 Gals [31], may cause damage may occur in some buildings, see Figure 5. Revisions are suggested to revisions to the regulations.

We make the selection of sample size, supported by a combination of two types probabilities are: the relative frequency probability and subjective, Canavos G.C., 1999, Soong T. T., 2004 and Levin R. I., 1988.

Thus, if n_t is the total number of trials and n_x is the number of trials where the event x occurred, the probability $P(x)$ of the event occurring will be approximated by the relative frequency as follows:

$$P(x) \approx \frac{n_x}{n_t} \qquad [3.1]$$

The subjective probability describes an individual's personal judgement about how likely a particular event is to occur. It is not based on any precise computation but is often a reasonable assessment by someone with experience.

A subjective probability is also conventionally expressed within the interval 0 to 1. A rare event has a subjective probability close to 0, a very common event has a subjective probability close to 1.

For this, the total of 3600 records that has the SMIS accelerations, only consider first a sample of 20 real acceleration records, including those who did not meet the design acceleration for a return period of 100 years of According to researcher of [CENAPRED Gutierrez C., 2004, see Figure 35]. The study area presents the acceleration values to consider are 298 Gals for the survey area of the State of Guerrero. For a return period of 100 years, but for cities like Acapulco and Ixtapa-Zihuatanejo is 406 value Gals and cities that have been attached to this port as the Renaissance city, Sale, and a city is a little way back Benitez Coyuca have an acceleration value 352 Gals.

In the history of humanity has witnessed seismic events that have caused extensive damage in cities of several countries, some examples are:

Date day/month/year	Region	Magnitude	Number of persons killed
26/12/2004	Off the west Coast of Northern Sumatra	9.1	227898
24/02/2004	Strait of Gibraltar	6.4	631
08/10/2005	Pakistan	7.6	80361
28/03/2005	Northern Sumatra, Indonesia	8.6	1313
26/05/2006	Java, Indonesia	6.3	5749
15/08/2007	Near the Coast of Central Peru	8	514
28/10/2008	Pakistan	6.4	166
12/05/2008	Eastern Sichuan, China	7.9	87587
06/04/2009	Central Italy	6.3	295

Table 7. Seismic events that have killed many people [USGS, [81]]

The following procedure is considered for the sampling, Canavos G.C., 1999, Soong T. T., 2004 and Levin R. I., 1988.

- CIRES, they sent me the last real records acceleration from 2004 until 2008, from seismic events with magnitudes greatest than Me, Mc, Ms, Mw and $Mc \geq 5.8$, see annex 4 of catalogue of magnitude, USGS, [81].

  Based on the research reports of [CENAPRED, Gutiérrez C., 2004], He considers necessary than when $PGA \geq 150 Gals$. He recommends to the governments in charge of the civil protection of the localities facing earthquakes make the reviews and check their codes of construction. So that all kinds of constructions and structures in the areas of greater seismic hazard, manage to survive and guarantee a high index of safety in the buildings, diminishing by this way the seismic risks to the population.

- Representative records of 3600 seismic information obtained since 1985 were analyzed, date in which the great earthquake has damaged Mexico City.
- The accelerograms correspond to the subduction zone that affects several states of The Mexican Republic, in the area of the Pacific Ocean. It is necessary to obtain a representative sample, for the coastal zones of the Guerrero State.
- The studies elaborated by the Mexican and investigative scientists of the [UNAM, [23]] and of others Institutions are of great importance for the argumentation of this work. Researches about the conditions of ground in the zone that is object of study; as well as the ones done by the scientists L. Esteva, M. Ordaz, V. Kostoglodov, S. K. Singh, G. Suárez, J. Pacheco, C. Gutiérrez, J. Anderson, R. Quaas, C. Valdés and D. A. Novelo [see Table 8]. Other publications elaborated by others scientists of other places of the world have been considered: the ones that have some reference to the seismic events of great magnitude that have caused damages and collapses in the buildings and structures [to see Table 7]. The representative sample of the real accelerograms takes into account: Magnitude, content of frequency, PGA, epicenter distance, depth of the fault between the plates, location relating to the population zone, and the azimuth with which the readings of the accelerograms were taken.
- To realize the study of structural reliability by means of the Incremental Dynamics Analysis (IDA), only one direction was considered i.e. where the PGA is bigger. Besides, because for the analysis were considered the following guidelines of probability and statistics:

By selecting the size of the representative sample of 20 real records acceleration in two directions of orientation are considered. In Mexico, some examples of events that have damaged earthquakes are presented in Table 8.

Date day/month/year	Magnitude	Region	Number of persons killed and material damages
29/07/1957	7.8	San Marcos, Guerrero	55 dead people, many material damage
02/08/1968	6.3	Pinotepa, Oaxaca	many material damage
30/01/1973	6.2	Colima	50 dead, 300 wounded, many damage
28/08/1973	6.8	Oaxaca-Puebla	600 dead, many wounded, 77 damaged cities
24/10/1980	6.5	Huajuapan, Oaxaca	50 dead, many damaged near to epicenter
19/09/1985	8.1	Michoacán	6500 dead, many damaged in cities
15/06/1999	7	Tehuacan, Puebla	17 dead and many damaged.
21/01/2003	7.8	Tecomán, Colima	29 dead, 300 wounded, many damaged
13/04/2007	6.3	Atoyac, Guerrero	many damaged

Table 8. Seismic events that have killed many people and originated many damage. [82]

The events chosen as a representative population of the records of significant accelerations and nearby to 150 Gals are based in the history of earthquakes that have caused damages and collapses in the last 20 years. They came from a whole set of 3600 records accelerations representative sample of 10 records that were analyzed in both directions of orientation is selected. Giving a whole set of 20 real accelerograms records, with magnitude M>6, they also fulfil the requirement that the soil response spectrum is greater than, or at least equal to the ordinate of the design spectrum [see Figure 3]. Annex 3 shows some of these spectra response compared with the design spectrum in Figure 28.

Then $n = 20$.

"Because, only 20 real records accelerations have a $PGA \geq 150 Gals$ and their value of pseudo-acceleration [Sa] is most bigger than Figure 28, see to Table 9".

Value of μ> 150 Gals. And with c > 0.44				Records	Value of **c** in design	Max. response of the ground	Period soil Ts[s]	Period mean Tm[s]
Seismic	Accelerographs		Distance to Epicenter	**PGA**				
Magnitude	Station	Direction	(km)	Gals	spectra	**c =[Sa/g]**	**ξ=0.05**	**ξ=0.05**
Me Mw7.3	CALE	SE90°	11	396	0.44	1.35	0.18	0.25
Me Mw7.3	CALE	SE0°	11	350	0.44	1.21	0.18	0.33
Me=6.5	PAPN	NW0°	20	293	0.44	1.14	0.15	0.16
Mc=6.6	BALC	NW0°	29	267	0.44	0.92	0.04	0.14
Mc=6.6	BALC	NW90°	29	177	0.44	0.81	0.04	0.15
Me=6.5	PAPN	NW90°	20	320	0.44	0.78	0.07	0.11
Ms=7.5	PAPN	NW90°	90	219	0.44	0.77	0.15	0.14
Mc=6.2	COPL	NW90°	10	293	0.44	0.76	0.10	0.30
Ms=7.5	PAPN	NW0°	90	243	0.44	0.74	0.09	0.17
Me=6.5	PETA	SE0°	16	267	0.44	0.67	0.09	0.20
Ms=8.1	UNIO	NW90°	121	148	0.44	0.64	0.24	0.36
Mc=6.2	COPL	NW0°	10	210	0.44	0.61	0.10	0.46
Me=6.5	PETA	SE90°	16	177	0.44	0.59	0.09	0.17
Ms=8.1	AZIH	NW90°	166	154	0.44	0.59	0.12	0.54
Ms=8.1	UNIO	NW0°	121	166	0.44	0.56	0.35	0.53
Ms=7.5	AZIH	NW90°	46	153	0.44	0.50	0.32	0.43
Ms=8.1	VILE	NW0°	78	125	0.44	0.49	0.55	0.66
Ms=8.1	PAPN	NW90°	218	110	0.44	0.48	0.12	0.22
Ms=8.1	PAPN	NW0°	218	153	0.44	0.45	0.12	0.26
Ms=8.1	CALE	NW0°	20	140	0.44	0.44	0.44	0.95

Table 9.Summary of the first sample with twenty real records acceleration seismic events that happened in State of Guerrero, Mexico. With the population mean $\mu \geq 150$ Gals and response of the Ground $c = (Sa, \xi = 0.05)/\, g$.[78]

For the table 9, the meaning of each symbol is:

c The seismic coefficient is one fraction of the value of gravity A/g.

Sa The pseudo-acceleration of the ground with $\xi = 0.05$

ξ Damping ratio

g The value of gravity.

T_S Is the predominant period, which corresponds to the acceleration response spectrum when it reaches its maximum value, calculated with damping ratio of $\xi = 5\%$. This value has been commonly employed in earthquake engineering to characterize an equivalent seismic loading on a structure from the earthquake ground motion. Usually, this spectrum of response of pseudo-acceleration is represented by its maximum value.

T_m Is the mean period. It was proposed by Rathje et al., [1998], is the best simplified frequency content characterisation parameter, because it takes in consideration all time-history, the duration and the content of frequency.

$$T_m = \frac{\left(\sum C_i^2 / f_i\right)}{\sum C_i^2}$$

Where

C_i are the Fourier amplitude, and

f_i represent the discrete Fourier transform frequencies between 0.25 and 20 Hz.

With the mentioned variables, it is considered everything with reference to the intensity, frequency content and duration, of all the real records of accelerations.

It is the degree of freedom that it considers the point from the procedure for the sampling.

The records of real accelerograms that are higher or close to 150 Gals, are considered to be harmful to the structures that are near the epicenter. For a level of significance 1- α = 99 % to predict that a structure will have considerable damages, the interval is good.

Confidence coefficient $1-\alpha$ = 99 percent

α Level significance where $\alpha = 0.01$

Anyway, the size of the sample continues to be very large to analyze 27 buildings. One needs to know the interval to be used with enough reliability. For this reason, we have to

look for the size N of values than gives one better and smaller sample to be considered, from the parameters for the sample of 20 accelerograms, we have: [85]

$$\left.\begin{array}{r} \text{Sample mean} = \overline{X} = 218 \text{ Gals}, \\ \text{Sample deviation standard} = S = 81 \\ \text{Mean population } \mu = 150 Gals \end{array}\right\} \quad [3.2]$$

As we know, the certainty of the variance σ^2 and the mean population $\mu = 150 Gals$ for the survey area, the only advice you have is the parameter (Gutierrez C., 2004).

To find a confidence interval one should follow the following procedure:

We may assume for our seismic events with magnitude and actual acceleration records normally distributed Z, by historical references of earthquakes that have caused damage, however, as the sample is small, a probability distribution like the normal distribution is the t-Student. Then starting from the central limit theorem [85], we have:

$$Z = \frac{\overline{X} - \mu}{\sigma / \sqrt{n}} \text{ and we expect that N tends to } N(0,1) \quad [3.3]$$

Where

Z is the Gaussian random variable

μ is the population mean with one parameter of reference, but for the survey area, it is still unknown

σ Is the deviation standard of the unknown variance

$\overline{X}$ is the sample mean

n it is degrees of freedom.

When an n increase, the t-distribution approaches a normal distribution, such as for reference parameter $n \geq 30$ is when practically have the same shape.

And for the theorem of Cochran [85] that says:

If $X_1, ..., X_n$ tends to $N(0,1)$ and there are random variables, then:

$$\overline{X} = \frac{1}{n}\sum_{i=1}^{n} X_i \text{ tends to } N(\mu, \frac{\sigma^2}{n}) \quad [3.4]$$

Where $\overline{X}$ is the mean

$$\sum_{i=1}^{n}\frac{\left(X_i-\overline{X}\right)^2}{\sigma^2} \text{ tends to } \chi^2_{n-1} \qquad [3.5]$$

Where: χ^2_{n-1} is chi-square with n-1 degrees freedom.

$$\overline{X} \text{ and } \sum_{i=1}^{n}\frac{\left(X_i-\overline{X}\right)^2}{\sigma^2} \text{ are the random variables independent.} \qquad [3.6]$$

And from equations 3.3 and 3.6 that are independent distributions. Starting from these relationships one can build a t-distribution or distribution Student with n-1 degrees of freedom.

Then one obtains:

$$T_{n-1}=\frac{Z}{\sqrt{\frac{1}{n-1}\chi^2_{n-1}}}=\frac{\frac{\overline{X}-\mu}{\sigma/\sqrt{n}}}{\sqrt{\frac{1}{n-1}\sum_{i=1}^{n}\frac{\left(X_i-\overline{X}\right)}{\sigma^2}}} \qquad [3.7]$$

Simplifying the previous expression [85], we have:

$$T_{n-1}=\frac{\overline{X}-\mu}{\hat{S}/\sqrt{n}} \text{ than tends to } t_{n-1} \qquad [3.8]$$

Where:

T_{n-1} is the t-distribution with n-1 degrees of freedom

μ is the population mean.

$\overline{X}$ is the sample mean

n it is degrees of freedom.

$\hat{S}$ Is a quasi standard deviation of the sample.

Knowing the sample variance, as we aim to reduce the size of the sample from a number "n = 20" to a smaller one, we also want to know the confidence interval for this new value.

We calculate the t-distribution as follows.

The number of degrees of freedom will be smaller. So, instead of using the sample standard deviation S in the t-distribution, we will replace for the quasi standard deviation $\hat{S}$, to estimate a bias value.

To calculate the sample standard quasi deviation $\hat{S}$, we proceed to take the following steps: If $X_1,...,X_n$ are independent random variables that are normally distributed, the sample mean is:

$$\overline{X}_n = (X_1 + ... + X_n)/n \qquad [3.9]$$

And the sample variance as:

$$S_n^2 = \frac{1}{n-1}\sum_{i=1}^{n}\left(X_i - \overline{X}_n\right)^2 \qquad [3.10]$$

The standard deviation of the sample we can obtain of the equation 3.10:

$$S_n = \sqrt{\frac{1}{n-1}\sum_{i=1}^{n}\left(X_i - \overline{X}\right)^2} \qquad [3.11]$$

Where: S_n is the sample standard deviation

and the quasi standard deviation:

$$\hat{S} = S_n\sqrt{\frac{n}{n-1}} \qquad [3.12]$$

It can be shown that the random variable

$$X^2 = \frac{(n-1)S_n^2}{\sigma^2} \qquad [3.13]$$

has a chi-square distribution with $n-1$ degrees of freedom. It is readily shown that the quantity.

This expression is normally distributed N (0, 1).

The sample mean $\overline{X}_n$ is normally distributed with mean μ and standard error $\sigma/\sqrt{n}$.

We also see from equation 3.13. The chi-squared distribution with (n-1) degrees of freedom. Furthermore, although we will not verify it here, it can be shown that $\overline{X}_n$ and S^2 are independent [85].

What differs from *Z* is that the exact standard deviation σ of equation 3.3 is replaced by the random variable $\hat{S}$ in the equation 3.8, has a Student's t-distribution as defined above. Notice that the unknown population variance σ^2 does not appear in *T*, since it was in both the numerator and the denominators.

When T has a *t*-distribution with $n-1$ degrees of freedom. by symmetry, that is, the same as saying that $A = t_{n-1;1-\alpha/2}$ satisfies the next equation:

$$\Pr(\overline{X} - A\frac{\hat{S}}{\sqrt{n}} < \mu < \overline{X} + A\frac{\hat{S}}{\sqrt{n}}) = 1-\alpha \qquad [3.14]$$

Where

$A = t_{n-1;1-\alpha/2}$ is the value tabulated.

$\overline{X}$ is the sample mean.

μ is the population mean.

$\hat{S}$ Is a quasi deviation standard

n is it degrees of freedom

$1-\alpha$ is the confidence level.

In inferential statistics, the statisticians to measure the dispersion are the most suitable unbiased. Therefore, we will leave aside the sample standard deviation, to use the typical quasi deviation $\hat{S}$:

For the above-mentioned, we can apply the equations to our values of the sample and with it to find the confidence interval in order to propose the new number of grades “n”:

$$\hat{S} = S\sqrt{\frac{n}{n-1}} = 81 * \sqrt{\frac{20}{20-1}} = 84$$

$\hat{S}$ Is a quasi deviation standard

n it is degrees of freedom

$$T = \frac{\left(\bar{x} - \mu\right)}{\hat{S}/\sqrt{n}} = \frac{(218-150)}{84/\sqrt{20}} = 3.74$$

Hence, from that the parameters from real PGA parameter given by (Gutierrez C., 2004), we can propose the following:

$$\text{Confidence coefficient } 1-\alpha = 99 \text{ percent}$$

$$\alpha \text{ level significance where } \alpha = 0.01$$

$$\alpha/2 = 0.005$$

The t-distribution is tabulated in any statistic book. When T has a *t*-distribution with $n - 1$ degrees of freedom. For instance, for the t-distribution and with these values finding $A = t_{n-1;1-\alpha/2}$:

$$\Pr(\overline{X} - A\frac{\hat{S}}{\sqrt{n}} < \mu < \overline{X} + A\frac{\hat{S}}{\sqrt{n}}) = 1-\alpha \qquad [3.14]$$

For know the Confidence intervals: $\Pr(\overline{X} - A\frac{\hat{S}}{\sqrt{n}} < \mu < \overline{X} + A\frac{\hat{S}}{\sqrt{n}}) = 1-\alpha$

then μ: $\mu = \overline{X} \pm A\frac{\hat{S}}{\sqrt{n}} = 218 \pm 2.861 * \frac{84}{\sqrt{20}}$ equal to $\mu = 218 \pm 2.861 * 18.69 = 218 \pm 54$

The reliable interval remains between the values of: **[164, 271]**

If we want to change the size of the sample to a smaller because of the time, we proceed to:

$$d = t_{n-1;1-\alpha/2} * \frac{\hat{S}}{\sqrt{N}} = \text{ Error of precision} \qquad [3.15]$$

$$d = t_{n-1;1-\alpha/2} * \frac{\hat{S}}{\sqrt{n}} = 2.861 * 18.69 = 54$$

Then to calculate N are takes into account a normal distribution. A small level of significance of 95 %, due we wish a smaller sample, and to, reducing the value of confidence level $1-\alpha$ to 95%.

$$N \geq \frac{Z^2_{1-\alpha/2} * S^2}{d^2} = \frac{Z^2_{0.975} * S^2}{d^2} = \frac{1.96^2 * 81^2}{54^2} = 8.91 \approx 9 \qquad [3.16]$$

With the result of the sample size with a value of N=9, we proceed to make the calculation of the Incremental Dynamics Analysis (IDA), using 9 records that give results

of structural reliability, that the scientists [Shome and Cornell, 2002] they consider that this it is a good size of the sample to give accuracy to our studies. Therefore, the nine records of real accelerations selected for this study are:

Value of μ> 150 Gals. And with c > 0.44				Records	Value of **c** in design spectra	Max. response of the ground **c =[Sa/g]**	Period soil Ts[s] **ξ=0.05**	Mean Period Tm [s] **ξ=0.05**
Seismic Magnitude	Accelerographs Station	Direction	Distance to Epicenter (km)	**PGA** Gals				
Me Mw7.3	CALE	SE90°	11	396	0.44	1.35	0.18	0.25
Me=6.5	PAPN	NW0°	20	293	0.44	1.14	0.15	0.16
Mc=6.6	BALC	NW0°	29	267	0.44	0.92	0.04	0.14
Ms=7.5	PAPN	NW90°	90	219	0.44	0.77	0.15	0.14
Me=6.5	PETA	SE0°	16	267	0.44	0.67	0.09	0.20
Ms=8.1	UNIO	NW90°	121	148	0.44	0.64	0.24	0.36
Ms=8.1	AZIH	NW90°	166	154	0.44	0.59	0.12	0.54
Ms=7.5	AZIH	NW90°	46	153	0.44	0.50	0.32	0.43
Ms=8.1	VILE	NW0°	78	125	0.44	0.49	0.55	0.66
The value of seismic coefficient [c = Sa/g] for survey area.								

Table 10. Summary of sample of seismic happened events in Guerrero State, Mexico. [78].

With the population mean $\mu \geq 150$ Gals and spectrum of response of the ground $c = (Sa, \xi = 0.05)/g$.

See Table 9 with 20 records PGA providing $\mu \geq 150$, in which we show the meaning of all the variables that we show in this Table 10.

All of the parameter of the mean population value are those recommends [CENAPRED, Gutierrez C., 2004].

In this study, we wish to show the index of reliability of the behavior of the buildings of concrete reinforced before the seismic events. Having comparative parameters the mentioned in the previous paragraphs and observing the Figure 3, Figure 28, Figure 34 and Figure 35, one may suggested make the corresponding recommendations for the coasts area of the status of Guerrero.

3.5 Calculation of the spectra of ground response

The response of the ground could be obtained from the interpretation of the actual records of real accelerations, and with the software Degtra [Ordaz M. and Montoya C., 2005] and also by the Seismosignal [Stelios Antoniou and Pinho Rui, (2002)]. The theoretical

aspects to develop spectrum of response to an acceleration $\ddot{u}_g(t)$ of motion of the ground we can find in the book [Anil K. Chopra, 2001] description, the following process, [see to Figure 37]:

"1. Numerically define the ground acceleration $\ddot{u}_g(t)$; typically, the ground motion ordinates are defined every 0.02 sec. For this study, we have 20 record accelerations defined to 0.01 sec.

2. Of a Single-degree-freedom [SDF] system, to select

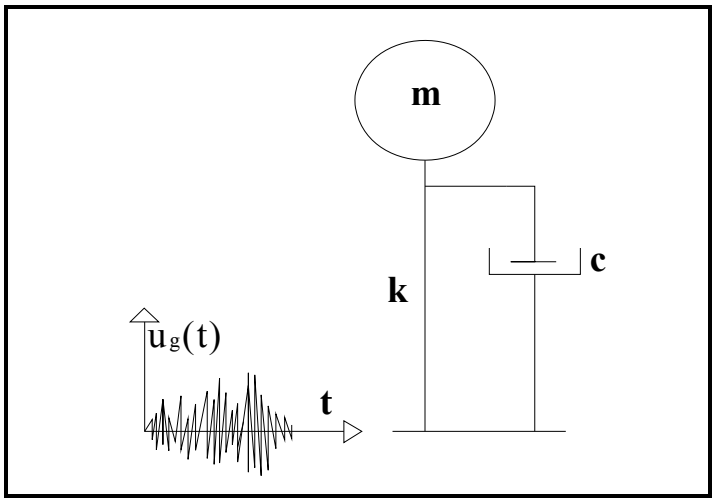

Figure 37 Single-degree-freedom system and ground acceleration.

T_n natural vibration period and

ξ damping ratio of an SDF system. We used $\xi = 0.05$

3. Compute the deformation response $u(t)$ of this SDF system due to the ground motion $\ddot{u}_g(t)$ by any of the numerical methods.[see Figure 38]

$$D = u_0, \qquad [3.17]$$

Where: u_0 Is the deformation response spectrum

D Is the value of u_0 determined for each SDF system at one point on the deformation response spectrum, that is to say, for a system with the given values of $u_0 = (T_n, \xi)$

4. Determine u_o, the peak value of $u(t)$.

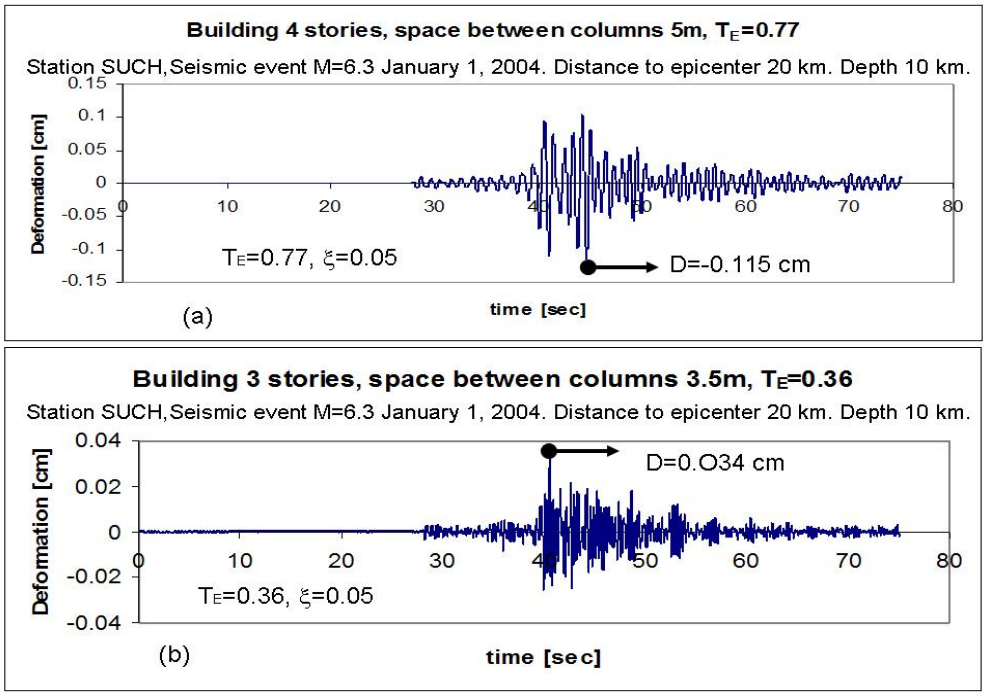

Figure 38 Deformation response of two SDF system with $\xi = 0.05$ and (a) T_E=0.77 and (b) T_E=0.36.[5]

That is to say, two system different have one response deformation for the same Earthquake

5. The spectral ordinates are:

$$V = \left(\frac{2\pi}{T_n}\right) D \qquad [3.18]$$

Where: V Is the pseudo-velocity response spectrum than considers a quantity V for an SDF system with natural frequency ω_n *related to its peak deformation* $D \equiv u_0$ *due to earthquake ground motion.*

$$A = \left(\frac{2\pi}{T_n}\right)^2 D \qquad [3.19]$$

Where: A the pseudo-acceleration response spectrum consider a quantity A for an SDF system with natural frequency ω_n *related to its peak deformation* $D \equiv u_0$ *due to earthquake ground motion.*

6. Repeat stops 2 to 5 for a range of T_n and ξ values covering all possible systems of engineering interest[17]

These curves for the pseudo-acceleration spectrum represent the properties of the earthquake at a particular site and are not depending on the properties of a structural system. A more explicit reference is found in the N. Nigam C. and Jenning P. C. (1968) See Annex 2 for further, one could run the algorithm for the construction of response spectra of the ground.

3.6 Location of epicenters through satellite image with the software Google Earth, distances between the epicenter and the station of the accelerographs, accelerograms and its response spectrum of the ground [Ts]

In this study, we show the location of the epicenters [see Figure 39], indicating the distance to the stations that were considered for this study, according to image of **Google Earth [27]**.

We will consider for each real record of sample accelerations, see figures in annex 3. The which:

a), the placement of their orientation, the distance between the station to the epicenter, the depth of the hypocenter and its **[PGA]**. In

b), we have the **response of pseudo-acceleration of the ground [Sa]** as a fraction of the gravity on the ordinate **[c=Sa/g]** against period on the abscissa, to facilitate its handling and then compare them with the spectra of seismic design used for the state of Guerrero, on the same graphic it is inserted for his comparison.

A summary of real records acceleration is provided in the Table 10 due to earthquake.

Thus, way it will be possible to determine if for return periods of 100 years of the terrain accelerations of 150 Gals. In this case, it will be necessary to consider the creation of construction regulations for the own state or municipality.

The seismic event in January 11, 1997 (see Figure 39), in which the epicenter distance is at 11.26 kilometres, present a value of PGA 396.21 Gals in the direction SE90° and a spectral ordinate due to the [Sa] of 1326 Gals [c=Sa/g=1.35]. In the other direction SE0 °

[17] Chopra Anil K. (2001), "Dynamics of Structures" Theory and Applications to Earthquake Engineering, Berkeley, USA., Second Edition,

a PGA of 350.27 Gals with a [Sa] of 1187 Gals [c=Sa/g= 1.21**]**, value to 800 Gals that indicate like parameter for [Veras L. and Ordaz M, 2004]. See Figure 34, and then compare it with Figure 69b in annex 3.

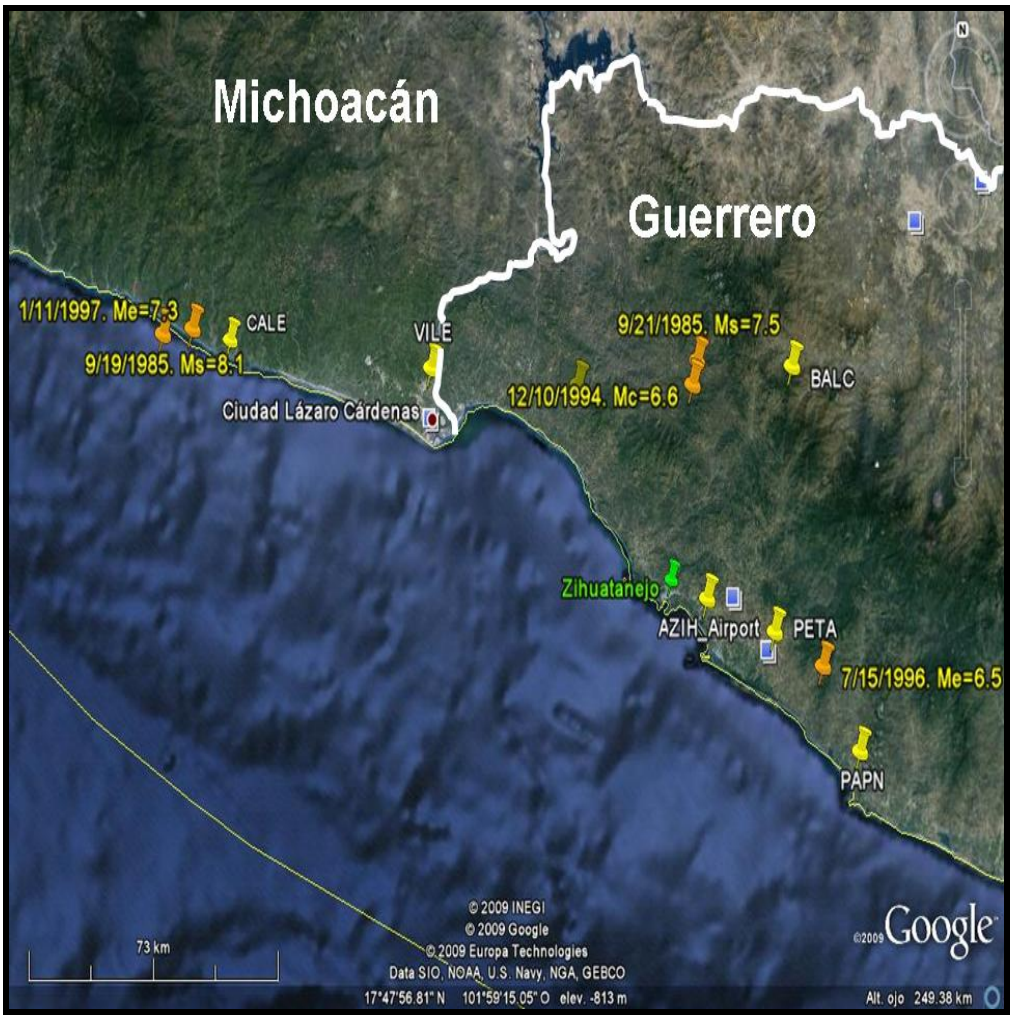

Figure 39 All epicenters nearby to the station of the accelerographs with their Magnitude and occurrence days are presented with their date as month/day/year. [27]

In Figure 39, we can observe the other stations where are located the accelerographs. But, as the distance to the epicenter is large, the amplitude is not enough representatives compared with the design spectrum that is in chapter 2, to see Figure 28. A particular order to be attention is required for the Figure 3, where the response spectrum of the ground is greater than the design spectra considered the old regulations of 1976. This may explain: the level of destruction that originated the earthquakes of September 19, 1985, with epicenter in Caleta de Campos, Michoacán, Mexico [see Figure 6a]. This earthquake

originated studies of micro zoning, but only for the region center of the country [to see Figure 1] and more in the Mexico City, Distrito Federal.

Figure 39, shows the epicenter corresponding to the seismic event of July 15, 1996, with a magnitude Me= 6.5. With the earthquake we can observe as the conditions of site of a determined region: for case of the records of acceleration at the station PAPN direction NW0° and PETA direction SE0°. The first one is 19.88 km and the second a 15.5 km. Nevertheless, the characteristic values of PAPN are: PGA of -292.86 Gals and a value of the [Sa] equal to 1122 Gals (see Figure 70b with [c=Sa/g=1.14], in annex 3). The parameters of PETA that is: PGA of –267 Gals and the response spectra of the ground of 660.7 Gals see Figure 73b c=Sa/g=0.67, in annex 3.

The previous values prove that there is another parameter as the content in frequency and the duration to affect the pseudo-acceleration spectrum of the ground [Sa]. Because the station PAPN in the address NW0° has a value of 1122 Gals that it is bigger than PETA with the address SE0° of 660.7 Gals, duration in seconds is 127 for PAPN and for PETA is 48.97 seconds.

Therefore, we observe that the proximity of the seismic event can generate intensities major amplitude corresponds to the stipulated in the code of construction.

The next seismic event is the unique with depth of 55.6 kilometers greater than the rest of the seismic events located at 20 kilometers depth. When checking the acceleration at the near stations, we observe are those the values to consider are the corresponding to the stations BALC. For direction NW0° the record in PGA is 267.002 Gals and another direction NW90° of -177.051 Gals. The [Sa] are: 899.92 and 798.8 Gals respectively. See Figure 71b for the first one where c=Sa/g=0.92, in annex 3.

The following seismic event does not exceed the value established by (Veras L. and Ordaz M., 2004) corresponding to the response spectra of the ground for a return period of 100 years, with the maximum value proposed as 800 Gals (see Figure 34). The excessive are those of the seismic coefficient for the soil under study (type I), which considers the regulation of Table 6: the value of 0.44 g, see Figure 28 and the comparisons in the figures of the parenthesis b of the annex 3.

For the seismic event happened on September 21, 1985, with magnitude Ms=7.5 for which were considered the records acceleration at the stations PAPN and AZIH, at this stations we observed the same behaviour explained for the magnitude Me=6.5. Then the

parameters for these two stations are: 83,8 and 46,28 kilometers. The PGA are -219.16 of PAPN NW90° and AZIH NW90° of -153.13 Gals. The [Sa] have the following values of 756,61 and 493,4 Gal respectively (see figures in annex 3, the 3.4b for PAPN station [c=Sa/g=0.77]) and AZIH (see Figure 76b [c=Sa/g=0.5]).

The following seismic event happened on October 24, 1993, near Copala town. For this reason, the station of the accelerographs takes this name with the initials COPL. With a magnitude Mc=6.2, the distance between the station and the epicenter is of 8.9 km, and PGA 209.59 Gals with [Sa] of 742.5 Gals, [c=Sa/g=0.757]

The duration time of these records is 17.15 seconds. It is the smaller event of all the records of acceleration under studies.

The seismic event has a small magnitude Mc = 6.2. At distance of 8.9 km to the epicenter, it caused a [Sa] value of the earthquake of September 19, 1985, that is shown below.

Actually, seismic event happened on the September 19, 1985, is located within the limits of the seismogenic zone boundary shown in Figure 36, but for the amount of released energy to the breaking of the tectonic plates. It generated an earthquake with the biggest duration of all events show here. In some stations of the accelerographs, the duration caused several pseudo-acceleration peaks, increasing the uncertainty of the resonance in the buildings.

The focus of the earthquake was found close in the zone of Trench. Even so, this event caused an enormous decrease of stiffness and resistance of the building. In the capital city this originated the collapse of the buildings for the phenomenon of the resonance. Several ordinates of the response spectrum of the ground were major to the design spectra indicate the regulation by (see Figure 3 and Figure 4) in the site SCT.

Then for the earthquake on September 19, 1985, we have records of acceleration of the stations of: UNIO, AZIH, VILE, PAPN and CALE. The station CALE has the nearest distance of 19.79 km, but it shows parameters of the response of ground pseudo-acceleration spectrum smaller than in other station accelerographs. Later the station of VILE located to 78.27 km and in the others, one distance superior to the 120 km, which explains the intensity of its responses pseudo-acceleration spectrum of the ground in particular characterizes that them for this event.

To see figures in Annex 3, for this seismic event in UNIO 3.6, AZIH 3.7, VILE 3.9.

3.7 Summary

In this chapter, we present the seismic hazard map, where we show the two types of fault due to the plates tectonic, but for our survey area, the most important is the subduction between the Cocos plate and the North American Plate.

To define the geometry of subduction and the zone of la major seismic hazard for the survey area, [Manea V. C. et al., 2004], that locate the subduction angle at approximately 10 ° degrees. There are two possible areas of rupture due to GAP that cause the Cocos Plate and the North American plate [Valdés C., and Novelo D.A., 1997] indicated this situation in their research, but they forgot to put the coordinates North, for to locate the most dangerous condition of two GAP. Hence, with the information provided by the research developed by [Suarez G. et al., 1990] and [Mendoza C., 1993.1995], they have calculated in an appropriate way the distance from the trench to the seismogenic zone, with these researches that help us, we propose some coordinates North that gave origin to the Figure 10. So that with this information, we have the distances to most important cities of the State of Guerrero, see Table 1 that shows the level from seismic risk.

With the previously mentioned, we could define the precise depth and distance where we locate the seismogenic zone, for the earthquakes expected to make damage and for the selection representative sample of earthquakes used in this study. This subduction between the plates produces differences in the frequency content and site effects.

With the conditions of response of the ground that we show in the annexe 3, we proposed the dimension for the RC buildings in the chapter 2, and to evaluate of the reliability index, we consider the research elaborated by Shome N. and Cornell C. A. (2002).

We proposed also an initial sample of twenty PGA that we can see in the Table 9, but to evaluate the corresponding reliability index and structural safety for several buildings that are designed according to the Mexican regulations, we considered nine seismic events, see Table 10. We considered the parameter recommended by the Mexican institutions and we have determined the characteristic periods of soil that are approximately of 0.034 to 0.549 seconds, however, the most prevalent value is in the range of 0.034 up to 0.36 seconds.

Chapter 4 Results

4.1 Introduction

This chapter aims to evaluate the structural safety regarding close seismic event in the Guerrero State. Some structural parameters are considered as random variables with selected probabilistic distributions. Several "existing buildings" designed according to Mexican regulation are analysed two situations:

- When they are to face for the first time an earthquake.
- When they have experienced post seismic events and have been partially damaged. The residual reliability is evaluated in case of occurrence of a new earthquake.

As previously discussed in chapter one concerning Geophysical studies, we wish to know how conservative is the seismic coefficient for the survey area, which is 0.44g. This value is the ordinate of the design spectra indicated by the regulations 2004. The flat part of the design spectra as far as we can find to uncertainty goes up to the period value of 0.6. The proposed buildings are small and with characteristic period of less than one second.

In chapter 3, we have mentioned up a parameter dedicated to the mean period of the response of the ground and proposed by (Rathje et al., 1998). In this chapter, we will compare this mean period with the characteristic value of the ground period commonly used in professional practice. Therefore, of Table 9, we analyses the influences and mentions as follows:

Ts to be compare with **Tm**

Sa the shape of the ordinate of the response pseudo-acceleration spectrum of the ground, (with the damping of $\xi = 0.05$) is compared with the seismic coefficient $c = 0.44$, which corresponds to the survey area.

To demonstrate and understand how vary the indexes of reliability; we need to put also attentions to the following factors:

- Variation of the buildings periods as shown in Table 12:
- Variation of the value and inelastic behavior, yield displacement in each of the building, see Figure 41.

- The spectrum of response of pseudo-acceleration of the ground considered with two approaches present in Table 9
- To observer the parameters of ductility developed by each proposed buildings, see Table 15.
- To study the influence of the variation in the materials, the uncertainty that affect the period of the buildings the structural behaviour. Also, if we observed the characteristic periods of the ground Ts and Tm and, we understand that the site effect is important as it influence the values of the reliability index.

Observing the **"list of symbols"** at the beginning of the thesis, understand the abbreviations in the figures and tables.

4.2 General Results on the Survey area

- **Survey area, observation**

Our concern for this study is to measure the level of safety in the case of an earthquake with a magnitude of Mw = 8.1 or Mw = 8.4, due to the GAP located in Guerrero (see Figure 9 and Figure 10) [Valdes C. and D. Novelo A., 1997].

The biggest fault line has an approximate distance of 220 km and the amplitude estimated according to other historical events and recent studies in Geophysics in the survey area, to see Figure 9. [Valdes C. and D. Novelo A., 1997] proposed 90 km, hence the rupture area is 220 x 90 km^2. Then with the relationship between the magnitude and the area [Singh S. K. et al., 1980], they gave a prospective maximum of magnitude of **Mw=8.4.** But, it is very important to remind that the seismic events shown in chapter 3, are smaller than the size of the expected earthquake Mw = 8.4 or Mw = 8.1.

It is worth to remind that the most important cities have an approximate distance to the epicenter that varies in an interval of 15 up to 67 km.

The variations in amplitude due to quake, depending on the distance (epicenter) and also the focus depth, the content on frequency, the Peak Ground Acceleration, duration.

In this study, we analyse the structural reliability according to the capacity of lateral resistance before a force induced by an earthquake, the construction types being the most commonly used by people in the Guerrero State.

Below are the results across the board for each analysis.

4.3 Results in the elastic status with the Dynamic Analysis Response to Spectrum [DARS]

In this part of the dynamic analysis, we known with better approach the interstorey drifts and this information is carried out with the design, based on the response of each building.

The commercial software ECOgcW is used to perform dynamic analysis of seismic response to spectrum, trying to optimize the buildings design, the main idea to make the comparative analysis is:

- The strength of concrete [$f'c$] with mean properties, this due to the consistency that gives the materials in the region of the state of Guerrero [Soto A., 2004]. They differ from the central region of the country, this difference in percentage being 2.13%.
- We propose degradation in the structural element (beam-column) in a random way, just after carrying out the preliminary tests in the process of selection of the real records in order to known the period of ground response.

To assume existing damaged, we consider: the first 20 real acceleration records selected. For this existing criterion of damaged, it is known that many of the houses have already more than 50 years and have experienced other degradation phenomena. The assumed values of possible degradation are summarized in Table 11 is:

This table is defined as follows:

- The first column shows the building.
- The degradation in number of columns of each storey, following a random parameter as it is shown in the Figure 40.
- Column 3 indicates the percentage of degradation obtained in the storey by the number of columns to which we apply degradation.
- In column 4 and 5, we proceed as in step 2 and 3, considering the beams, in both directions.

Nomenclature for the next table is, for example, 2-3.5m. Mean building with 2 stories with separation between columns of 3.5 meters.

Building	number of columns	% of columns damaged	numeber of beams	% of beams damaged
2-3.5m	8	50	8	33
3-3.5m	8	50	8	33
4-3.5m	4	25	6	25
2-5m	8	50	8	33
3-5m	8	50	8	33
4-5m	4	25	6	25
5-5m	4	25	6	25
7-5m	4	25	6	25
The degradation was of a value of 20% in the the module of elasticity of concrete				

Table 11. Stories damaged considered for the buildings.

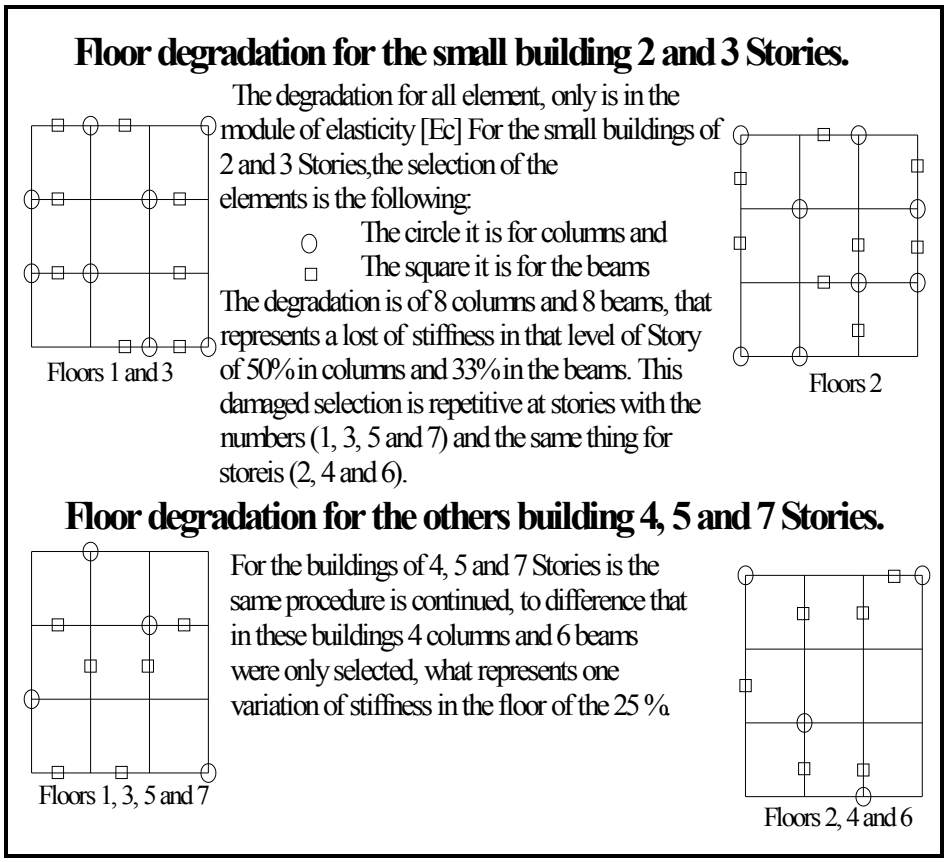

Figure 40 Distribution of the degradation observed in plant of the buildings.

In the first point for the structural behavior, are the following variations, in the periods.

Nomenclatura of the building, for example, 2-3.5m, that is, Building with two stories and space between columns of 3.5 meters, T_E it is period fundamental of the building			
Building	Soto T_E	RCDF T_E	Damaged T_E
2-3.5m	0.31	0.31	0.32
2-5m	0.44	0.44	0.45
3-3.5m	0.36	0.36	0.37
3-5m	0.53	0.53	0.55
4-3.5m	0.52	0.52	0.54
4-5m	0.77	0.77	0.79
5-5m	0.85	0.85	0.87
7-5m	0.87	0.88	0.90

Table 12. Fundamental Period due to the properties means and degradation proposed for the buildings.

It is of importance for us to present each detail of the results, because each variation rebounds in the indexes of reliability, for that in the following figure we showed the variation of the fundamental period [T_E] in percentage of the Table 12.

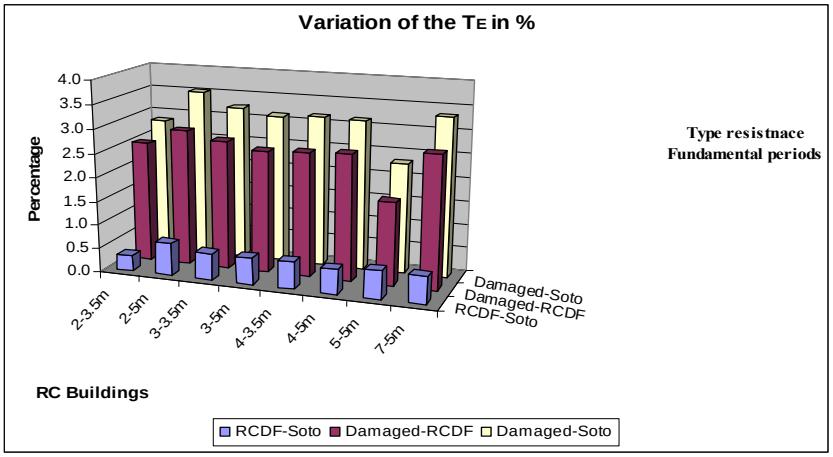

Figure 41 Variation in percentage among the fundamental periods of the mean resistance and a proposed of degradation.

In Figure 42 shows the variation of yield displacement for the first mode on the roof, in the node of interest shown in Figure 15a, Chapter 2. These values are still in the elastic range and meet the specifications of the regulations 2004. With the exception of buildings damaged by the degradation, for which we estimate that there a damaged state from the optimal structures RCDF, this means that already in the permissible limits, this situation reflected In Figure 42 very large differences between resistance damaged with reference to the other two resistance considered.

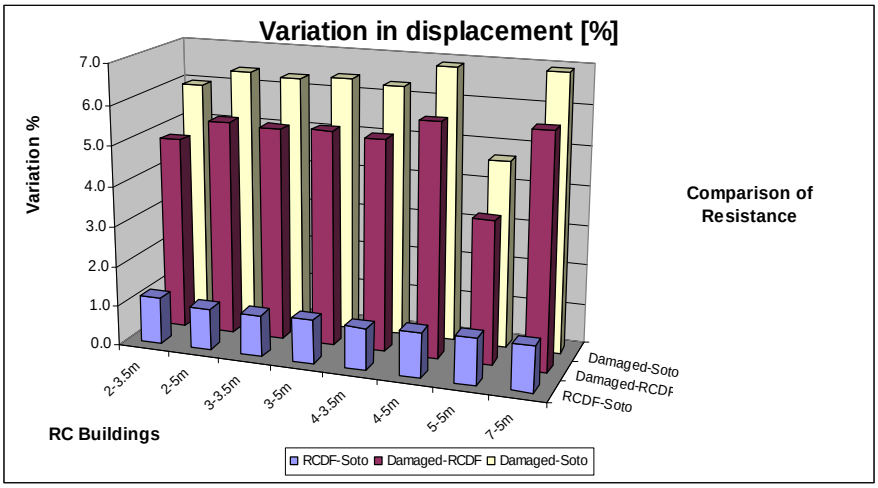

Figure 42 Variation in percentage of the yield displacement with the DARS method.

In Table 13 and Figure 43 are the results of these analyses, in this summary are the two main variables affecting the capacity of lateral load of the building, for the variation show up of $f'c$ and E_c.

Summary in the elastic range in [%]			
Variable	Soto-Degraded	RCDF-Degraded	Soto-RCDF
TE	3.09	2.55	0.55
δy	6.23	6.00	1.65
Ec	20.86	20.00	1.07
f'c	37.36	36.00	2.13

Table 13. Variation in the elastic state due to the properties f'_c and E_c of the RC

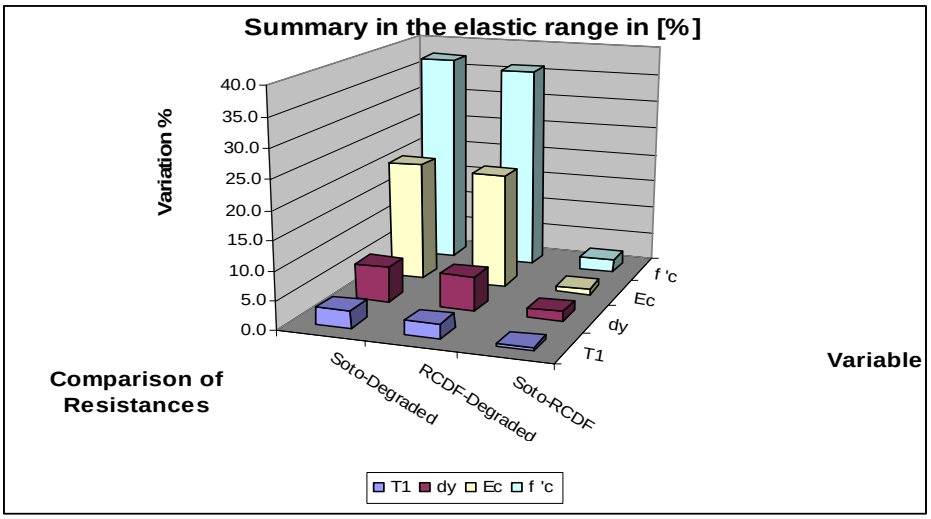

Figure 43 Variation in percentage due to variables of f'_c and E_c of the RC

From the database [SAS, installed in the State of Guerrero] with a total 3600 real records acceleration, for the historical background discussed in the Table 7 and Table 8. We have considered all seismic events with magnitude greater than 6, as shown in Table 9 and Table 14. We have shown the total number of earthquakes occurred in the survey area from the year 1985 with magnitudes large than 5.

History of the seismic events in the State of Guerrero, Mexico between the period from September 19, 1985 until October 12, 2009			
Year	Range, 5 until 5.99	Range, 6 until 6.99	Range, 7 until 8.1
1985	1	1	1
1986	1	1	---
1989	4	1	---
1990	6	---	---
1993	3	1	---
1994	2	1	---
1995	1	---	1
1996	1	1	---
1997	1	1	---
1999	3	1	---
2001	4	---	---
2002	3	---	---
2004	1	1	---
2006	2	---	---
2007	5	1	---
2008	3	---	---
2009	4	---	---
Totals	45	10	2
From January 1, 1998 until October 12, 2009. There have been 995 Seismic events of magnitude in the range of 4 to 4.99.			

Table 14.History of the seismic events in the State of Guerrero, Mexico, in the period between September 19, 1985 until October 12, 2009.[78]

In the years, (1991, 1992, 1998 and 2005), the registers earthquakes did not exceed the magnitude of 5.

Having greater resistance in the materials induces bigger intervals in the displacement. The displacement values can be found even in the elastic range, but when the opposite happens, it is necessary to observe that it happens with the ductility of the building of which it will be discussed in the relation of the two following topics.

With the observations of the response of the buildings seismic behavior in the linear range and variations due to changing in the properties of the concrete materials in conjunction

with the uncertainty generated by an earthquake, we observed the variation of displacement, characteristic periods of ground and buildings.

4.4 Results of Static Adaptive Pushover Analysis [Displacement-base, DAP]

The software SeismoStruct was used, [S. Antoniou and R. Pinho, 2004].

The results show a variation of 1% between the resistances to the basal shear maximum of the buildings with the resistance of Soto for the State of Guerrero in comparison with the resistance of the Regulation 2004 [RCDF], as shown in Figure 44.

On the other hand, when the structure is deteriorated, the comparisons between this resistances degraded with respect to the previous two is at a minimum order of 5% and a maximum value of 23.4% of variation.

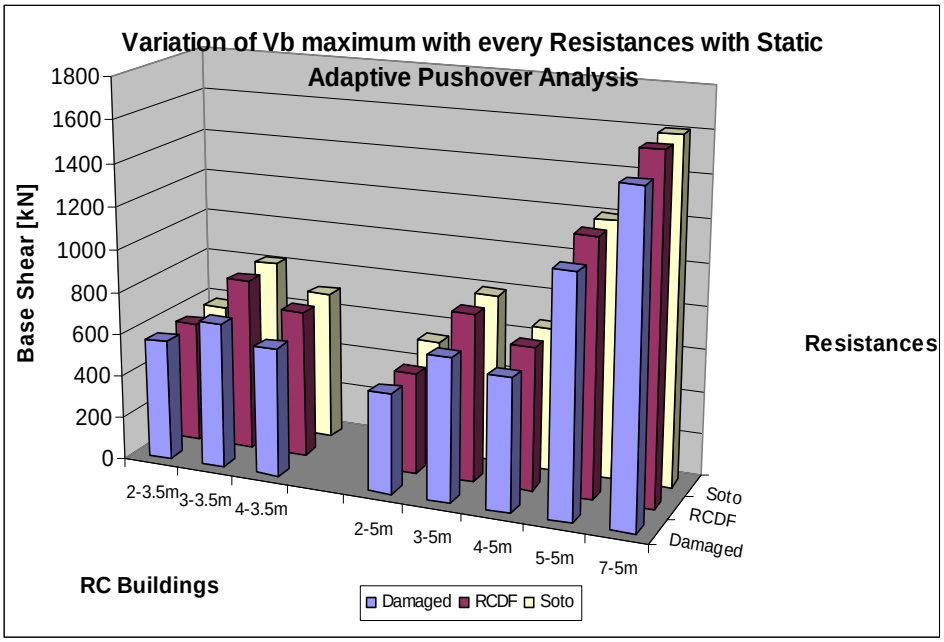

Figure 44 Variation of the lateral capacity of the maximum basal shear.

With the pushover curves, we obtained two important parameters to consider. Actually, the consequence of change in materials properties of concrete show that the interest of this analysis is, mainly measured by ductility of the buildings and their capacity to resist shear.

Therefore, in the following sub-theme, which is the most important in the pushover, we present the results of the ductility parameter.

4.4.1 Ductility in the buildings

With the previous theme, we can find the relations of the building ductility.

In buildings with two levels with the restrictions make by [regulation 2004], about the size of the section of structural elements, this causes great stiffness. We compare these same buildings, when adapting a different separation between columns: One of them has a 5m separation ductility of 47%, and the other with its 3.5m ductility is of 26%. So we can conclude that the more rigid buildings have lower ductility and therefore increasing their likelihood of collapse, as shown with the building of 2 stories in Table 15

Static Adaptive Pushover Analysis [Results with the DAP]			
RC Building	RCDF Ductility ((δu-δy)/δu)*100	Soto Ductility ((δu-δy)/δu)*100	degradation Ductility ((δu-δy)/δu)*100
Building with separation between columns of 5 m.			
2 Stories	47	44	44
3 Stories	82	81	84
4 Stories	70	71	70
5 Stories	28	28	23
7 Stories	67	67	67
Small building with separation between columns of 3.5 m.			
2 Stories	26	26	29
3 Stories	85	85	86
4 Stories	73	74	74

Table 15.Ductility developed by the proposed buildings

As for other buildings that have more levels, looking at the dimensions it has in sections of the beam-column shown in Chapter 2. We can see the following: when it is gradually decreasing as the sections in the case of buildings with three stories; (where each level has a different section of column), it helps to reduce the weight and therefore the mass of the stories, that generates a minor force of inertia that damages the structure. It is also found that the stiffness decreases, but the benefit is more significant for the reduction of structural mass in the stories. The section of beam is constant at all levels of this building. It can be concluded that this building had the best performance due to the gradually increased load by pushover, in both cases; in the building with three Stories and separation between columns of 5m and 3.5m are obtained the better structural behavior.

For the 4 stories building we proposed two sections of columns and maintained the section of beam for all stories. The building is symmetrical in plan and has the same height for all stories levels. It results in decreasing slightly ductility with reference to the

building, so that it can be concluded that this is the second building that showed better ductility.

The building of 5 levels, remained with the same section of beam for the entire building and on the column sections of a change in the stories section of the first second after switching section to the fourth level, and finally from fourth to fifth level. It is observed that the maintenance section of beams in buildings, that are growing vertically, is not recommended as decreasing the ductility in this building up to 28% by purpose of maintaining the beams.

Finally, in the building of seven stories, the changes in the section of beams and columns are gradual. For the first three stories, we long undamaged the two sections of beam and column. Fourth and fifth suffered slight decrease sections of both structural's elements. Finally, with the same decreasing trend for the last two levels, it produces a 66.7% of the ductility level in this type of building.

4.5 Results with the method of the Incremental dynamic analysis – [IDA]

In this dynamic analysis of the increase (IDA), the records were taken from real acceleration and entered into the software. Before starting the analysis, where there is we can change the registry values through a factor.

The characteristics of this type of analysis were described in Chapter 2. In the Chapter 3 are detailed the real records of acceleration in Gals and their response spectra as well as their absolute ground acceleration as a fraction of gravity. We aim to compare the spectrum of design (see Figure 28 and Figure 3).

As mentioned above in Table 15, it can be said that the results achieved since the first increase in the acceleration of the seismic event, result in great efforts in building. It cause serious damage and initiation of the plastic of hinges. In Figure 45, shows the roof displacement at the node of interest in the buildings at the station for the seismic event of PAPN with the magnitude Me = 6.5. The Buildings supported the first increase of the acceleration in real seismic record and their period of the ground, as is very small and approaches the characteristic period of the buildings [see Table 10 and Table 9]. This behavior occurs also with the same event for the station accelerographs with the name of PETA.

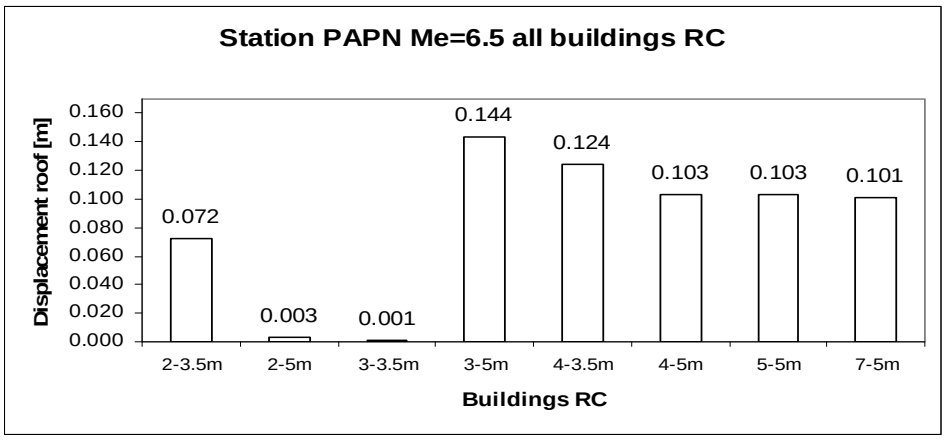

Figure 45 Observing the displacement of roof with the first increase in acceleration for the station PAPN of magnitude Me = 6.5.

We can see that the structures have probably collapsed because of the amount of displacement in the roof of the buildings referenced: 2-3.5m and 3-5m.

In the Incremental Dynamic Analysis of these displacement values are very superior to the displacements calculated with the method DARS and to the displacement of the Static Adaptive Pushover Analysis. It is certain that if an earthquake with a magnitude Mw = 8.1, occurs with the epicenter located near the buildings will suffer considerable damage and this will cause the total collapse. The most vulnerable buildings will be the smallest, those that are near the period of the ground, that is to say, the buildings 2, 3 and 4 levels. For this study, it is checked using the model that the building with minor space between columns will collapse more quickly than the buildings with the smaller space between columns.

If the period of the structure is on the flat part of the design spectrum, the constructions regulation suggests not making any reduction of seismic force that is induced into the building. However, the value which characterizes the seismic coefficients of the spectra is really very big [see Table 6]. The Engineers use a value of seismic behavior factor that reduces the seismic force design spectrum. This value, must have certain characteristics, for example, we can mention: Regularity, Material used and Types the connections between them, see Figure 46.

Therefore, the most common is that engineers, to minimize costs, respect the criteria to reduce the strength of the design spectrum. Then, the value that is most commonly used

for the factor of seismic behavior is Q = 2. This value that does not require other more rigorous review, this would reduce the spectrum as shown in Figure 46.

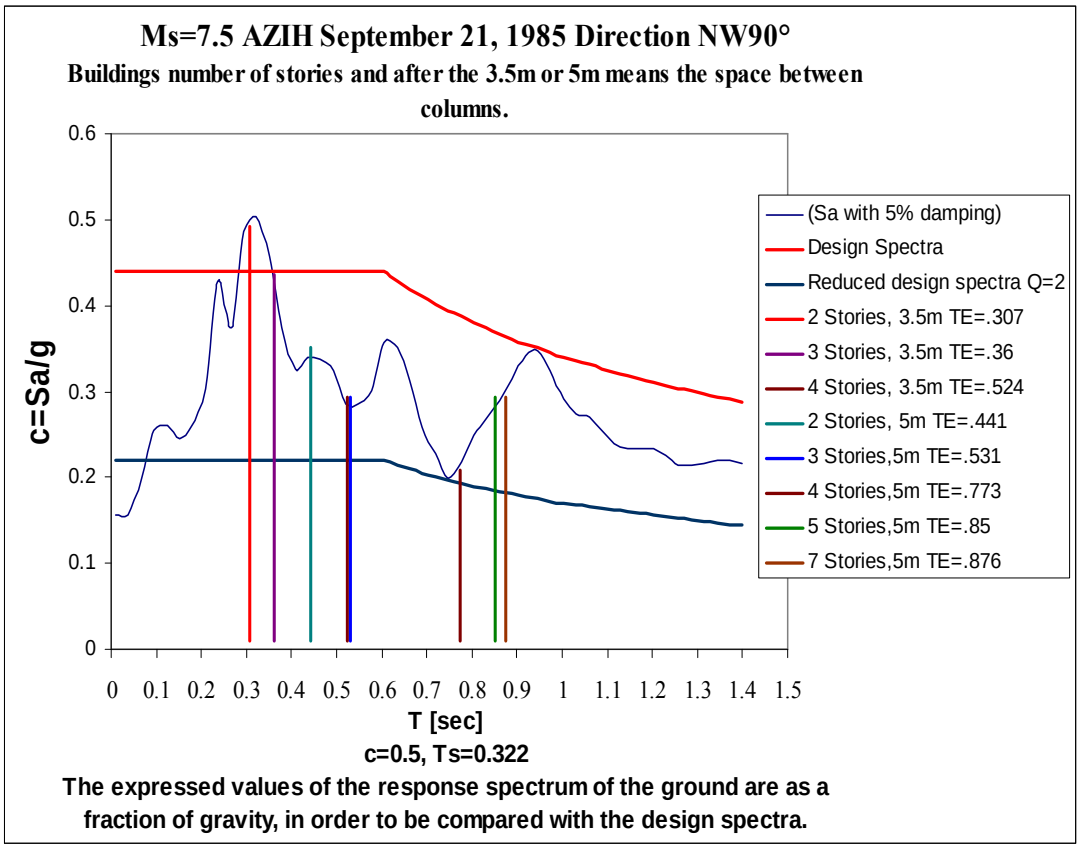

Figure 46 Parameters of the soil and the buildings.

Here, we can observe that the unscaled acceleration record has a distance from the station accelerographs to the epicenter of 46 km. We can notice, that all response values of the buildings pass the value of the seismic reduced coefficient, which implies that buildings entered the inelastic range, but the ductility that these buildings have to help them minimize the impact of a sudden collapse. Some small buildings if they suffer great damage, as shown in Figure 5. Others more if they collapse. In this Figure 46 shows that the building of two Stories with 3.5 m separation between columns is close to collapse by the phenomenon of resonance.

4.6 Indexes of reliability.

The effects of site that were observed are in relation to the characteristic period response of the ground [Ts] with the mean period of the ground [Tm]. As an example of these site effects, we present the seismic stations with the name and AZIH and PAPN, comparisons

in the same direction, but with different magnitude and distance to the epicenter. A second observation is carried out for the same seismic event of magnitude Ms=8.1 at different distances from the epicenter, and then we will present in the next figures.

a) Site effects considering different magnitudes, duration and different distances from the epicenter to the station of the accelerographs, to see Table 16.

With the special attention, we should observe the station AZIH, where we locate the accelerograph. The first event happens in the area of the trench with magnitude Ms=8.1 and duration 72.74 seconds, and its aftershock come two days after in the seismogenic zone with magnitude Ms=7.5 and duration 57.47 seconds. This last earthquake presents several peaks of the spectrum pseudo-acceleration of the ground that characterize it, presenting a great uncertainty even for buildings that can end up having up to 12 stories, see the following figure.

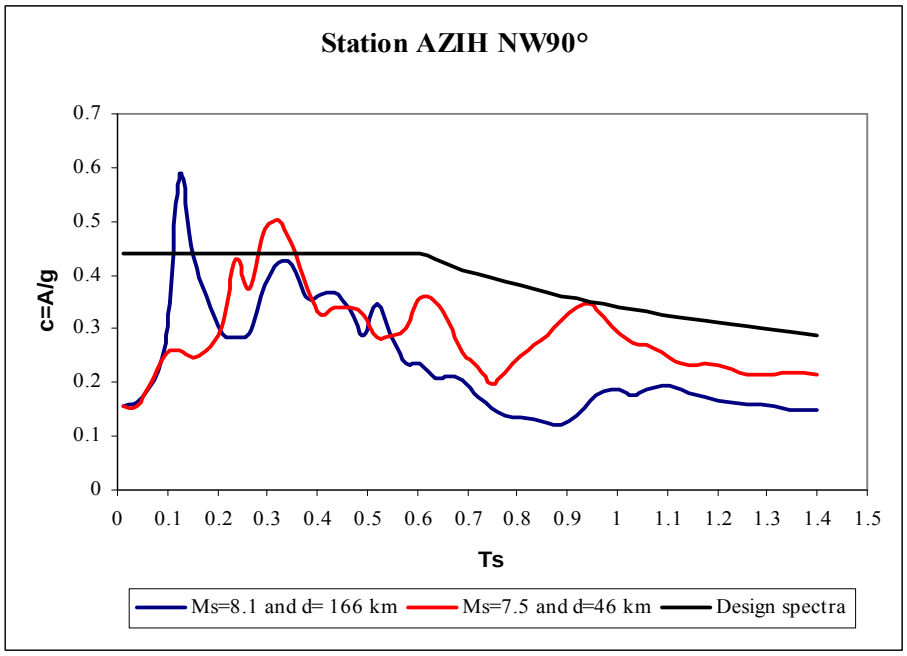

Figure 47 Site effects in the station AZIH with different magnitude and distances from station to the epicenter.

The same procedure performed with PAPN station, but contrary the previous station, the seismic events of great magnitude Ms=8.1 and Ms=7.5 is located very retired of the station of the accelerograph, to see the following figures.

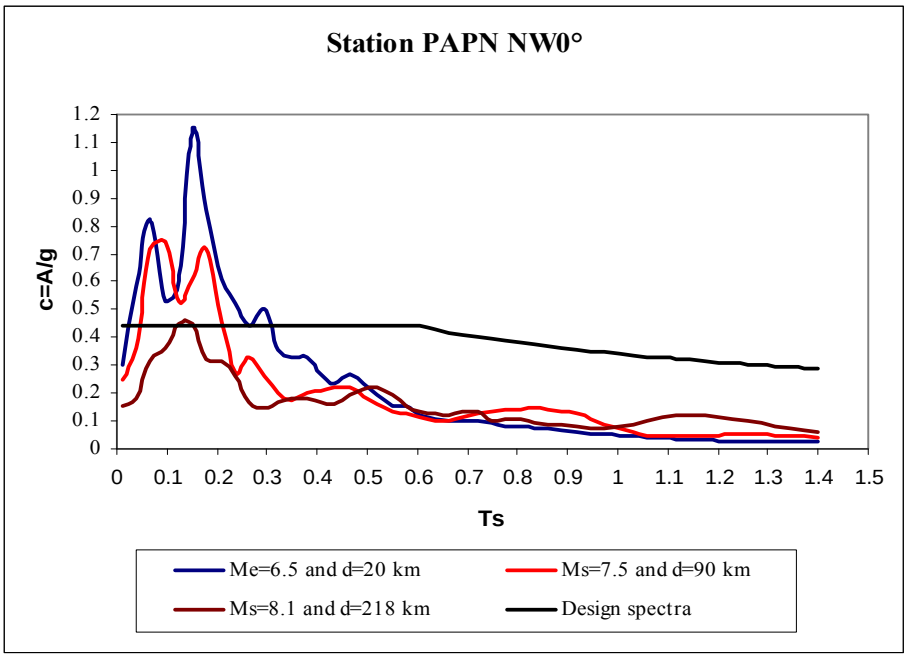

Figure 48 Site effects with different magnitudes, distances and duration, station PAPN NW0°.

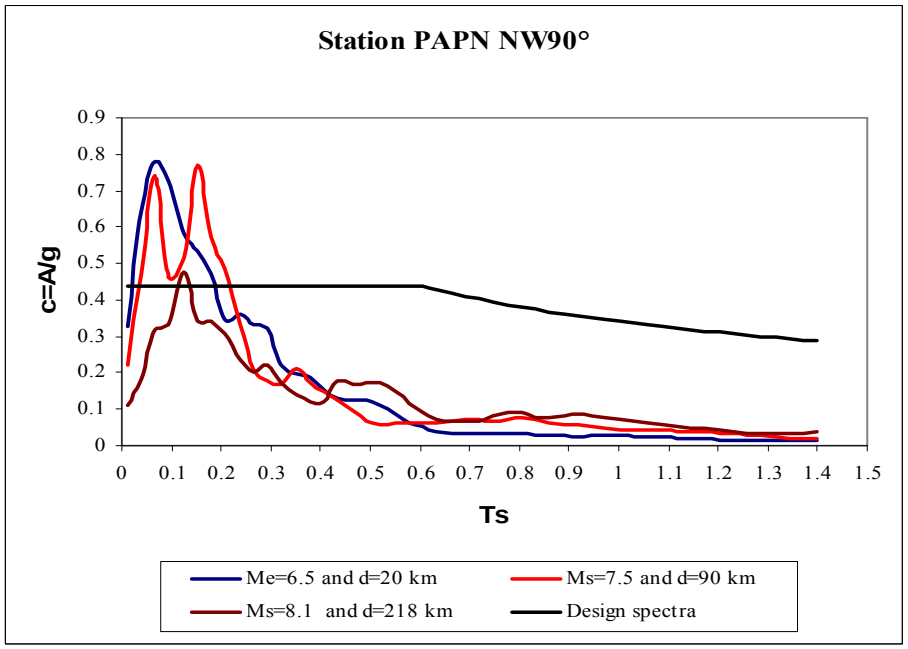

Figure 49 Site effects with different magnitudes, distances and duration, station PAPN NW90°.

b) Site effects considering the distance

Observing the values of the Table 10 of the item 4.3, for the same seismic events Ms=8.1 we present the following figures.

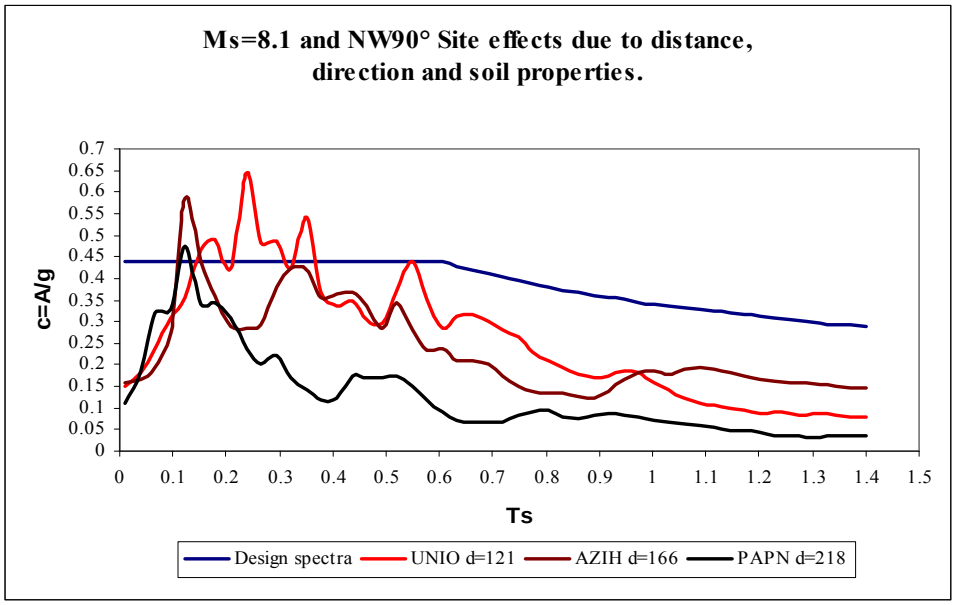

Figure 50 Site effects for Ms=8.1 at different distances, direction NW90°.

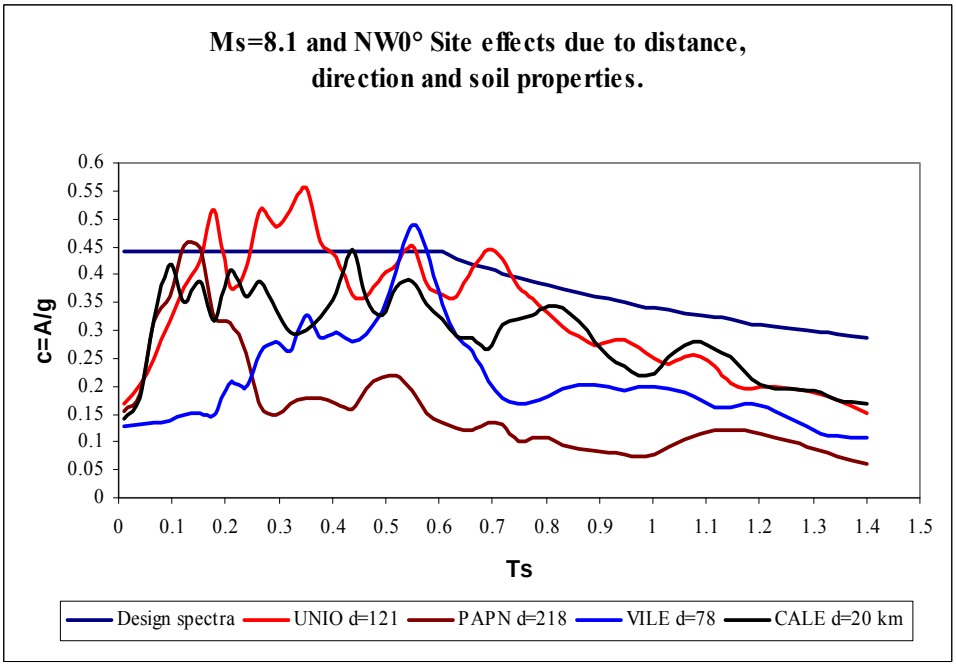

Figure 51 Site effects for Ms=8.1 at different distances, direction NW0°.

We should remember of the Figure 39 that this seismic event occurred in the trench, where the subduction area begins and it is the only event that is registered with this magnitude. We can see there is great uncertainty and for this reason, we presented below two other parameters that we would help us to interpret the variation of the indexes of reliability next.

T_S Is the predominant period has been commonly employed in earthquake engineering to characterize an equivalent seismic loading on a structure from the earthquake ground motion. Usually, this spectrum of response of pseudo-acceleration is represented by its maximum value, calculated with damping ratio of $\xi = 5\%$.

T_m Is the mean period, it was proposed by Rathje et al., [1998], is the best simplified frequency content characterisation parameter, because it takes in consideration all time-history, the duration and the content of frequency.

Then:

Magnitude	Seismic Station	Direction NW90° Ts [s]	Tm [s]	Direction NW0° Ts [s]	Tm [s]	Distance to epicenter [km]
Me=6.5	PAPN	0.066	0.114	0.150	0.157	20
Ms=7.5	PAPN	0.150	0.140	0.090	0.169	90
Ms=8.1	PAPN	0.120	0.222	0.120	0.264	218

Magnitude	Seismic Station	Direction NW90° Ts [s]	Tm [s]	Distance to epicenter [km]
Ms=8.1	AZIH	0.120	0.537	166
Ms=7.5	AZIH	0.320	0.427	46

Table 16. Effects of site that change the index of reliability in the buildings.

The index of reliability that are observed in the following figures, vary with:

- Magnitude of seismic events: This can be observed by comparing the Figure 52 to Figure 54. This shows that the lower the magnitude of the event, the greater reliability indices of the buildings.
- Duration of the seismic event, as shown in Figure 12, that the greater the seismic magnitude and duration of the seismic event, the bigger is the damage to the building.

To better understand the results of the index of reliability in the buildings, then we present the response spectrum of the ground [See Table 10 and Table 12]. In order to clarify idea the site effect phenomena. This table was ordered from highest to lowest value of the Figure 69b to Figure 77b [Annexe 3]. The figures are comparing with the spectrum of design, see Figure 28. That to enveloped to put the Figure 28. on the Figure 69b to Figure 77b, gives the results as the Figure 3. This explains the great damaged and collapse in the city of Mexico in the year 1985.

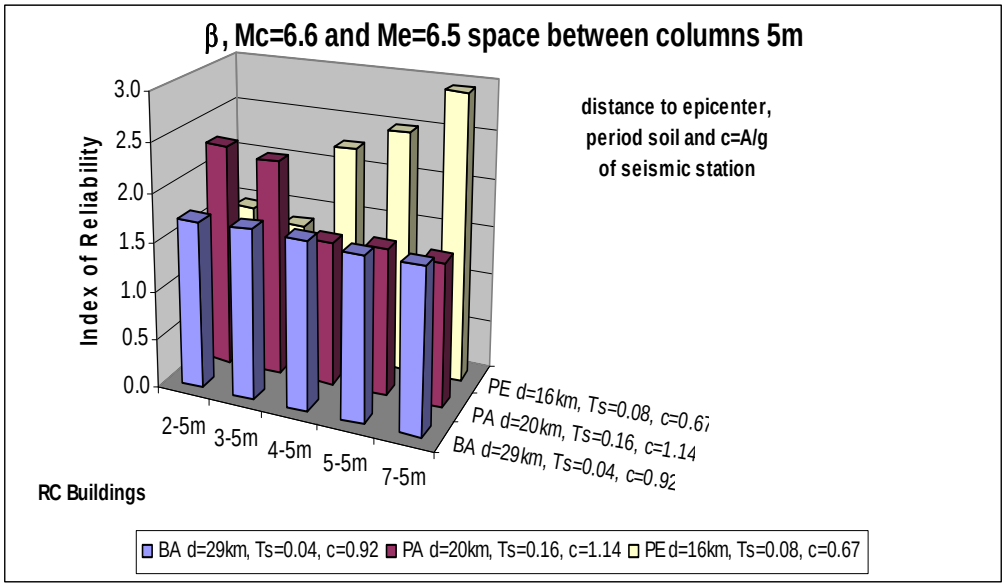

Figure 52 Index of reliability of RC buildings with separation between 5 meters columns, once submitted to the force seismic action in the base with M<6.7.

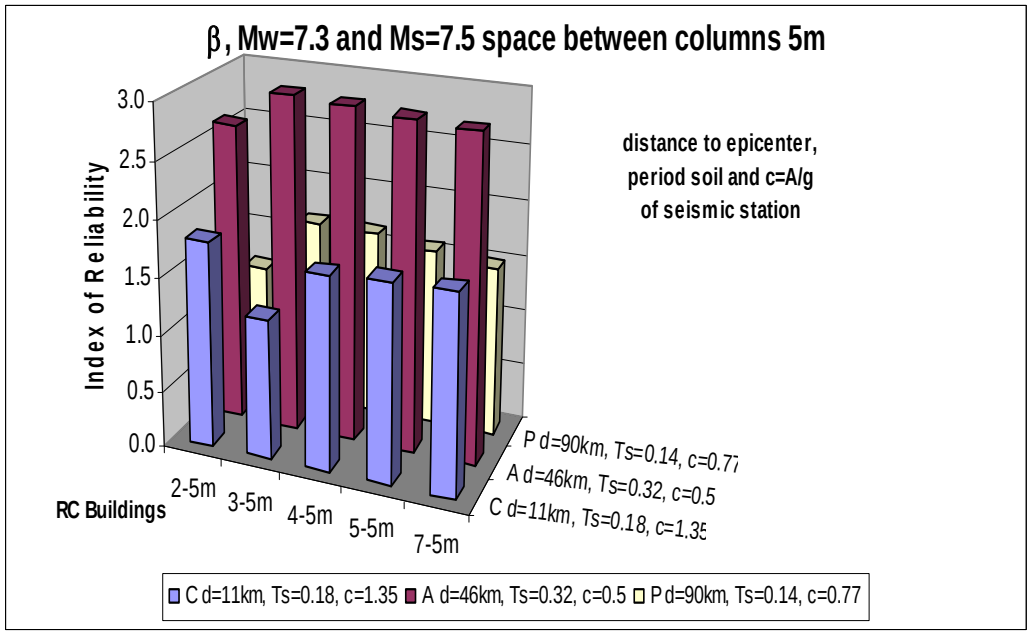

Figure 53 Index of reliability of RC buildings with separation between 5 meters columns, once submitted to the force seismic action in the base with M<7.6.

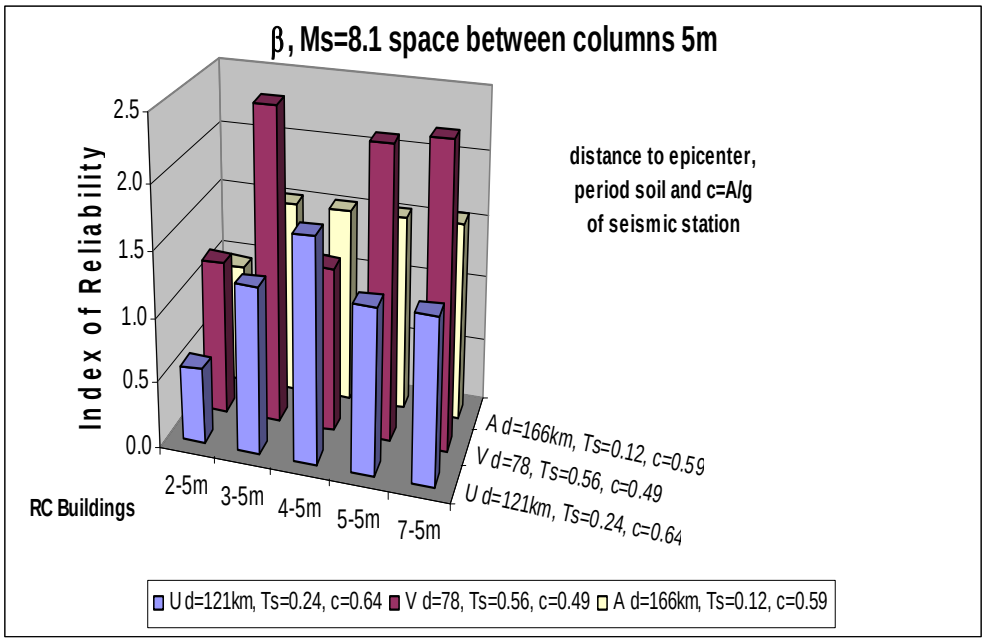

Figure 54 Index of reliability of RC buildings with separation between 5 meters columns, once submitted to the force seismic action in the base with M<8.2.

The effects of the site of the ground characteristics, has influence significant in the response of the building, as shown by Figure 54 with the building of three stories. It should also be noted that the column sections of the building were reduce gradually with/height. This enabled a reduction of inertia forces that helped significantly to improve its ductility and increase the level of security in the building.

Then, we can say that in the case of Ms = 8.1 seismic event occurred at the seismic station of Vile, the response characteristic of the soil gives a value of Ts = 0.549 seconds. But the Sa/ g = c has a value of 0.49 [see Figure 77b]. Comparing this value with the spectrum of design shown in Figure 28. We see that there is a small difference shows, that it to say, 0.49-0.44 = 0.05, equivalent to 10%. But returning to the Figure 28 we see that the spectrum of design begins to decline at a value of Tb = 0.6, where Tb is the boundary that includes the regulation of a spectrum of response characteristic of the soil to the ground type I, considered as hard.

In Figure 52, we can observe the effect of site because as the characteristic period of ground [Ts] is very small, the buildings 4, 5 and 7 stories, which have a period of the structure [T_E] bigger to that of the ground, as a result presents great index of reliability. In this sense, we can go to observe the same trend with the other figures. However, when the

periods of soil and building closer, they come closer to the phenomenon of resonance that makes collapses of buildings and their index of reliability decreases.

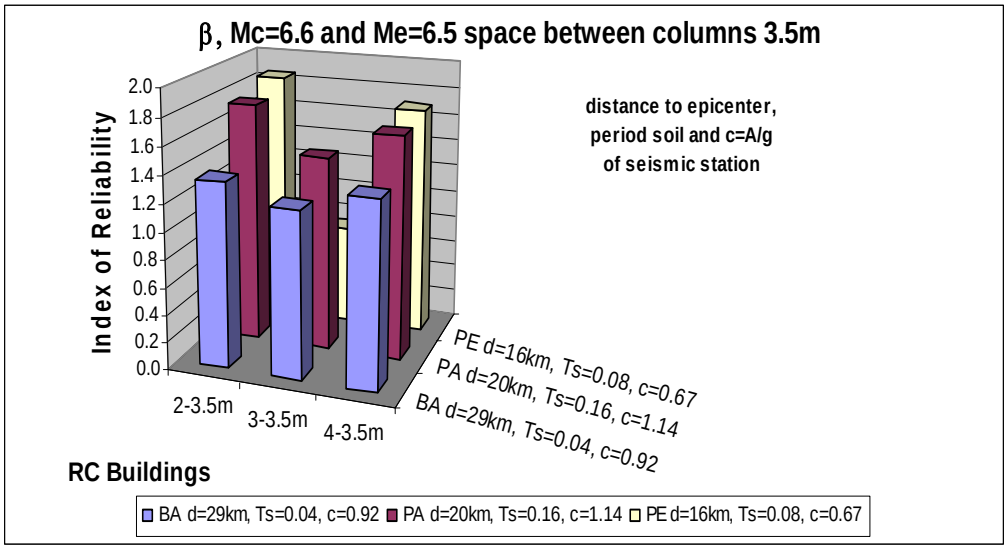

Figure 55 Index of reliability of RC buildings with separation between 3.5 meters columns, once submitted to the force seismic action in the base with M<6.7.

When we decrease the space between columns for the small buildings, the stiffness grows and this reduces their the probabilities of surviving a seismic event with near epicenter and major magnitude to M≥6.6. As shown in the Figure 55 up to Figure 57.

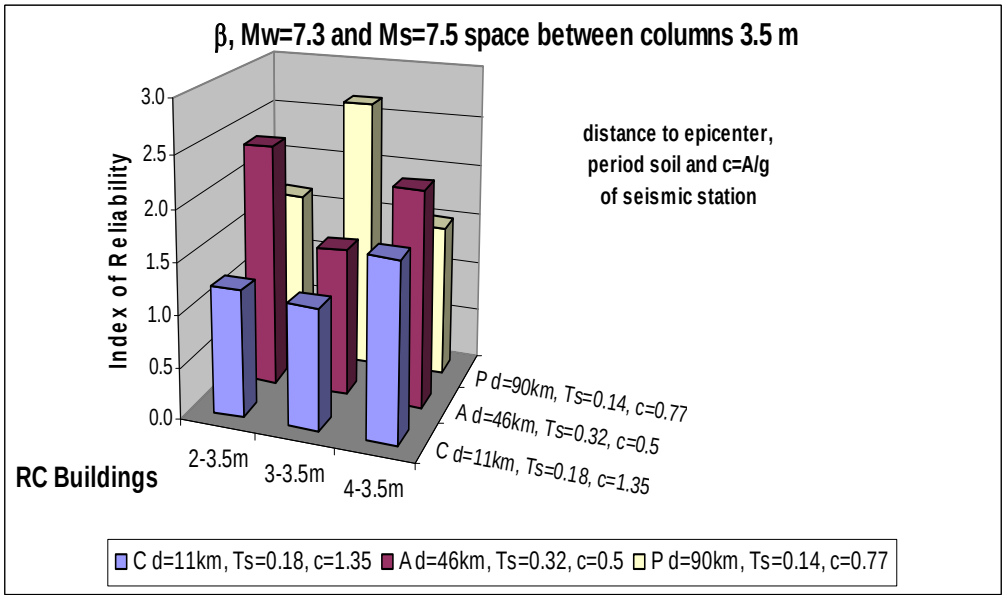

Figure 56 Index of reliability of RC buildings with separation between 3.5 meters columns, once submitted to the force seismic action in the base with M<7.6.

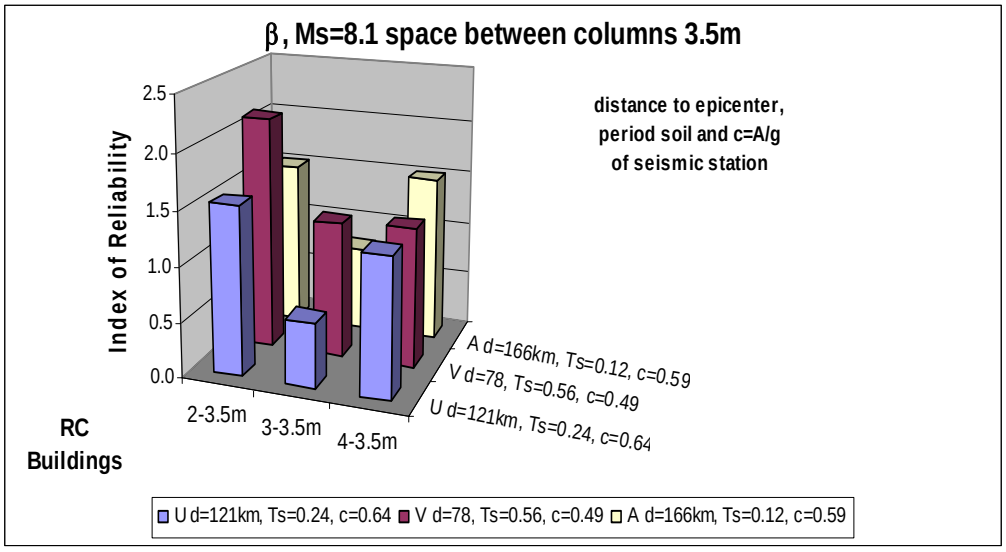

Figure 57 Index of reliability of RC buildings with separation between 3.5 meters columns, once submitted to the force seismic action in the base with M<8.2.

The buildings fundamental period of 3 stories is T_E = 0.531s. So that we could secure a possible state of resonance of the building. But with the ductility developed by the building and the status of the site effects, the structure presents a high security. This same behavior had for the building of 2 levels, presenting a high level of reliability, but for being away from the characteristic period of soil for the same seismic event of the Station VILE, to see Figure 57. The following figures show the index of reliability with degradation in the buildings.

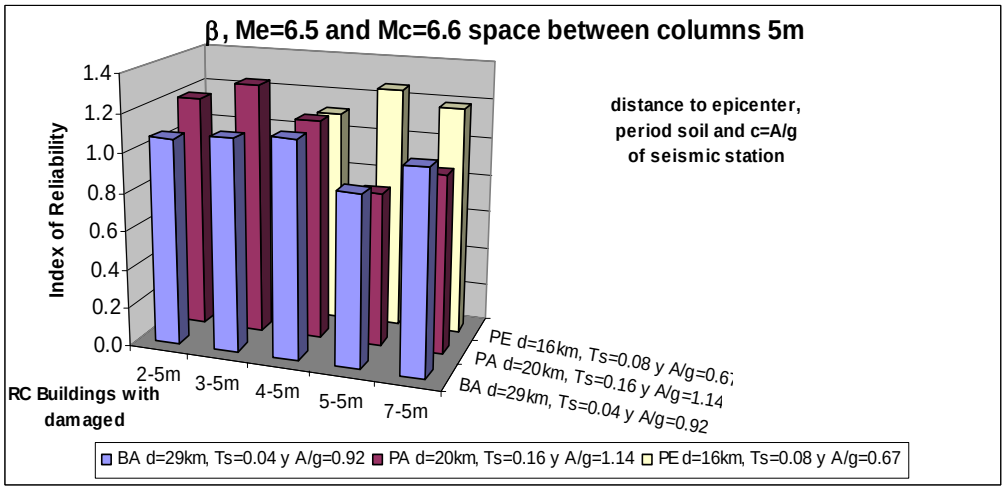

Figure 58 Index of reliability of RC building with degradation and separation between columns of 5 meters, for the earthquake with M<6.7

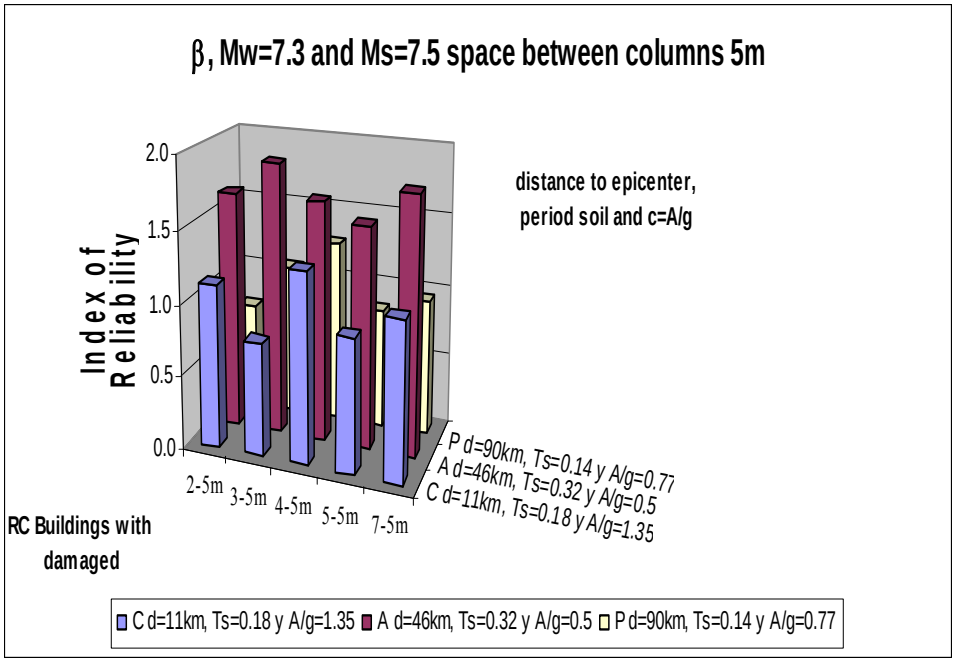

Figure 59 Index of reliability of RC building with degradation and separation between columns of 5 meters, for the earthquake with M<7.6

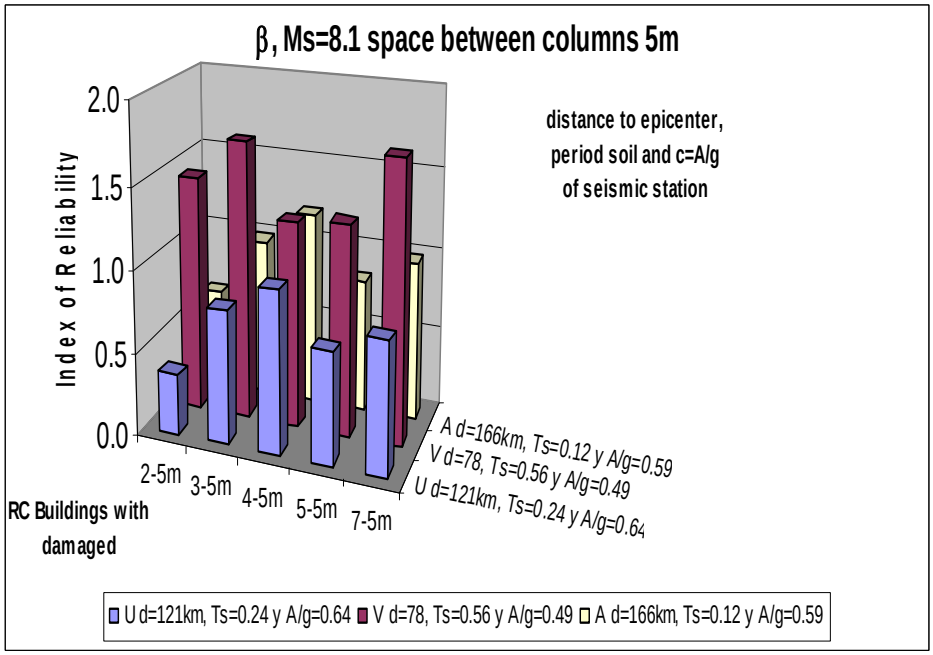

Figure 60 Index of reliability of RC building with degradation and separation between columns of 5 meters, for the earthquake with M<8.2

And for the building with space between columns of 3.5 meters we have:

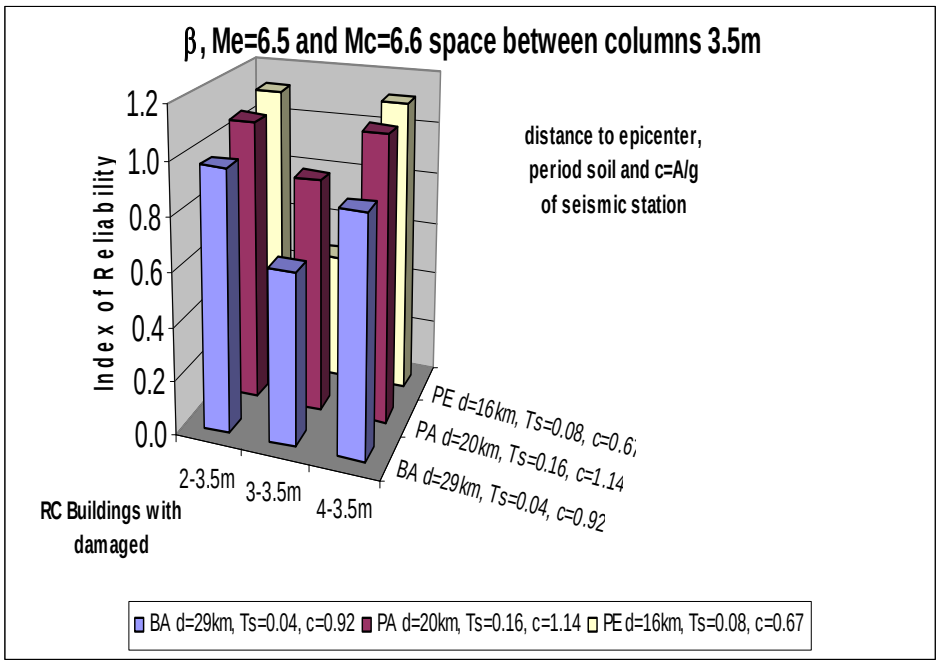

Figure 61 Index of reliability of RC building with degradation and separation between columns of 3.5 meters, for the earthquake with M<6.7

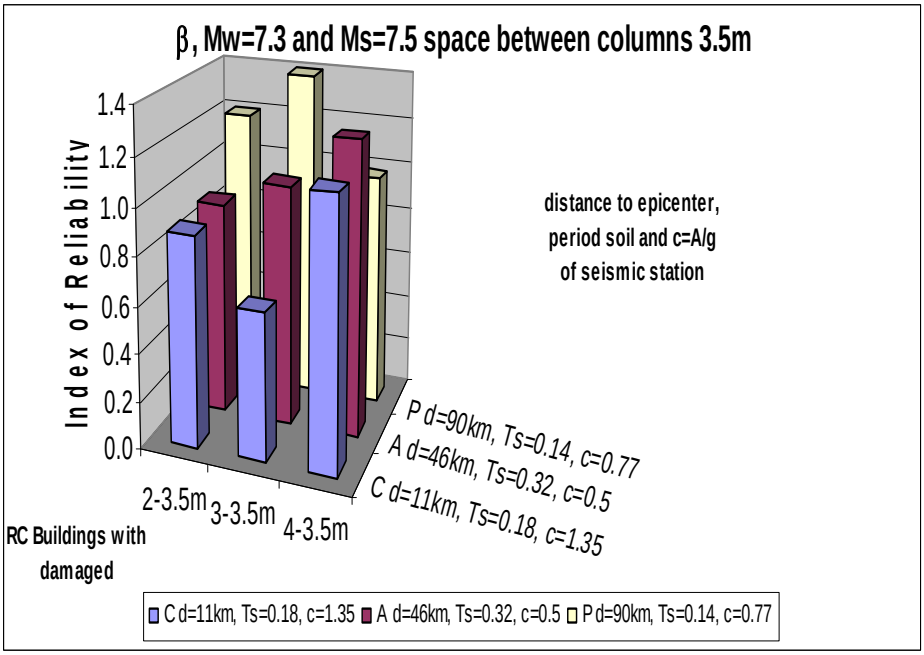

Figure 62 Index of reliability of RC building with degradation and separation between columns of 3.5 meters, for the earthquake with M<7.6

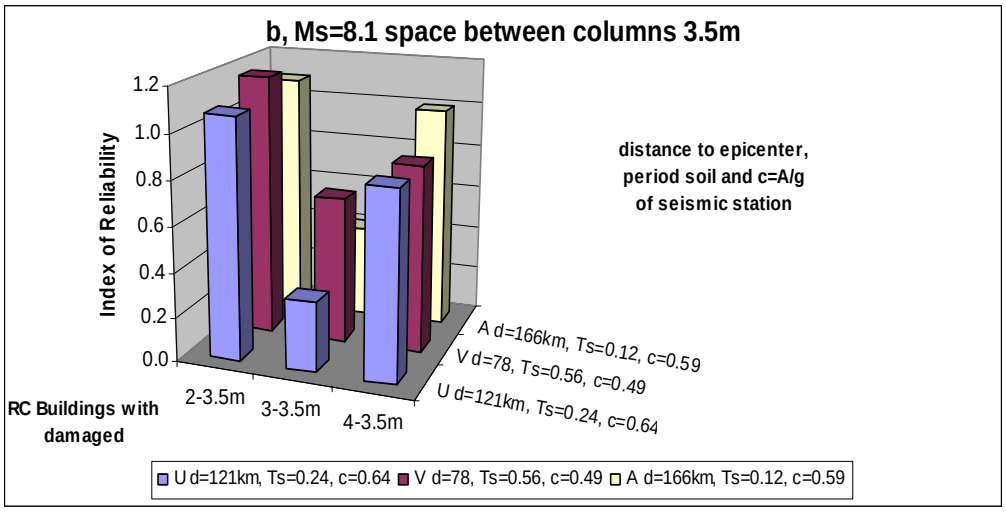

Figure 63 Index of reliability of RC building with degradation and separation between columns of 3.5 meters, for the earthquake with M<8.2

The indexes of reliability for the buildings that were degraded, diminished considerably their possibility of survive a seismic event at near source. The behavior is shown in Figure 58 up to Figure 63. The results do not follow a trend which we emphasize, because the site effects in the field vary. Each earthquake has a content of frequency that depends on the Magnitude, topography, duration, according to the type of terrain.

(Bruce R. E. and Kanda J., 2005), based on the Eurocode 1, published in their book "Safety and Its Quality Assurance", some reliability indices based on the consequences for the loss of human lives and economic conditions, as follows:

- CC3. High consequence for loss of human life or economic, social or environmental consequences very great
- CC2. Medium consequence for loss of human life or economic, social or environmental consequences considerable
- CC1. Low consequence for loss of human life or economic, social or environmental consequences small or negligible.

Reliability	Target values for β with your reference periods	
Class	1 year	50 years
CC3	≥ 5.2	≥ 4.3
CC2	≥ 4.7	≥ 3.8
CC1	≥ 4.2	≥ 3.3

Table 17. Recommended target reliability in structural Eurocode. [13]

In the Annex A, the French norm, AFNOR (1996), Eurocode 1, in Table 18:

Status Limit	Index target of reliability duration of use of project	Index target of reliability One year
Last	3.8	4.7
Fatigue	1.5 to 3.8[1)]	--------
Serviceability (irreversible)	1.5	3
1) Depend on the level of reliability, of reparability and tolerance to the damages.		

Table 18. Indicative values of index target of reliability β [1]

The values in Table 17, are the indexes of reliability for 50 years. Of the lifetime calculations for this study are higher, than the tangent indicated by the French norm [1996], of Eurocode 1. We observe the index of reliability for duration of project specifications in of 100 years, according to Mexican regulation 2004. We consider the type of buildings selected, then we can say that for most of the buildings with real resistances [Soto and RCDF]. They are in the acceptable range. The values show some reliability index slightly low. They correspond to the cases when the period of the structure is close to the ground. This can be explained by the resonance phenomenon that increases the probability of collapse in the building.

The buildings that have suffered degradation, according to Table 17 and Table 18, show unacceptable level of index of reliability. That is to say, it is very unlikely that these buildings will survive a seismic event of magnitude higher than $M \geq 6.5$, as Figure 58 show the Figure 63.

4.7 Summary

With the index of reliability obtained, we have precise ideas of the factors that affect most the structural behavior for the region of the state of Guerrero. However, to be able to accomplish affirmations to the 100% effective, we would require more seismic events with similar characteristics. As the Site effects have influence on the movement of the ground, the important parameters are: content of frequency of each earthquake, the duration, in some cases the amplification of the wave, topography, soil hardness, the distance and depth of the seismic event. We could see the Figure 47 until the Figure 63.

The parameters that may affect the structural behavior of the building are: the orientation of the building, type of foundation, the construction process and the properties of their materials. However, with the obtained results we can indicate the general conclusions, according to the results of this chapter and with the references indicated of the Eurocode 1 and Bruce R. E. and Kanda J., 2005.

Chapter 5 Conclusion and recommendations

The study consists in an analysis on the great seismic hazard for the extensive coastal region of Guerrero, Mexico. We define the Geometry of the survey area with greatest seismic risk. We calculated the distances more unfavourable due to the seismic event in the Guerrero State, as there is a seismic GAP. The most important cities that are therein are localized in Guerrero State, to which correspond the worst-distances:

"Acapulco [15 km], Ixtapa-Zihuatanejo [59 km], Chilpancingo [67 km], Ometepec [62 km] and Tierra Colorada [27km]".

The seismic GAP of $220x90km$, is so that may the expected earthquake of Mw = 8.4. According to historical earthquake records in the region, can have magnitude period of return for major seismic events is likely to be found in a range from 35 up to 70 years. This show the importance to the topics considered in the present thesis project.

On the bases of a total of 3600 records, we have selected the seismic event with magnitude $M \geq 6$. The processing of the seismic records (acceleration records) was performed with the software Degtra and Seismosignal in which we observed: near epicenters, duration of earthquakes, depths, contents in frequency that to cause very quick variation of the amplitudes for given magnitude on some ground categories. Therefore the records of real acceleration once selected, provided large values than the spectra design of the constructions code for the Guerrero State, Mexico.

For the survey zone, the characteristic response of the ground, gave results of characteristic periods ranging from Ts=0.034 to Ts = 0.36 seconds. A selected size of the buildings samples is then calculated in order to perform a sensitivity and reliability analysis.

A smaller separation between the spaces of the columns increases the stiffness and the likelihood of a more abrupt collapse, for the structures between 2 up to 4 levels which have characteristic periods near the period of the soil.

With the method of Static Adaptive Pushover Analysis, we see that the lateral load capacity in the building is seriously affected by a high coefficient seismic design, because it changes the parameters of flexibility that can develop a structure. This also shows that the ductility varies in proportion to the geometric sections of the structural elements that increases or decreases the mass of the building.

The results of the displacement method with IDA have already exceeded the permissible values stipulated in the regulations [2004]. Whereas the recommendations advises that if the ground accelerations are greater than 150 Gals, the specifications of the regulation should be revise. Almost all the selected records accelerations violated the permissible limit. Furthermore, the seismic coefficient that is obtained by calculating the response spectrum of the ground are very higher.

The indexes of reliability according to the proposed limit state function are evaluated for some selected seismic events and for some buildings in a state limit of fatigue, but they are still within an acceptable range.

The main factors that affect the indexes of reliability are:

- The site effects
- The ductility to be developed by the building. This may in some cases define the level of survival for the structures. The limit size for the section in the regulation [2004] stipulates that column, mainly damages the dynamic response of the buildings of 2 stories and more damage is observed for the building with a separation between axes of columns of 3.5m.

With respect to the earthquake, we have the variables:

Content of frequency and the PGA, i.e.:

We observed great changes that happen on the ordinate of pseudo-acceleration [Sa], that make vary to the characteristic period of soil [T_S]. The content on frequency into from the quake, to affect the variation from the mean period [Tm] has increased compared to the period dispersion characteristic.

With respect to the distance (between the City and the epicenter), duration and magnitude, we have:

The consistency of the soil has influence in to the amplification of the seismic wave, which is directly related to the magnitude and duration of the quake, it does change the characteristic period of ground a short distance with different magnitudes. This same tendency is reflected with the dispersion between the characteristic period [T_S] with respect to the mean period [Tm].

In Reference to the buildings, the indexes of reliability varied due to:

The properties of the materials that is, one of the main objectives in this research, so when we observe the variation in the seismicity, although there is little variation in reference to f 'c, in percentage it has a value of 2.13%. In the displacements, this variation is almost twice. The other uncertainties are about the geometry in the structural element and the architectural distribution.

For example, an important aspect of the buildings of 3 stories is: that projecting the dimensions of the sections of beam-column elements so as to gradually reduce the height of a story when passing at the following level, it provide a better structural behavior, as seen in the ductility of the and some indices of reliability.

When the buildings have suffered degradation from past seismic events, the values of reliability indices are reduced by over 50%.

The site effects are of vital importance in the behavior of the structure. This effect changes significantly the indexes of reliability. In order to define more accurately the results, we need to have more available seismic events with great magnitude earthquakes in the seismogenic zone. We will know better the structural behavior, as the response of the soil changes a lot. Only two seismic events with magnitude Mw = 7.3 and Ms = 8.1, occurred in the zone of the trench. The only event in the seismogenic zone was the earthquake aftershock of September 21, 1985, with magnitude Ms = 7.5, which caused several buildings collapse, as many were partially damaged by the quake occurred two days earlier with a magnitude Ms = 8.1.

If there is a seismic event with magnitude of Mw=8.1 or Mw=8.4 and with near epicenter, at distances minors than 60 km the following may be observed and we can say according with the Table 18 of the Eurocode 1, in the new buildings, they could enter in the range of the fatigue of the building and/or they can collapse, their level of survival will depend on its ductility and of the response of the ground where was built.

The level of survival of the buildings depends on.

- The earthquake feature: the seismic magnitude, the content of frequency, duration, distance of the epicenter to the cities.

- The buildings feature: the properties of the materials, the geometry of their structural element and their architectural distribution, as has been observed in several countries over the world.

Researchers have mainly focused their studies on the central region of the country Mexico. The main geophysical studies have as objective to measure the seismic wave and as they affect greatly the structural behavior of buildings for that region of the country. We have considered those studies for this thesis to observe the index of reliability for the Guerrero State.

Some recommendations for future study topics related to earthquake engineering in the state of Guerrero, are:

- Complete and provide maps of seismic vulnerability in the most important cities, taking into consideration the age of the buildings and the seismic events that have suffered in their lifetime.
- Perform micro-zoning studies to improve the designing coefficients for earthquake.
- An earthquake of magnitude Mw=8.1 would generate tsunami. This may cause a wave threatening the structures close to the seashore.
- Consider the aspects of the topography and the effects of the interaction soil-structures in the buildings.
- Include the torsion phenomenon on the buildings and measure the damage it may cause for this zone.
- Establish coordinated works with chemical engineers to study the decrease of steel resistance due to corrosion, in buildings nears to seashore.
- Establish coordinated work with the architects specialized in urban planning in order to define heights of the buildings.
- Obtain mathematic relationships that optimize the cost benefit to the projection of the urbanization in major cities of the Guerrero State.

Annex 1

General explanation of the procedure for obtaining the mechanical Dynamic Analysis of Response to Spectrum

The Mexican Code contemplates the follow load combinations, which are:

$$1.4*(CM \pm CV\max)$$

That is to say:

$$1.4*(CM + CV\max) \text{ And } 1.4*(CM - CV\max)$$

Which is equivalent for two combinations, the same would be for the following equation

$$1.1*(CM \pm CVa \pm CS)$$

That is,

$$1.1*(CM + CVa + CS) \qquad 1.1*(CM + CVa - CS)$$

$$1.1*(CM - CVa + CS) \qquad 1.1*(CM - CVa - CS)$$

Where:

CM is the dead load that considers the concrete volume multiplied by its specific weight, and this also considers the type of material that composes it, for example, the class one concrete needed for this study has a f'c value equals to 250 kg/cm$^{2.}$, and is used mainly for the elements beam-column. The Mexican Code stipulates a superior specific weight of (2.2 tons/m^3 but generally is used the value of 2.4 ton/m^3) 22 kN/m^3 and 24 kN/m^3.

CVa is the instant live load that depends on the use of the building, which is the value that the code assigns, this load is being used to combine it with the induced load produced by and earthquake and wind.

CS is the load due to an earthquake, for which is used the design spectrum.

CVmax is the maximum live load and is employed for the structural design, review of immediate settlements in the soil, and the structural design of the foundation.

With the specifications of the regulation [2004], we explain the process with the building of 5 stories shown in Figure 64 of the analysis of seismic response spectrum, supported in the software manual and developed even more in the books of "Cálculo sísmico de

estructuras" [Alex H. Barbat, 1982] Chapter 4, "Dynamics of Structure" [Anil K. Chopra [2001] Chapter 13.

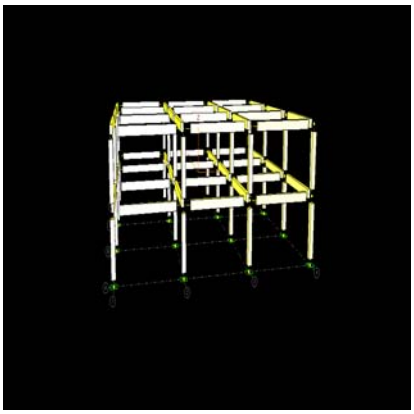

Figure 64 Building of 2 Stories symmetric.[20]

A multi-level structure shown in Figure 64, we can idealize as a multi-tiered porch with diaphragm rigid body assuming that the mass is concentrated at each level [See Figure 65], the columns are supposed to axially inextensible but flexible laterally. The dynamic response of the system is represented by the lateral displacement of the masses with the number of degrees of freedom dynamic o n vibration modes that are equal to the number of masses. The resulting vibration of the system is given by the superposition of vibration of each mass. Each individual mode of vibration has its own period and can be represented by a simple system of the same period.

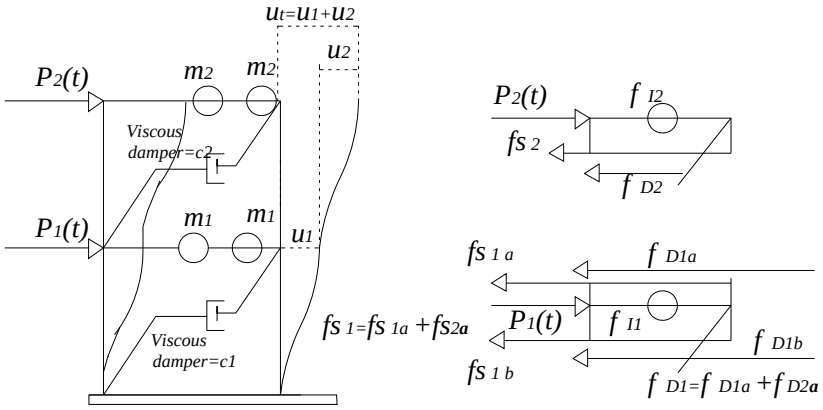

Figure 65 Hypothesis of the concentrated mass, a) Two stories shear frame, b)forces acting on the two masses.[17]

Using Newton's Second Law of Motion, we have the next equations mathematical.

For the masses, of the figure 2b we have:

Each Story represents a massive degree of freedom of a dynamic equilibrium equation is in general:

$$\begin{Bmatrix} f_{I1} \\ f_{I2} \end{Bmatrix} = \begin{bmatrix} m1 & 0 \\ 0 & m2 \end{bmatrix} \begin{Bmatrix} u_1 \\ u_2 \end{Bmatrix} \quad [1]$$

$$\{F_I\} = [M] \cdot \{\ddot{U}\} \quad [2]$$

Where:

$\{F_I\}$ It is the vector of force of inertia,

$[M]$ Is the matrix of mass and

$\{\ddot{U}\}$ is the vector of accelerations.

It should be noted that the mass matrix is diagonal sums for a clustered system, without considering coupling between the masses. In coordinate systems on a more widespread, there is often coupling between the coordinates, which complicates the solution. This is a primary reason for using the method of concentrated masses.

The forces depend on the displacement and using stiffness influence coefficients can be expressed as:

$$K_j = \sum_{columns} \frac{12EI}{L} \quad [3]$$

Where:

K_j It is the lateral stiffness of each element of the buildings.

E Is the elastic modulus, which depends on the resistance of the element.

I Is the inertia that depends on the geometry of the structural element.

L Is the length of each structural element.

With the storey lateral stiffness defined, we can relate resisting forces fs_1 and fs_2 to the displacement interstorey, u_1 and u_2. For one force shear $Vj = k_j \Delta_j$ and the expression for the building of the Figure 65, is:

$$fs_1 = k_1 u_1 + k_2(u_1 - u_2) \quad \text{and for} \quad fs_2 = k_2(u_2 - u_1)$$

In matrix form, the expression is:

$$\begin{Bmatrix} fs_1 \\ fs_2 \end{Bmatrix} = \begin{bmatrix} K1 + K2 & -K2 \\ -K2 & K2 \end{bmatrix} \begin{Bmatrix} u_1 \\ u_2 \end{Bmatrix} \quad [4]$$

or

$$\{F_s\} = [K] \cdot \{U\} \quad [5]$$

Where

$\{F_s\}$ is the vector of force elastic,

$[K]$ is the matrix of stiffness and

$\{U\}$ is the vector of displacement

The damping matrix, result:

$$\begin{Bmatrix} f_{D1} \\ f_{D2} \end{Bmatrix} = \begin{bmatrix} c1 + c2 & -c2 \\ -c2 & c2 \end{bmatrix} \begin{Bmatrix} \dot{u}_1 \\ \dot{u}_2 \end{Bmatrix} \quad [6]$$

By analogy, the damping forces of the following equation can be expressed as:

$$\{F_D\} = [C] \cdot \{\dot{U}\} \quad [7]$$

$\{F_D\}$ is the vector of force of damping,

$[C]$ is the matrix of damping and

$\{\dot{U}\}$ is the vector of velocity.

In general it is impractical to determine the damping c is expressed in terms of the damping coefficient of (ξ).

With the application of the equation of equilibrium dynamic of the figure 2 of motion is:

$$\{F_I\} + \{F_D\} + \{F_S\} = p(t) \quad [8]$$

Which is equivalent to:

$$m\ddot{u} + c\dot{u} + ku = p(t) \quad [9]$$

With one displacement quasi-static influence by un vector ι that represents the displacement which represents the displacement at time t of a accelererogram, then we can say that for the second term of equation 9 equals:

$$P_{eff}(t) = -m \ddot{u}_g(t) \qquad [10]$$

Where

$\ddot{u}_g(t)$ are the records of accelerations.

To solve the equation of motion of a system of several degrees of freedom, we have:

METHOD MATRICIAL[6]

As the Dynamic response of a structure depends of frequency or period of vibration and of the displaced shape (form modal), the first step in an analysis of a system of several degrees of freedom is finding frequencies and shapes of modes of free vibration. In this case external forces do not exist and damping is considered zero.

Each degree of freedom provides a dynamic equation of dynamic equilibrium, the resulting vibration of the system consists of n of these equations, and can be expressed in matrix form for free vibration is not damped as:

$$[M] \cdot \{\ddot{U}\} + [K] \cdot \{U\} = 0 \qquad [11]$$

The matrix of damping [C] it can express like a linear combination of the matrix of stiffness and of mass:

$$C = \alpha_1 M + \beta K \qquad [12]$$

Where α and β are constants. This equation defined the damping of Raleigh.

But to simplify the problem, we can consider $\beta = 0$, and therefore we have:

$$[C] = 2[\beta][M] \qquad [13]$$

The matrix contains in its main diagonal damping factors corresponding to each of the shocks of the dynamic model of Figure 65

For the natural vibration frequencies and modes, we can calculate for means of the free vibration in one of his modes of natural vibration can be described mathematically for:

$$\{u(t)\} = [\Phi]\{n(t)\} \qquad [14]$$

[6] Barbat A. H., (1982), "Cálculo sísmico de las estructuras", primera edición, editors técnicos y asociados, S. A. BARCELONA. Capítulo 4.

Where:

$\{u(t)\}$ Is the displacement of the modal

$[\Phi]$ The modal matrix

$\{n(t)\}$ is a vector whose elements n (t) characterize the amplitudes of motion in each mode, called the vector of generalized coordinates.

$$[M]\{\ddot{u}(t)\}+[C]\{\dot{u}(t)\}+[K]\{u(t)\}=-[M]\{1\}a(t) \qquad [15]$$

Where

a(t) it is the horizontal acceleration record to be considered for the analysis.

Substituting the equation we have [14] in [15] :

$$[M][\Phi]\{\ddot{n}(t)\}+[C][\Phi]\{\dot{n}(t)\}+[K][\Phi]\{n(t)\}=-[M]\{1\}a(t) \qquad [16]$$

Multiplying now the equation [16] for $[\Phi]^T$ results:

$$[\Phi]^T[M][\Phi]\{\ddot{n}(t)\}+[\Phi]^T[C][\Phi]\{\dot{n}(t)\}+[\Phi]^T[K][\Phi]\{n(t)\}=-[\Phi]^T[M]\{1\}a(t) \qquad [17]$$

Of the equation [13] and remembering the conditions of orthogonal of the system, the values out of the main diagonal in the equation transform [17] themselves in zeros:

We introduce the next notations:

$$[M^*]=[\Phi]^T[M][\Phi] \qquad [18]$$

$$[C^*]=[\Phi]^T[C][\Phi]=2[\beta][M^*]=2[\upsilon][\Omega][M^*] \qquad [19]$$

where:

$$[\Omega^2]=\begin{bmatrix}\omega_1^2 & 0 & 0 & 0\\ 0 & \omega_2^2 & 0 & 0\\ 0 & 0 & \omega_i^2 & 0\\ 0 & 0 & 0 & \omega_n^2\end{bmatrix} \qquad [20]$$

And for $[K^*]$

$$[K^*]=[\Phi]^T[K][\Phi]=[\Omega^2][M^*] \qquad [21]$$

Where each one of these equations is:

$[M^*]$ Matrix of mass general

$[C^*]$ Matrix of damping general

$[K^*]$ Matrix of stiffness general.

Now we substitute these in the equation [18, 19, 21] in [13] and we have the form:

$$[M^*]\{\ddot{n}(t)\}+[C^*]\{\dot{n}(t)\}+[K^*]\{n(t)\}=-[\Phi]^T[M]\{1\}a(t) \qquad [22]$$

This has decoupled equation [15], i.e. that the equations in [22] no longer a system of differential equations, but n independent differential equations, due to the shape of the diagonal matrices of coefficients that multiply vector of unknown functions $\{n(t)\}$.

Pre-multiplicand equation [15] for $[M^*]^{-1}$ the resulting equation is:

$$\{\ddot{n}(t)\}+2[\upsilon][\Omega]\{\dot{n}(t)\}+[\Omega^2]\{n(t)\}=-[M^*]^{-1}[\Phi]^T[M]\{1\}a(t) \qquad [23]$$

Where

$$[\upsilon]=\begin{bmatrix} \upsilon 1 & 0 & 0 & 0 \\ 0 & \upsilon 2 & 0 & 0 \\ 0 & 0 & \upsilon_{n-1} & 0 \\ 0 & 0 & 0 & \upsilon_n \end{bmatrix} \qquad [24]$$

$[\upsilon]$ It is the matrix of the fraction of critical damping of the structure.

An ordinary equation i of the equation [23] it can show like:

$$\ddot{n}_i(t)+2\upsilon_i\omega_i\dot{n}_i(t)+\omega_i^2 n_i(t)=-\frac{1}{M_i^*}\{\phi_i\}^T[M]\{1\}Sa(t) \qquad [25]$$

Where

a(t) it is the horizontal acceleration record to be considered for the analysis.

Factor of participation

The equations of motion for each degree of freedom do not depend on the modes of vibration and have similar shape to the equation of motion of a system of a single degree of freedom. The factor of participation, for systems of several degrees of freedom this defined in shape matrix by Williams, A. [1998].

$$[P] = \frac{[\Phi]^T \cdot [M] \cdot \{1\}}{[\Phi]^T \cdot [M] \cdot [\Phi]} \qquad [26]$$

Where {P} vector of coefficients of participation for all the considered modes

{ 1 } unitary vector.

For a system in specific, the factors of participation have the properties of:

$$\Sigma P_n \cdot \phi_{1n} = 1 \qquad [27]$$

Where P_n is the factor of associated with participation the mode n.

ϕ_{1n} is the component, for the first knot of the system of the associated eigenvector the mode n.

The matrix of maximum displacements this defined for:

$$\begin{aligned} [U] &= [\Phi] \cdot [P] \cdot [D] \\ [U] &= [\Phi] \cdot [P] \cdot [V] \cdot [\Omega]^{-1} \\ [U] &= [\Phi] \cdot [P] \cdot [A] \cdot [\Omega^2]^{-1} \end{aligned} \qquad [28]$$

where [D] diagonal matrix of spectra displacement.

[V] Diagonal matrix of spectra velocity.

[A] Diagonal matrix of spectra acceleration.

The matrix of lateral forces in each node of the system is given by second law of Newton:

$$[F] = [K] \cdot [U] \qquad [29]$$

[K] Matrix of stiffness

[U] Vector of displacement

[F] vector of forces

The vector of shear forces at the base is given by:

$$[V] = [F]^T \cdot \{1\} \qquad [30]$$

Known values of the maximum dynamic response in each of the Nm vibration modes of interest; it is possible to obtain a good estimate of the maximum value of the structural response through combination of appropriate criteria that take into account the correlation between modes of close frequencies.

Ri and Rj are the highest values of response i and j modes, respectively.

The most probable value R or probable maximum value is given by:

$$R = \left\{ \sum_{i=1}^{N_m} \sum_{j=1}^{N_m} C_{ij} R_i R_j \right\}^{1/2} \qquad [31]$$

Where is the correlation coefficient between modes i and j, giving the following formula:

$$C_{ij} = \frac{8\xi^2 (1+r) r^{2/3}}{(1-r^2) + 4\xi_i^2 r (1+r)^2}, \quad r = \frac{\omega_j}{\omega_i} \qquad [32]$$

As ξ is the damping coefficient on the structure, the same for all modes of vibration. Getting them the complete quadratic combination (CCC), the forces applied on the obtained diagram considering the static eccentricity with respect to their center of mass and generate the loading.

In buildings of 2, 3, 4 and 5 levels, various tests were carried out and designs, from the start of the study on the topic of doctoral thesis was performed with pre-masonry walls and concrete, which was published a first article Congress in Malta (Mebarki D. and A. Perez, 2007). Hence, by the time it takes time for any project, we chose to consider only the buildings consisting of beam and column, which includes in its analysis a system solid slab floor that is rigid, thus we want to get your period after the key to know the characteristic period of the land that was in Chapter 3. It appears better behavior in small buildings, such as being the most approaching the period of the soil, then there 4 proposals for each of the buildings 2, 3 and 4 stories. The variation that exists in the proposals for these buildings is the clear separation between the columns is a design 3.5 m and another 5m.

Annex 2.

Explanation of the algorithm for develop the program

for the calculation Spectrum response of the soil.[44]

The spectrum of response is obtained by integrating the following equation: Navin C. Nigam and Paul C. Jennings (1968)

$$\ddot{u} + 2\omega c\dot{u} + \omega^2 u = -Ac(t) \qquad [1]$$

Where

ω Circular frequency in radians.

c Damping (related to critical damping)

Ac (t) Value of the acceleration in the time t due to an accelerogram

t time of the accelerograms

$\ddot{u}, \dot{u}, u$ Acceleration, velocity and displacement of the oscillator which correspond to a given frequency.

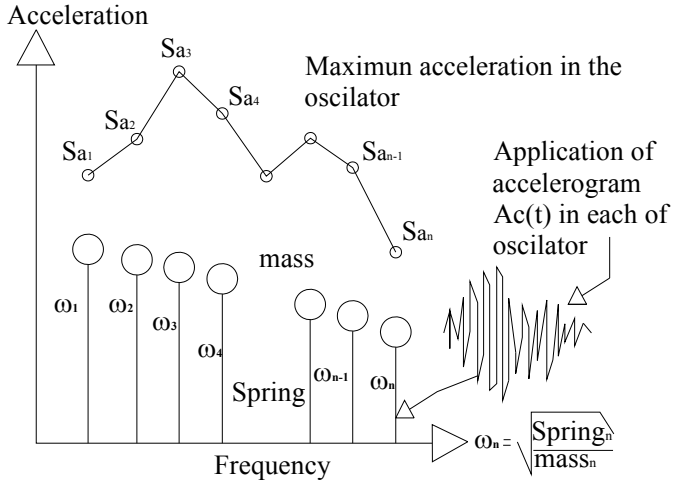

Figure 66 Graphic representation of the frequencies of the oscillator of 1GDL that introduces in the equation 1.

[44] Navin C. Nigam and Paul C. Jennings (1968), "Digital calculation of response spectra from strong motion earthquake records", California Institute of Technology

In Figure 66, Sa is the value of the spectrum of response that have of ground with a value of damping considered for analysis.

It is considered that the accelerograms varies linearly between each designated point, so the equation [1] becomes:

$$\ddot{u} + 2\omega c\dot{u} + \omega^2 u = -Ac_i - \frac{\Delta Ac_i}{\Delta t_i}(t - t_i) \qquad t_i \le t \le t_{i+1} \qquad [2]$$

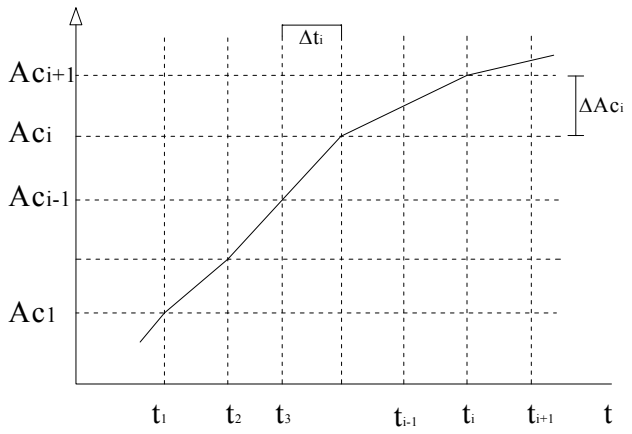

Figure 67 Graphic of acceleration time for the algorithm development.

$$\Delta t_i = t_{i+1} - t_i$$

$$\Delta Ac_i = Ac_{i+1} - Ac_i$$

The solution for $t_i \le t \le t_{i+1}$ the relative displacement is:

$$u(t) = e^{-c\omega(t-t_i)}\left[c_1 \cos \omega d(t - t_i) + c_2 sen\omega d(t - t_i)\right] - \frac{Ac_i}{\omega^2} + \frac{2c\Delta Ac_i}{\omega^3 \Delta t_i} - \frac{\Delta Ac_i}{\omega^2 \Delta t_i}(t - t_i) \quad [3]$$

Where

$$\omega d = \omega\sqrt{1 - c^2} \qquad [4]$$

ωd Represents the damped frequency

The constants of integration c_1 and c_2 equation [3] are evaluated for: $u = u_i$, $\dot{u} = \dot{u}_i$ and $t = t_i$

$$c_1 = \frac{1}{\omega d}\left[c\omega u_i + \dot{u}_i - \frac{\left(2c^2 - 1\right)\Delta Ac_i}{\omega^2 \Delta t_i} + \frac{c}{\omega} Ac_i \right] \qquad [5]$$

$$c_2 = u_i - \frac{2c\Delta Ac_i}{\omega^3 \Delta t_i} + \frac{Ac_i}{\omega^2} \qquad [6]$$

Substituting the constants in the equation [3] of displacements we have to u and $\dot{u}_i$ in $t = t_{i+1}$ they are give by:

$$\overline{u}_{i+1} = A(c, \omega, \Delta t_i)\overline{x}_i + B(c, \omega, \Delta t_i)\overline{A}c_i \qquad [7a]$$

Which:

$$\overline{u}_i = \begin{Bmatrix} u_i \\ \dot{u}_i \end{Bmatrix} \qquad \overline{A}c_i = \begin{Bmatrix} Ac_i \\ Ac_{i+1} \end{Bmatrix} \qquad [7b]$$

$$A = \begin{bmatrix} a_{11} & a_{12} \\ a_{21} & a_{22} \end{bmatrix} \qquad B = \begin{bmatrix} b_{11} & b_{12} \\ b_{21} & b_{22} \end{bmatrix} \qquad [7c]$$

Substituting in [7a] we have:

$$\begin{Bmatrix} u_{i+1} \\ \dot{u}_{i+1} \end{Bmatrix} = \begin{bmatrix} a_{11} & a_{12} \\ a_{21} & a_{22} \end{bmatrix} \begin{Bmatrix} u_i \\ \dot{u}_i \end{Bmatrix} + \begin{bmatrix} b_{11} & b_{12} \\ b_{21} & b_{22} \end{bmatrix} \begin{Bmatrix} Ac_i \\ Ac_{i+1} \end{Bmatrix} \qquad [7d]$$

Where the matrices A and B of the equation [9] are given by:

$$\left.\begin{aligned} a_{11} &= e^{-c\omega\Delta t_i}\left[\frac{c}{\sqrt{1-c^2}} sen\,\omega d\Delta t + \cos \omega d\Delta t_i \right] \\ a_{12} &= \frac{e^{-c\omega\Delta t_i}}{\omega d} sen\,\omega d\Delta t_i \\ a_{21} &= -\frac{\omega}{\sqrt{1-c^2}} e^{-c\omega\Delta t_i} sen\,\omega d\Delta t_i \\ a_{22} &= e^{-c\omega\Delta t_i}\left[\cos \omega d\Delta t_i - \frac{c}{\sqrt{1-c^2}} sen\,\omega d\Delta t_i \right] \end{aligned}\right\} \qquad [7c\text{-}1]$$

$$b_{11} = e^{-c\omega\Delta t_i}\left[\left(\frac{2c^2 - 1}{\omega^2 \Delta t_i} + \frac{c}{\omega} \right) \frac{sen\,\omega d\Delta t_i}{\omega d} + \left(\frac{2c}{\omega^3 \Delta t_i} + 1 \right) \cos \omega d\Delta t_i \right] - \frac{2c}{\omega^3 \Delta t_i}$$

$$b_{12} = e^{-c\omega\Delta t_i}\left[\left(\frac{2c^2-1}{\omega^2\Delta t_i}\right)\frac{sen\ \omega d\Delta t_i}{\omega d}+\left(\frac{2c}{\omega^3\Delta t_i}\right)\cos\ \omega d\Delta t_i\right]-\frac{1}{\omega^2}\frac{2c}{\omega^3\Delta t_i}$$

$$b_{21}=e^{-c\omega\Delta t_i}\left[\left(\frac{2c^2-1}{\omega^2\Delta t_i}+\frac{c}{\omega}\right)\left(\cos\omega d\Delta t_i-\frac{c}{\sqrt{1-c^2}}sen\omega d\Delta t_i\right)-\left(\frac{2c}{\omega^3\Delta t_i}+\frac{1}{\omega^2}\right)\left(\omega d sen\omega d\Delta t_i+c\omega\cos\omega d\Delta t_i\right)\right]$$
$$+\frac{1}{\omega^2\Delta t_i}$$

$$b_{22}=e^{-c\omega\Delta t_i}\left[\left(\frac{2c^2-1}{\omega^2\Delta t_i}\right)\left(\cos\omega d\Delta t_i-\frac{c}{\sqrt{1-c^2}}sen\omega d\Delta t_i\right)-\left(\frac{2c}{\omega^3\Delta t_i}\right)\left(\omega d sen\omega d\Delta t_i+c\omega\cos\omega d\Delta t_i\right)\right]$$
$$-\frac{1}{\omega^2\Delta t_i}$$

Every equation b_{11}, b_{12}, b_{21} *and* b_{22} belong to the equation [7c-2]

From equation [2], the absolute acceleration, $\ddot{z}_i$, is given by:

$$\ddot{z}_i = \ddot{u}_i + Ac_i = -(2c\omega\dot{u}_i + \omega^2 u_i) \qquad [8]$$

Here, if the displacement and velocity of the oscillator are known for some time t_o, the state of the oscillator at all subsequent times can be calculated exactly in a step by step implementation of the equations 7 and 8.

Finally the spectrum of response is given for each frequency and damping as:

$$S_d = Max.Abs[u_i]_{i=1\ \ a\ \ n} \qquad \text{Spectral displacement} \qquad [9]$$

$$S_v = Max.Abs[\dot{u}_i]_{i=1\ \ a\ \ n} \qquad \text{Spectral Velocity} \qquad [10]$$

$$S_a = Max.Abs[\ddot{u}_i]_{i=1\ \ a\ \ n} \qquad \text{Spectral Acceleration} \qquad [11]$$

The scheme of the algorithm we can see in Figure 68, which indicates the sequence to be scheduled

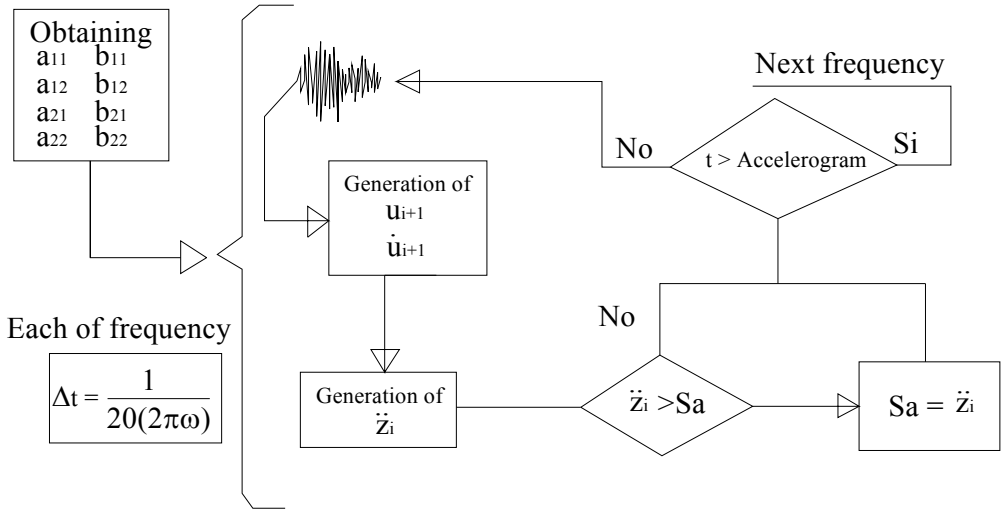

Figure 68 Algorithm for make the spectrum of response

Annex 3

Next, we present the records of real acceleration Gals and Pseudo-acceleration spectrum $(c = Sa/g)$, that is, as a fraction of gravity, the entire sample of the Table 10. It is attached to the Pseudo-acceleration spectrum of response of the ground, the corresponding to the design spectra of the Figure 28, which is the value assigned by the regulations 2004, of the Table 10 from our survey area.

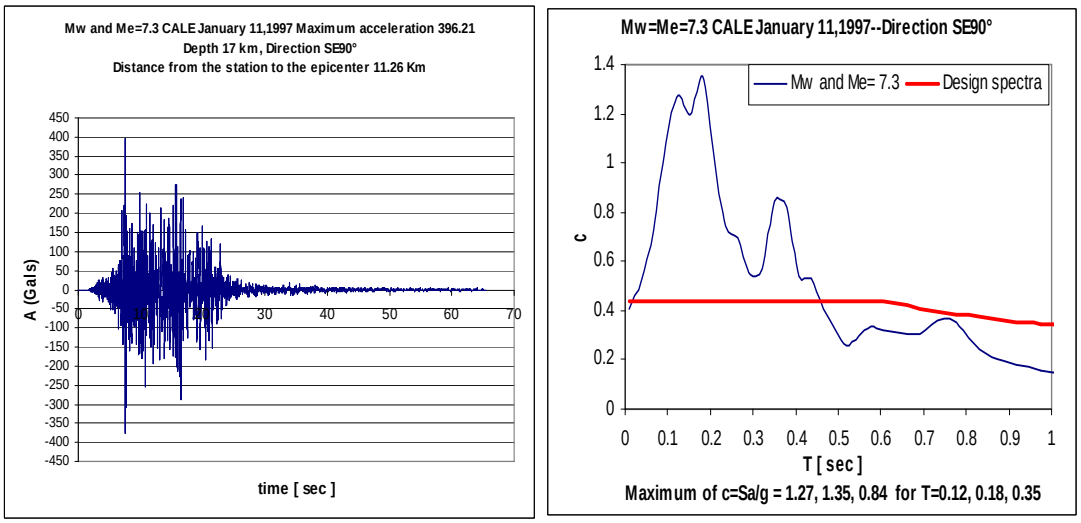

Figure 69 Station accelerograph CALE with Me=Mw=7.3 a) Record Acceleration, b) Pseudo-acceleration response spectra with $\xi = 0.05$

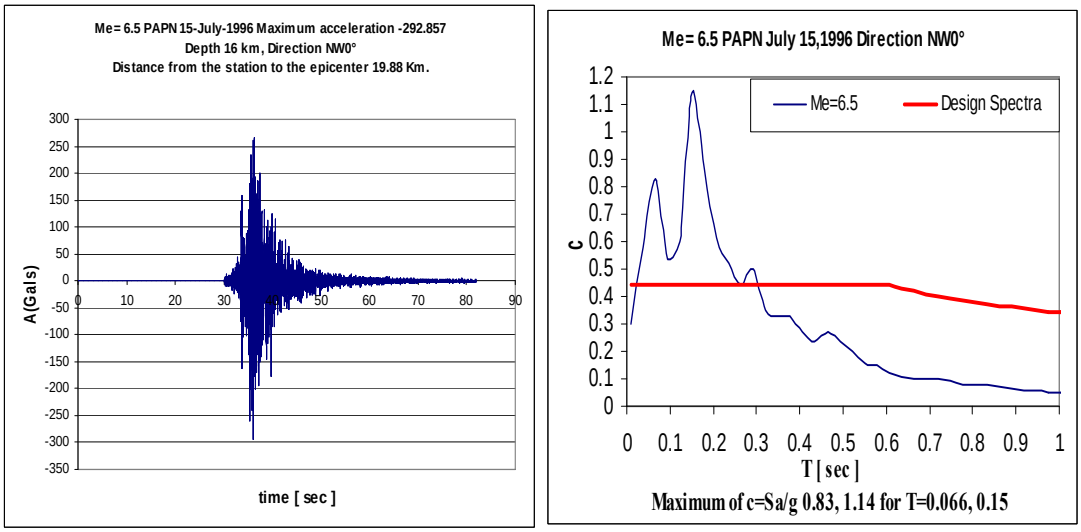

Figure 70 Station Accelerographs PAPN with Me =6.5 a) Record Acceleration b) Pseudo-acceleration response spectra with $\xi = 0.05$

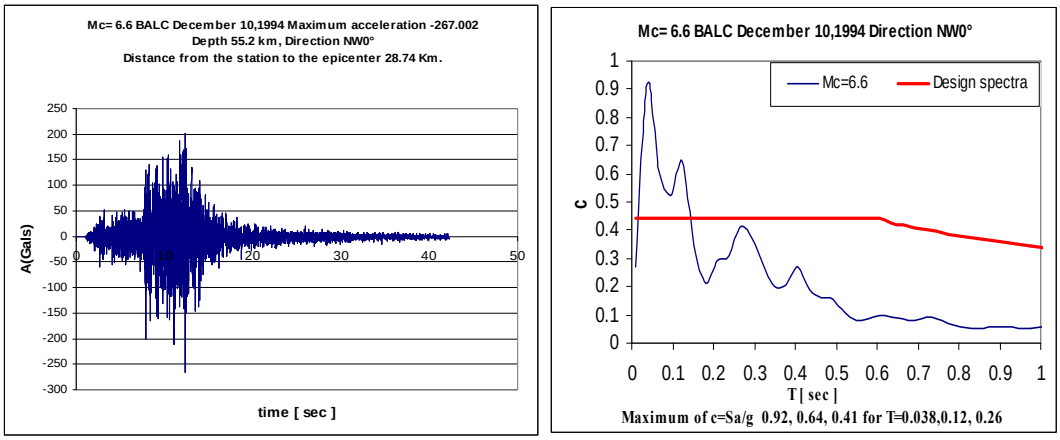

Figure 71 Station accelerograph BALC with Mc= 6.6 a) Record Acceleration, b) Pseudo-acceleration response spectra with $\xi = 0.05$

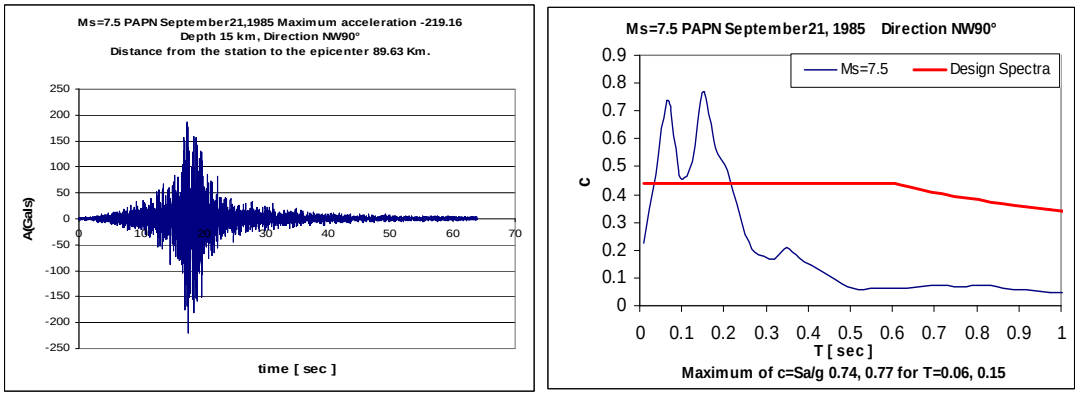

Figure 72 Station accelerograph PAPN with Ms=7.5 a) Record Acceleration, b) Pseudo-acceleration response spectra with $\xi = 0.05$

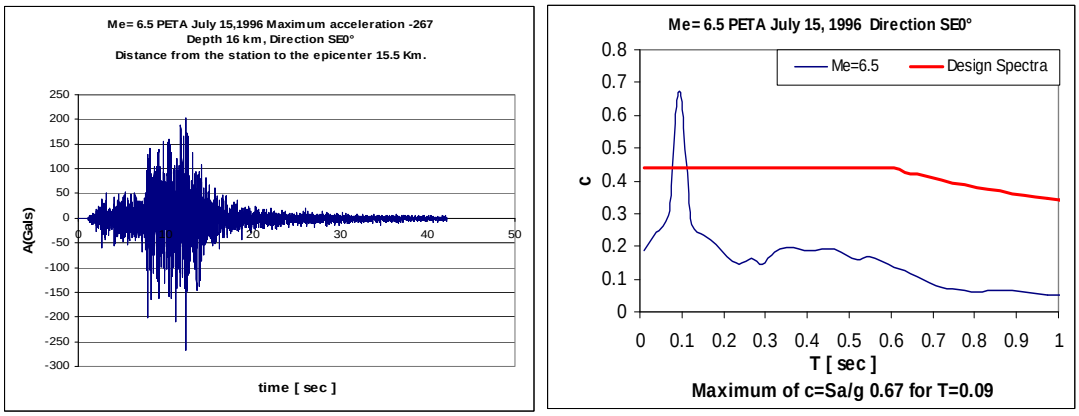

Figure 73 Station accelerograph PETA with Me=6.5 a) Record Acceleration, b) Pseudo-acceleration response spectra with $\xi = 0.05$

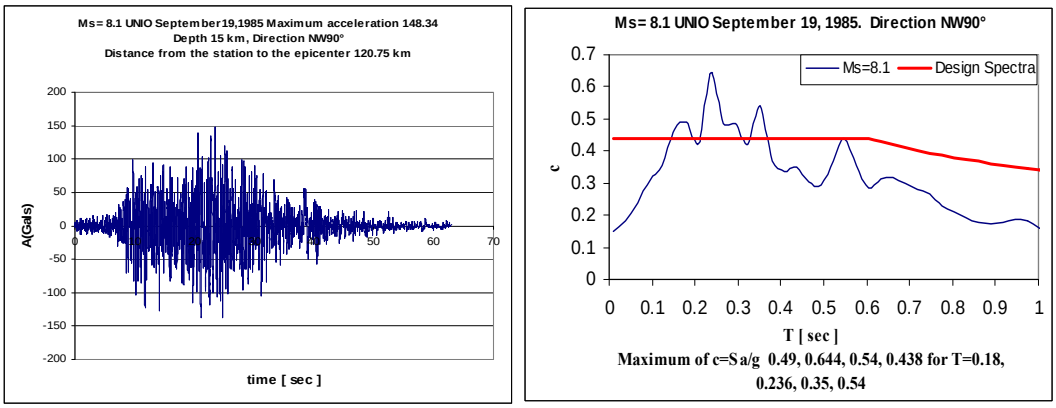

Figure 74 Station accelerograph UNIO with Ms=8.1 a) Record Acceleration, b) Pseudo-acceleration response spectra with $\xi = 0.05$

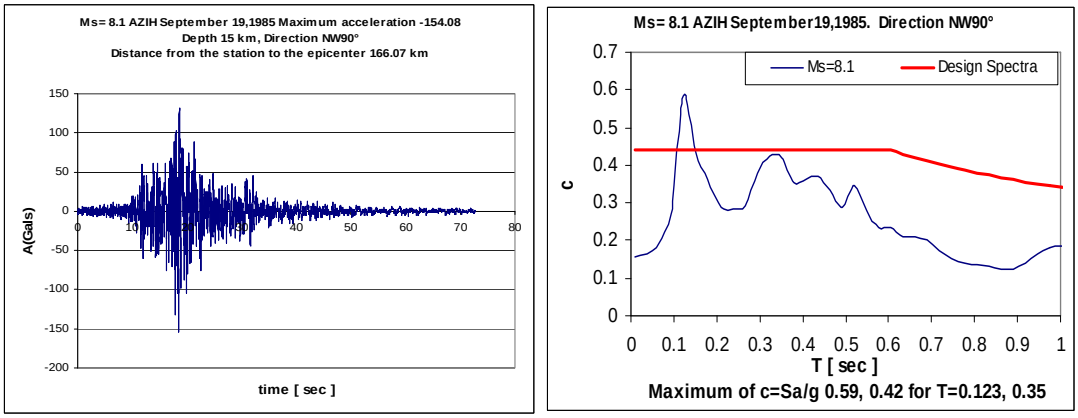

Figure 75 Station accelerograph AZIH with Ms=8.1 a) Record Acceleration, b) Pseudo-acceleration response spectra with $\xi = 0.05$

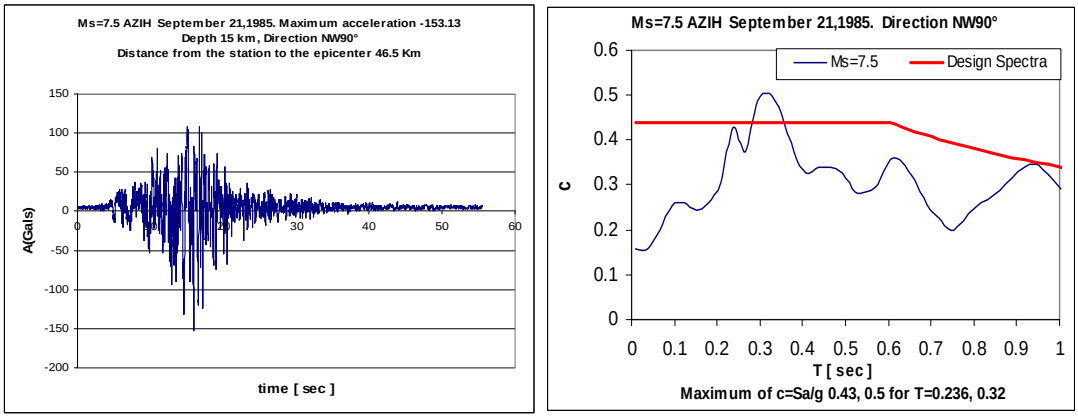

Figure 76 Station accelerograph AZIH with Ms=7.5 a) Record Acceleration, b) Pseudo-acceleration response spectra with $\xi = 0.05$.

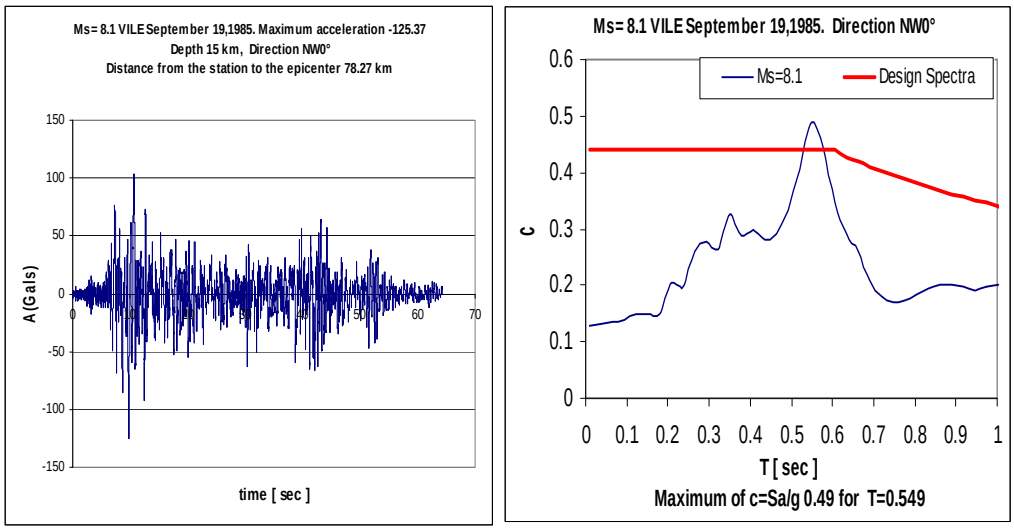

Figure 77 Station accelerograph VILE with Ms=8.1 a) Record Acceleration, b) Pseudo-acceleration response spectra with $\xi = 0.05$

Annex 4

Catalog of earthquake magnitude used.

Ms Magnitude that measures the surface waves and the expression mathematic is:

$$M_S = \log10\ (A/T) + 1.66 \log10\ D + 3.30 \qquad [4.1]$$

M_S is computed from a bandwidth between approximately 18 to 22 s.[81]

Where :

A is the amplitude of ground motion (in microns).

T is the corresponding period (seconds)

D is the distance to epicenter in (degrees)

Me Magnitude based on energy radiated by an earthquake, and the formula is:

$$M_e = 2/3\ \log_{10}E - 2.9 \qquad [4.2]$$

Where:

E is the energy expressed in Ergs.

The energy radiated by an earthquake is a measure of the potential for damage to man-made structures. Theoretically, its computation requires summing the energy flux over a broad suite of frequencies generated by an earthquake as it ruptures a fault. Because of instrumental limitations, most estimates of energy have historically relied on the empirical relationship developed by Beno Gutenberg and Charles Richter:

$$\log_{10}E = 11.8 + 1.5M_S \qquad [4.3]$$

It is now known that the energy radiated by an earthquake is concentrated over a different bandwidth and at higher frequencies. With the worldwide deployment of modern digitally recording seismograph with broad bandwidth response, computerized methods are now able to make accurate and explicit estimates of energy on a routine basis for all major earthquakes. [81]

Mc Also know by the name Coda-length, an estimate of local magnitude (ML), is calculated using a relationship developed for Washington State:[84]

$$Mc = 2.82 \log (D) - 2.46 \quad [4.4]$$

where

D is the duration of the observed event.

In Mexico the researchers, Marcos Chavacán Avila y Javier Lermo Samaniego, Coordinación de Ingeniería Sismológica, Instituto de Ingeniería, UNAM, for calculating the coda magnitude Mc used the relationship by Lee et al.(1972):

$$Mc = -0.87 + 2 \log T + .0035 D (1) \quad [4.5]$$

Where: T is the duration of the event in seconds and D is the epicentral distance in kilometers. To calculate the amount of time we used the expression of Kanamori (1977):

Mw magnitude based on seismic moment **Mo**, therefore first we will define the magnitude **Mo**. [81]

Mo considering the geometry of the fault, the orientation of the fault, direction of fault movement, and size of an earthquake can be described by the fault geometry and seismic moment. These parameters are determined from waveform analysis of the seismograms produced by an earthquake. The differing shapes and directions of motion of the waveforms recorded at different distances and azimuths from the earthquake are used to determine the fault geometry, and the wave amplitudes are used to compute moment. The seismic moment is related to fundamental parameters of the faulting process.

$$M_O = \mu S\langle d\rangle , \quad [4.6]$$

Where μ is the shear strength of the faulted rock,

S is the area of the fault, and

d is the average displacement on the fault.

Because fault geometry and observer azimuth are a part of the computation, moment is a more consistent measure of earthquake size than is magnitude, and more importantly, moment does not have an intrinsic upper bound. These factors have led to the definition of a new magnitude scale M_W, where the expression mathematic is:

$$M_W = 2/3 \log_{10}(M_O) - 10.7 \quad [4.7]$$

The units of Mw are dyne*cm. [81]

References and Bibliography

[1] AFNOR (1996), "Bases of design and action on structures and national application document", Part 1: Basis of design, Annexe A, "Méthode des coefficient partiels",Tableau A.2., page 59.

[2] Antoniou S. and Pinho R., (2004), "Development and verification of a displacement-based Adaptive Pushover procedure", Journal of Earthquake Engineering, Vol. 8, No. 4

[3] Antoniou S. and Pinho R., (2004), "Advantages and limitations of adaptive and non-adaptive force-based pushover procedures", Journal of Earthquake Engineering, Vol. 8, No. 5

[4] Antoniou S. and Pinho R., (2004), "Software SeismoStruct", Version 4.0.3 Temporary License 31/12/2009.

[5] Antoniou S. and Pinho R., (2004), "Software Seismosignal", Version 3.3.0 Temporary License 31/12/2009.

[6] Barbat A. H., (1982), "Cálculo sísmico de las estructuras", primera edición, editors técnicos y asociados, S. A. BARCELONA. Capítulo 4.

[7] Bathe K. J. (1982), "Finite element procedures in engineering analysis", Prentice-Hall Inc.

[8] Bazán E. y Meli R. (1999), "Diseño sísmico de edificios", Editorial LIMUSA, S.A. de C.V., grupo Noriega Editores, Figura 1.12, pp. 27 and Chapter 1.

[9] Boore D. (1973), "The effect of simple topography on seismic waves: implications for the accelerations recorded at Pacoima dam, San Fernando Valley, California". Bulletin of the seismological society of America, 63 (5), pp. 1603-1609.

[10] Boore D. y Joyner W. (1997), "Site amplification for generic rock sites", Bulletin of the seismological society of America, 87 (2), pp. 327-341.

[11] Bozzo L. M. and Barbat A. H. (1999), "Diseño sismorresistente de edificios Técnicas convencionales y avanzadas", Editorial Reverté, S. A. pp. 162.

[12] Bracci J. M., Kunnath S. K. and Reinhorn A. M. (1997), "Seismic performance and retrofit evaluation of RC structures, Journal of structural engineering, 123, 3-10.

[13] Bruce R. E. and Kanda J., (2005), "Safety and its Quality Assurance", edition of the Augoust 1, Structural Engineering Institute, ASCE

[14] Canavos G. C. (1999), “Probabilidad y Estadística Aplicaciones y Métodos”, Editorial McGraw-Hill, chapter 9, página. 388.

[15] Centro Nacional de Prevención de Desastres [CENAPRED](2004), “Guía Básica para la Elaboración de Atlas Estatales y Municipales de Peligros y Riesgos”, 1a Edición, diciembre 2004. Capítulos 3 y 4.

[16] Cheng G., Li G. and Y. Cai (1998), “Reliability-based structural optimization under hazard loads”, Structural optimization, Springer-Verlag 1998.

[17] Chopra Anil K. (2001), “Dynamics of Structures” Theory and Applications to Earthquake Engineering, Berkeley, USA., Second Edition, Chapter 6, pp. 205-216, chapter 9, pp. 373-374, Chapter 13, pp. 555-561.

[18] CIRES, (2009), “Informe del 4 de abril de 2009”, Macrosimulacro 2007, Secretaría de Protección Civil, Gobierno del DF., http://www.proteccioncivil.df.gob.mx/macrosimulacro /objetivo_macrosimulacro _3.html , comunicación personal con el investigador del Instituto de Geofísica de la UNAM, Singh S. K.

[19] Clough R. W. and Penzien J. (1995), “Dynamics of Structures”, Computers & Structures, Inc., Berkeley, USA., Third Edition, Chapter 25, pp. 575-607.

[20] Corona G. (2002), “ECOgcW, ANEMgcW”, Análisis y diseño de Edificios de Concreto, Software. gcorona@gcingenieria.com

[21] Dhillon B.S. (2006), “Maintainability, maintenance, and Reliability for Engineers”, Published by CRC Press Taylor & Francis Group, ISBN -0-8493-7243-7. pp. 3.

[22] Ellstein R. (2003), “La Interacción Sismo – Suelo – Estructura y su influencia en el diseño de edificios urbanos”. XIV Congreso de León Guanajuato, México. Director de Laboratorios Tlalli, S. A de C. V.

[23] Esteva L., Díaz O., Mendoza E., Cruz O., Alamilla J. y Pérez D. (2000), “Confiabilidad de sistemas Estructurales ante sismos”, Proyecto CONACYT REF 3663PA.

[24] Esteva L. and Ruiz S. (1989), “Seismic failure rates of multistory frames”. J. Structural Div., ASCE, 115 (ST2)

[25] Esteva L., Díaz O. and Mendoza E. (1994), “Espectros de Diseño Sísmico de Confiabiliad Congruente, Etapa 1. Espectros de Isoconfiabilidad en la zona blanda del DF, Proyecto No. 3558, Instituto de Ingeniería, UNAM, Septiembre.

[26] Gaceta Oficial del Distrito Federal, (2004) “Normas Técnicas Complementarias”, Tomo I y II, BIS 103.

[27] "Google Earth (2009)". Software

[28] Hancock J. and Bommer J. (2006), "A state-of-knowledge review of the influence of strong-motion duration on structural Damage", Earthquake Engineering practice, 22 (3), pp. 827-845.

[29] Huerta B. y Reinoso E. (2002), "Espectros de energía de movimientos fuertes registrados en México", Revista de Ingeniería Sísmica de la red de revistas Científicas de América Latina y el Caribe, España y Portugal, enero-junio No. 066, Sociedad Mexicana de Ingeniería Sísmica, A. C., pp. 45-72

[30] Hamburger R. O., Foutch D. A. and Cornell C. A. (2000), "Performance basis of guidelines for evaluation, upgrade and design of moment-resisting steel frame", Proceedings of the Twelfth World Conference on Earthquake Engineering, Auckland, New Zealand, paper No. 2543.

[31] Informe rápido al EERI, SMIS, CENAPRED y GIIS sobre el sismo de Colima, México, 21 de Enero de (2003).

[32] Kanamori, H. (1977), "The energy release in great earthquake", Journal of Geophysic Research, 82, 2981-2987.

[33] Laouami N., Slimani A., Bouhadad Y., Chatelain J. L. and Nour A. (2006), "Evidence for fault-related directionality and localized site effects from strong motion recordings of the 2003 Boumerdes (Algeria) earthquake: Consequences on damage distribution and the Algerian seismic code", Soil Dynamics and Earthquake Engineering, Elsevier, pp-991-1003.

[34] Larson K. M., Lowry A. R., Kostoglodov V., Hutton W., Sánchez O., Hudnut K. and Suárez G. (2004), "Crustal deformation measurements in Guerrero, Mexico". Journal of Geophysical Research, Vol. 109, pag. 1-19.

[35] Lee W. H. K., Bennet R.E. and Meagher K. L., (1972), "A method of estimating magnitude of local Earthquake from signal duration", Geol. Surv. Open-File Rep. (E.U.A.), 28.

[36] Lemaire M., and collaboration avec Chateauneuf A. et Mitteau J. C. (2005), "Fiabilité des structures couplage mécano-fiabiliste statique", Publications Hermes Science.

[37] Levin R. I. (1988), "Estadistica para administradores", Prentice-Hall Hispanoamericana, S. A., ISBN 968-880-152-6. Capítulo 8.

[38] Mander J. B., Priestley M.J.N. and Park R. (1988), "Theoretical stess-strain model for confined concrete", Journal of Structural Engineering, Vol. 114, No.8, pp. 1804-1826.

[39] Manea V. C., Manea M., Kostoglodov V., Currie C. A. And Sewell G., (2004) , "Thermal structure coupling and metamorphism in the Mexican subduction zone beneath Guerrero", Journal Geophysics, April 14, No. 158, pp. 775-784.

[40] Martinez-Rueda J.E. and Elnashai A.S. (1997), "Confined concrete model under cyclic load", Materials and Structures, Vol. 30, No. 197, pp. 139-147.

[41] Meli R. (1976), "Bases para los criterios de Diseño Estructural del proyecto del Reglamento de Construcciones para el Distrito Federal", Instituto de Ingeniería, UNAM, Informe Interno, septiembre.

[42] Meli R. y Mendoza C. J. (1991). "Reglas de verificación de calidad del concreto", Revista de ingeniería LXI, México.

[43] Mendoza C. (1993), "Coseismic slip of two larga Mexican earthquake from teleseismic body waveforms: implications for asperity interaction in the Michoacan plate boundary segment", Journal Geophysics, Res. 98, 8197-8210.

[44] Mendoza C. (1995), "Finite-fault analysis of the 1979 March 14 Petatlan, Mexico, earthquake using teleseismic P waveforms", Journal Geophysics, Int. 121, 675-683.

[45] Navin C. Nigam and Paul C. Jennings (1968), "Digital calculation of response spectra from strong motion earthquake records", California Institute of Technology

[46] Nishenko S. P. and Singh S. K. (1987a), "Condicional probabilities for the recurrence of large and great interpolate earthquake along the Mexican subduction zone". Bull. Seismol. Soc. Am. 77, 2094-2114.

[47] Nishenko S. P. and Singh S. K. (1987b), "The Acapulco-Ometepec, Mexico, earthquake of 1907-1982; evidence for a variable recurrence history". Bull. Seismol. Soc. Am. 77, 1359-1367.

[48] Nowak A. S. and Collins K. V. (2000), "Reliability of Structures", McGraw-Hill Higher Education, ISBN 0-07-048163-6. Chapter 5.pp. 91-143.

[49] Ordaz M. y Montoya C., (2005), "Software Degtra", Versión 5.4.0 UNAM (25/07/2005), 1990-2002.

[50] Ortiz B. L., (1998), "Elasticidad", McGraw-Hill, ISBN 84-481-2046-9.

[51] Papanikolaou V. K., Elnashai A. S. And Pareja J. F., (2005), "Limits of applicability of conventional and Adaptive Pushover Analysis for seismic response

assessment", Mid-America Earthquake Center civil and environmental engineering Deparment University of Illinois at Urban Champaign,

[52] Park R. and Paulay T. (1984), "Reinforced Concrete Structures", New York, J Wiley and Sons.

[53] Pelin G., Guido de R., Geert D. and Wong K.K.F (2007), "Site dependent response spectra and analysis of the characteristic of the strong ground motion due to the 1999 Duzce earthquake in Turkey". ScienceDirect

[54] Pérez D. and Mebarki A.(2007), "Optimal Design of Reinforced Concrete Structures Erected on Hard Soils", Civil-Comp Press, 2007, Proceeding of the Eleventh International Conference on Civil, Structural and Environmental Engineering Computing, BHV Topping (Editor), Civil-Comp Press, Stirlingshire, Scotland.

[55] Periodico Oficial del Gobierno del Estado de Guerrero, Poder Ejecutivo, "Reglamento de Construcción para los municipios del Estado de Guerrero", Artículo 206, pp. 108.

[56] Petersons N. (1964), "Strength of concrete in finished structures", Trans. Royal Institute Technology, No. 232, Estocolmo.

[57] Philippe C. C., (2005), "Mathematical Elasticity", Vol. 1, pp. 250-251.

[58] Rathje E. M., Abrahamson N. A. and Bray J. D. [1998], "Simplified frequency content estimates of earthquake ground motions", Journal of Geotechnical and Geoenvironmental Engineering, Vol. 124, No. 2, pp. 150-159.

[59] Reinoso E. and Ordaz M. (2001), "Duration of Strong ground motion Turing Mexican earthquakes in terms of magnitude, distance to the rupture area and dominant site period", Earthquake Engineering and Structural Dynamics, pp. 653-673.

[60] Reyes J., Hernández J. L. y López O. (2003), "Espectros inelásticos para estructuras precoladas de concreto reforzado", XIV Congreso SMIS León Guanajuato, Art. VII-05.

[61] Reyes C., Meli R. y Leonar L. (2003), "El efecto de la magnitud y el amortiguamiento en los espectros de diseño asociados al estado límite de servicio", XIV Congreso SMIS León Guanajuato, Art. V-02.

[62] Sasaki K. K., Freeman S. A. and Paret T. F.(1998), "Multimodal pushover procedure (MMP)", A method to identify the effects of higher modes in a pushover analysis, proceedings of the sixth US National Conference on Earthquake

Engineering (Oakland, California, 1998) (computer file), Earthquake Engineering Research Institute, 12 pages.

[63] Shome N. and Cornell C. A. (2002), "Probabilistic seismic demand analysis of nonlinear structures. Report No. RMS-35 program, Stanford University.

[64] Singh S. K., Bazan E. and Esteva L. (1980), "Expected earthquake magnitude from fault". Bull. Seismol. Soc. Am. 70, 903-914.

[65] Singh S. K. and Mortera F. (1991), "Source time functions of large Mexican subduction earthquake, morphology of the Benioff zone, age of the plate and their tectonic implications". Journal Geophysics, Res. 96, 21487-21502.

[66] Soong T. T. (2004), "Fundamentals of Probability and Statistic", Edition John Wiley & Sons Ltd, ISBN 0-470-86814-7. pp.298

[67] Soto A., (2004), "Determinación del modulo de elasticidad del Concreto simple, con Resistencia f 'c=250 kg/cm2, para el municipio de Chilpancingo de los Bravos, Guerrero". Tesis para obtención del grado de Maestría en la Universidad Autónoma de Guerrero, México. Septiembre 2004.

[68] SriVidya A. and Ranganathan R. (1995), "Reliability based optimal design of reinforced concrete frames". Elsevier Science Ltd., Computer and Structures Vol. 57, No. 4, pp. 651-661.

[69] Suárez G., Monfret T., Wilttlinger G. and David C., (1990), "Geometry of subduction and depth of the seismogenic zone in the Guerrero GAP, Mexico". Nature 345, 336-338.

[70] Valdés C. and Novelo D.A. (1997), "The Western Guerrero, Mexico, seismogenic zone from the microseismicity associated to the 1979 Petatlan and 1985 Zihuatanejo earthquake", Instituto de Geofísica, Universidad Nacional Autónoma de México, ELSEVIER, Tectonophysics, 3 Septembre 1997.

[71] Val D., Bljuger F. and Yankelevsky D. (1997), "Reliability evaluation in nonlinear analysis of reinforced concrete structures", Elsevier Science, Structural Safety, Vol. 19, No. 2, pp. 203-217.

[72] Vamvatsikos D. and Cornell C. A. (2002), "Incremental Dynamic Analysis", Earthquake Engineering and Structural Dynamic, Vol. 31, No. 3, pp. 491-514.

[73] Veras L. y Ordaz M. (2004), "Criterios generales para la definición de espectros sísmicos de sitio", Aplicaciones prácticas a la ingeniería, congreso SMIE, 2004.

[74] Villanueva J. M. y Meli R., (1984), "Análisis Estadístico de Propiedades Mecánicas de Aceros de Refuerzo Producidos en México", Instituto de Ingeniería, UNAM, Informe Interno, Septiembre.

[75] Wai-Fah C. and Scawthorn C. (2003), "Earthquake Engineering Handbook", Edition by CRC Press LLC, ISBN 0-8493-0068-1. Chapter 13, pp. 13-8 and 13-9

[76] website: http://tlacaelel.igeofcu.unam.mx/~vladimir/gpsred/acapulco/acap01.jpg website of Instituto de Geofísica de la Universidad Nacional Autónoma de México (UNAM)

[77] website: http://www.cires.org.mx Centro de Instrumentación y Registros Sísmicos, Asociación Civil

[78] website: http://www.smis.org.mx Sociedad Mexicana de Ingeniería Sísmica [SMIS].

[79] website: http://tlacaelel.igeofcu.unam.mx/~vladimir/gpsred/acapulco_yates/acya_ne_01.jpg website of Instituto de Geofísica de la Universidad Nacional Autónoma de México (UNAM)

[80] website: http://tlacaelel.igeofcu.unam.mx/~vladimir/sismos/100%Floshtml Instituto de Geofísica de la Universidad Nacional Autónoma de México (UNAM)

[81] website: http://earthquake.usgs.gov/ United States Geological Survey Earthquake Hazard Program. Vocabulary and many other aspects of their Earthquake Hazards Program. The figure 1.2.11 from "Lisa Wald".

[82] website: http://www.ssn.unam.mx Servicio Sismológico Nacional de México.

[83] website: http://www.inegi.gob.mx INEGI

[84] website: http://hsap.pnl.gov/catalogues.asp, US DEPARTMENT OF ENERGY, Pacific Northwest, National laboratory.

[85] website: http://www.bioestadistica.uma.es/libro/node80.htm#teo:t5:cochran, "Bioéstadistica: Métodos y Aplicaciones", U. D. Bioestadística. Facultad de Medicina de la Universidad de Málaga. ISBN 847496-653-1.

[86] website: http://www.seru.metu.edu.tr/Istanbul/Presentations/pinho.pdf

[87] Pinho R., Antoniou S., Casarotti C. And López M. (2005), "A displacement-based adaptive pushover for assessment of building and bridges", Istanbul.William, Alan (1998), "Seismic Design of Buildings and Bridges" , 2ª edición, Editorial Engineering Press, Austin-Texas, Estados Unidos. pp 22-23 [ref. 4]

[88] Wilson E. L., (2002), “Three-Dimensional Static and Dynamic Analysis of Structures”, A physical approach with emphasis on earthquake engineering”, University of California at Berkeley. Computer & Structures Inc., Third Edition January 2002.

[89] Xianguo Y., Jiaru Q., and Kangning L. (2004), “Shaking table test and dynamic response prediction on an earthquake-damage RC building”, Earthquake Engineering and Engineering vibration, Vol. 3, No.2.

[90] Kanamori, H. (1977). "The energy release in great earthquakes", Journal of Geophysical Research, 82, 2981-2987

[91] Lee, W.H.K., R.E. Bennett and K.L. Meagher. (1972). "A method of estimating magnitude of local earthquakes from signal duration", Geol. Surv. Open-File Rep. (EUA), 28.